THE CONTROL OF A PLASTICATING EXTRUDER WITH FLIGHT NOISE AND PRESSURE SURGING

By

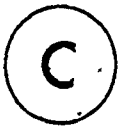

MARK HENRY COSTIN, B.Eng.

A Thesis

Submitted to the School of Graduate Studies

In Partial Fulfilment of the Requirements

for the Degree

Master of Engineering

McMaster University

June 1981

To my family, Mom, Dad, Paul, Uncle Hy and Aunt Bernice

MASTER OF ENGINEERING (1981) McMASTER UNIVERSITY
(Chemical Engineering) Hamilton, Ontario

TITLE : The Control of a Plasticating Extruder with Flight Noise and Pressure Surging

AUTHOR : Mark Henry Costin, B.Eng. (McGill University)

SUPERVISORS : Professor P.A. Taylor

Professor J.D. Wright

NUMBER OF PAGES : x, 193

ABSTRACT

Dynamic models for a plasticating extruder melt pressure are formed from steady state, step test and time series analysis data. The extruder pressure response to steps in screw speed is modelled by a first order transfer function with a time constant of approximately 0.2 s. The noise associated with the extruder pressure consists of a pressure surging at 0.125 Hz frequency and a longer term drift associated with the die temperature controller. This drift has a period of approximately 3.0 min. The pressure also has a signal noise at the same frequency as the screw rotation caused by the screw flight passing the tip of the pressure transducer.

The digital PI and the self-tuning regulator control algorithms are used to control the extruder. These controllers are implemented in combination with various filters which remove the flight noise. The most successful controller/filter combination is a digital PI controller used with a filter constructed from 2 poles and 2 zeroes.

The dynamic response of a disturbance caused by changing the input polymer quality is also examined. The use of Box and Jenkins seasonal time series models as bandstop filters is studied and it is concluded that they have little practicality as filters. Another topic covered by the thesis is the effect that including filters in the forward transfer function part of a process has on the self-tuning regulator algorithm.

ACKNOWLEDGMENTS

I wish to acknowledge the work and time spent on this project by my supervisors Prof. P.A. Taylor and Prof. J.D. Wright. I would also like to acknowledge Xerox Research Center of Canada, the employers of Prof. Wright for allowing him time to supervise this project. The donation of the polymer used in the experimental portion of this project by Union Carbide of Canada is acknowledged. The help of the following people is also gratefully appreciated: Prof. J.F. MacGregor, Dept. of Chemical Engineering, for our discussions in the area of stochastic identification and control, Prof. J. Vlachopoulos, Dept. of Chemical Engineering, for his help in the area of polymer processing, Prof. S. Haykin, Dept. of Electrical Engineering, for his help in filtering theory and practice and my fellow graduate student Enno Agur for his help in running the equipment involved in this project. The financial support of the Government of Canada, in the form of an NSERC scholarship, and McMaster University is also acknowledged.

On a more personal level, I would like to thank my friends, the graduate students of the Department of Chemical Engineering who are responsible for all my fond memories of McMaster. I am especially grateful to Alan and Janet Melnyk whose incredible generosity during my last weeks in Hamilton will always be remembered.

I would also like to thank Mrs. Heather Avedesian for typing my manuscript into a thesis.

TABLE OF CONTENTS

LIST OF TABLES

LIST OF FIGURES

CHAPTER ONE

INTRODUCTION

One of the most important pieces of equipment used in the processing of plastics, is the plasticating extruder. With plastics finding more and varied uses, that require exacting standards, a method of increasing polymer production without degrading the product quality is needed. Presently most industrial extruders are run with analog PI controllers to regulate wall temperatures and melt pressure. The application of more modern process control techniques to the extruder has the potential for great savings in the polymer industries.

This thesis describes the modelling and control of a small industrial scale extruder. Many authors (e.g. Tadmor and Klein(1978)) have reported pressure surges due to the breakup of the tip of the solid region and a signal noise due to the rotation of the screw. However, the previous attempts, reported in the literature, of modelling and controlling the extruder pressure have completely neglected these disturbances. The previous stochastic control studies, which had great potential to identify and control these disturbances, stopped at the modelling stage without applying control to the actual process.

The objective of this thesis is to experimentally identify the noise models and transfer functions for an extruder, using the screw speed as the manipulated variable and the pressure as the measured variable. Once the dynamic model for the extruder is identified,

various control schemes are implemented on the extruder in an attempt to regulate the process.

This thesis also studies the effect that filters with cutoff frequencies close to the control frequency have on the closed loop control. Various filters are examined and implemented to remove the flight noise from the pressure signal in an attempt to improve the quality of control of the extruder pressure.

Time series models based on filtered data are compared to the one developed for the unfiltered case. The effects of filters on the control achieved by the self-tuning regulator algorithm is discussed in detail.

The thesis is outlined as follows:

Chapter Two: A literature survey on the application of process control to the extruder is presented. The chapter is divided into three sections discussing classical control studies, modern control studies and extruder disturbance studies.

Chapter Three: The extruder equipment and computer facilities are described.

Chapter Four: This chapter presents steady state runs and step tests performed on the extruder. Estimates for process parameters and disturbances are made.

Chapter Five: A time series model for the extruder is presented.

Chapter Six: The extruder pressure is regulated by the digital PI algorithm using the screw speed as manipulated variable. Experimental results for unfiltered pressure data and pressure data filtered by various methods are presented. Filtering theory and Bode diagrams

for the individual filters are discussed.

Chapter Seven: The application of the self-tuning regulator in combination with various types of filters for the control of the pressure is presented. The control of extruder pressure in general is summarized.

Chapter Eight: The results of this thesis are summarized and recommendations and conclusions are presented.

CHAPTER TWO

LITERATURE SURVEY

2.1 Classical Control Studies

Recently, the problems presented by the dynamic behavior of extruders has attracted the attention of many research teams in the field of plastic processing. Most of these workers have proceeded by using classical techniques for both model identification and process control applications. Classical methods use dynamic models of the process expressed in terms of transfer functions. These models are generally determined from open loop step response data. Control algorithms are analog or digital versions of the PI or PID algorithms which are tuned either off-line from the models or on-line by trial and error. This section describes most of this work, all of which has been published in the last decade.

Dormeier(1979) outlines the use of digital PID algorithms. He regulates the melt temperature on a 45 mm screw diameter extruder with 3 heating zones. The barrel heater nearest the screw tip is used as disturbances. The digital PID controller is tuned off-line using a simulation study that is developed in another paper. It is found to be superior to conventional analog control for both disturbances and set point changes. However, set point changes and disturbances each have a different set of tuning parameters and no details are given on the tuning of the analog controller. This paper shows that the combination of heater power and the digital PID algorithm can be quite effective in regulating long term temperature disturbances. The

controller is tested by set point changes and disturbances caused by steps in the second zone heater power. The figures presented show that a disturbance rejection or set point change reaches steady state within 10 min. Unfortunately, the system time constant, controller sampling time or any description of typical process disturbances associated with the melt temperature are not presented. Also no consideration is given to the effect on the process of disturbances other than the second zone heater step disturbances.

Fingerle(1978) describes a control system designed to regulate the temperature in an extruder. The melt temperature is controlled by heat generated by viscous dissipation from the polymer. This is called autogenic control. In this system the temperature is controlled by manipulating a plunger which varies the length of an annular section at the end of the screw. By varying this length, more or less heat will be generated by viscous dissipation. The extruder used in the experiments has a screw diameter of 60 mm and 25:1 length to diameter ratio. The responses of melt temperature and pressure for step changes in both annular length and screw speed are reported. The steps in screw speed were large, 40r/min, and Fingerle samples too slowly, at 15 s, to see any high frequency disturbances. However, the steps are performed for many different operating conditions, showing that the extruder gain is linear for the range 40-120 r/min and 12-43 mm annular length. The pressure responds almost immediately to a change in screw speed, rising to a maximum after 15 s (one sampling period). The pressure then falls to a new steady state level as the temperature rises. The pressure response shows an overshoot of over 40% in comparison to

the final level. The melt temperature has a first order response, with a small period of delay (0.25 min), to changes in screw speed and annular length with time constants of 2.5 min and 1.5 min respectively. The transfer functions relating annular length to pressure are presented for various screw speed operating conditions. The transfer functions presented have higher order numerator (lead) terms than denominator (lag) terms. This is physically unrealizable as it implies that the output predicts the input. However, Fingerle also reports that the gain for the transfer functions relating annular length to die pressure is so small that these models are neglected. The pressure and annular length are then considered to be uncorrelated variables. The controller implemented appears to be a variation of Dahlin's algorithm (Smith(1972)) using annular length to control the melt temperature.

Rastogi(1978) and Frederickson(1978) of Measurex Corporation describe a general industrial system used to control extrudate thickness and throughput for extruders with flat dies. This system uses a microcomputer which can be programmed to handle many different control functions and sensors in a simple and flexible manner. These include an option of retuning control variables based on a process model and the current operating level. The control algorithm most generally used appears to be Dahlin's algorithm (Smith(1972)).

The system only controls thickness and throughput. No mention is made of any other variables such as temperature or pressure. Experimental data showing the effectiveness of the system in controlling thickness and throughput are presented. Rastogi shows a two-thirds

reduction in thickness variance. The controller takes approximately 2.5 min to complete a setpoint change, sampling approximately every 10 s. Frederickson's data shows that the control is very effective in eliminating any offset or long term drift in thickness. However, the thickness shows considerable high frequency thickness variations, too fast for the take up mechanism to handle. It appears that this controller would have trouble regulating high frequency (greater than approximately 0.01 Hz) thickness variations.

Tadmor et al(1974) develop a dynamic simulation of an extruder, based on theoretical models. This simulation uses instantaneous mass and energy balances to identify the pressure, temperature, throughput and width of the solid unmelted polymer bed, as a function of time and distance down the extruder barrel. The simulation is used to model a 63.5 mm diameter extruder. The length of the barrel is not given.

The results for large changes in screw speed level (from 60 r/min to 100 r/min) are presented. The pressure response is described by a gain with no dynamics, followed by a slow decay to a new steady state level, as the temperature rises. The temperature rise overshoots its final value by approximately 30% and slowly oscillates as it decreases to the steady state level. The temperature response time constant is of the order of 10 s.

Brauner et al(1978) use the same model as Tadmor et al(1974) to model the dynamic behavior of the extruder when the rheological properties of the feed polymer are varied. They study two cases, a minor change in apparent viscosity corresponding to minor variations in feed material and a major change in apparent viscosity corresponding

to an entirely different feed material.

Brauner et al's simulation shows that a small step change in feed polymer apparent viscosity forms a pressure wave in the melting zone. The die does not sense the increase in pressure until the pressure wave arrives. Both the temperature and pressure rise until the wave reaches the die, one full residence time in the extruder. With the arrival of the wave at the die, all the variables have a dramatic change in their dynamic behavior. The die pressure and throughput perform very fast dynamic steps (the steps appear to be almost instantaneous with the arrival of the new polymer) to new steady state values. At this point the temperature also levels out to its steady state value.

The case of the major change in apparent viscosity has the same response as the previous case with one important addition. When the new polymer reaches the die, the flow rate is greatly changed. This causes a shift in the position of the start of the melting region. This in turn causes an oscillation in solid bed width which is sustained as late as one residence time after the new material has reached the die.

Brauner et al propose simplifying changes to the model, mainly in the form of linearizations of some of the simulation's partial derivatives. No results for the approximate model are presented.

Brauner et al's results are not verified by experiments and Tadmor et al's are verified only qualitatively on an extruder different from the one modelled. Both their results deviate from those obtained experimentally in this thesis. An especially surprising result for the disturbance in feed quality, is that the die pressure does not

change until the new polymer reaches the die. A pressure spike in a fluid carrying pipe would travel much faster than the fluid velocity. A similar result would be expected in the extruder system. A comparison of the simulation results of Tadmor et al and Brauner et al with the experimental results presented in this thesis appears in Chapter 4.

Schott(1971) studies extruder dynamics by performing step tests in screw speed and in polymer quality on a 44.4 mm diameter extruder with a 24:1 L/D ratio. His screw speed steps are relatively large, 20 r/min (from 40 to 60 r/min), and he observes a highly underdamped second order response in melt pressure. Impulse tests in screw speed lead him to believe that the extruder behaves like a differentiator. He postulates a transfer function model, equation (2.1) relating pressure to screw speed.

$$\frac{P(s)}{U(s)} = \frac{(1 + as)^4}{\tau^2 s^2 + 2\tau \xi s + 1} \qquad (2.1)$$

where $a = 0.42$, $\xi = 0.08$ and $\tau = 0.85$ s are fitted from experimental data. However, this transfer function has a higher order numerator (lead) terms than denominator (lag) terms which implies that the output predicts the input. This system is physically unrealizable.

Schott's steps in polymer quality are performed by suddenly switching from one polymer to another. The pressure response to these steps is modelled as a second order plus dead time transfer function. This model has a dead time corresponding to the system residence time, approximately 5.3 min, a time constant equal to 8.44 min and a 0.706 damping coefficient. In this thesis, Schott does not describe any

inherent disturbances in the extruder. Pressure surges, such as those described in section 2.3, are not observed. Schott samples at 1 Hz which would be fast enough to see any surging if it is present. Schott makes no recommendations for the application of any of his models for process control.

Fontaine(1975) uses step tests to develop relatively complex transfer function models relating throughput, adapter pressure and exit temperature to back pressure valve setting, barrel heater power and screw speed. He uses a 63.5 mm diameter extruder with a 24:1 L/D ratio which produces polystyrene sheets. His steps in screw speed are a more reasonable magnitude of +8.15 r/min, from an 85. r/min initial level, as compared to the steps of Schott. His data show a rapid pressure rise (time constant less than 5 s) followed by a slow decline as the temperature increases. The melt temperature has a time constant of the order of minutes. He actually presents two models, one for the long term, and the other for short term responses, in order to take the sizable difference in the time constants into account. Fontaine also reports the presence of cyclic fluctuations in pressure and temperature with a period of 11 s and pressure variations as large as 200 kPa. These fluctuations are found to be inherent to the extruder in that configuration. These cycles are determined to be actual process information and are not found to be correlated to the screw speed. These fluctuations are therefore not due to any effects caused by the rotation of the screw. No mention is made of controlling or modelling the 11 s surging even though the pressure deviations due to these fluctuations are almost one-half the magnitude of the pressure response to a change

in screw speed of +8.15 r/min. Fontaine almost completely ignores these disturbances even though they are quite large and would therefore affect product quality. They are only briefly discussed and are filtered from all but one figure. In most parts of the data analysis, the cycling is removed by digitally filtering the data. A filter used to remove a noise with an 11 s period would have affected a process with a 5 s time constant. Fontaine does not consider this filtering problem and no detail as to the nature of the filter is presented. Fontaine recommends a control strategy using the PI algorithm for the control of the die and adapter wall temperatures and a flow resistance valve to regulate the long term condition of the throughput.

Dormeier(1980) gives an overview of extrusion control. He gives examples of classical control strategies for the control of screw speed, screw temperature, barrel wall temperature including melt temperature regulation via cascade terms to the barrel temperature controllers, melt pressure and viscosity. However, there is no clear presentation of the control problems encountered in the plastics industries. Neither does he make statements describing the effectiveness of the control schemes or discuss areas that require more research.

Wright(1978) uses a microprocessor interfaced to an extruder to control screw speed and barrel temperature profiles. The system handles upsets to the barrel temperature caused by screw speed changes or changes in feed material quality. He concentrates mainly on the computer system as the objective of the thesis is to design a low cost computer control system for a general extruder. His experimental results are very similar to Fontaine's (they used the same extruder). Unlike Fontaine,

all of Wright's figures do show the sizable pressure surging with an unspecified period. Wright does not try to control the pressure. The surging is attributed to solid bed breakup and is not discussed further. The feed material quality changes are caused by switching from pellets to flaked feed material and by changing types of polystyrene. The resulting responses are very similar to those observed by Schott. No models for the disturbances or transfer functions are presented.

In summary, all these researchers justify studying the extruder in an attempt to eliminate disturbances in the melt temperature and pressure, it is hoped that the other properties of the final product (i.e. viscosity) will be maintained constant, minimizing off-specification material. However, all of the researchers concentrated on the control of the relatively long term drifts and disturbances, with time constants in the order of minutes. There is no comprehensive appreciation of the disturbances encountered in extruders in general or even the particular extruders examined. This is probably why there have been so many experimental dynamic modelling studies published and so little work presented on actual process control implementation.

2.2 Time Series Modelling Studies

In addition to the studies presented in the previous section, there have been some attempts to use more modern control techniques to model the extruder dynamics. Most of this work concentrates on using Box and Jenkins(1976) time series analysis techniques to develop these models.

In this method, a sequence (usually a pseudo-random binary sequence (PRBS)) is used to determine the setting of the manipulated

variable. The sequence usually has an implementation period smaller than the process response time. By studying the auto and cross correlations of the input series and the corresponding output data, a model of the following form can be constructed:

$$Y_t = \frac{\omega(Z^{-1})}{\delta(Z^{-1})} \; Z^{-f-1} \; X_t + N_t \qquad (2.2)$$

where f is the number of sampling period of delay, $\delta(Z^{-1})$ is a polynomial representing the system dynamic terms, $\omega(Z^{-1})$ is a polynomial with terms to compensate for past inputs and Z^{-1} is the backwards shift operator $Z^{-1} X_t = X_{t-1}$. N_t is a noise model which can in turn be specified by equation (2.3):

$$N_t = \frac{\theta(Z^{-1})}{\nabla^d \phi(Z^{-1})} \; a_t \qquad (2.3)$$

where a_t is a white noise sequence and $\nabla = 1 - Z^{-1}$ is the difference operator with d having an integer value to compensate for non-stationary disturbances. Most models use d = 1 which allows the noise model to follow step disturbances. This will force the inclusion of integral action in the discrete controller designed to control this process for minimum variance. The ∇ term will eliminate an offset due to step changes in the process. $\theta(Z^{-1})$ and $\phi(Z^{-1})$ are polynomials in Z^{-1} relating the a_t to past a_t's and the input and output sequences.

The parameters of the combined model (2.2) and (2.3) can be determined by using a least squares analysis on the a_t sequence. Because this technique can involve many more parameters than simple first order plus dead time models, the process and its related noise

can be modelled more accurately. The noise is not modelled and therefore not considered by classical techniques. Once one knows the type of disturbances associated with a process, one can determine their probable cause and the most effective means of eliminating them. The time series method also contains the means for determining the goodness of the model fit, by examining the cross and auto correlations between the residual a_t's and the input sequence.

From Box and Jenkins models one can easily determine a minimum variance control strategy which implies that the controlled variable has the smallest possible variation. Tuning procedures are therefore simplified. In addition the structure and the initial parameters for self-tuning regulators can be determined from the minimum variance controller. More detail on time series analysis can be obtained from Box and Jenkins(1976).

Parnaby and his co-workers are the first to use time series analysis and other stochastic identification techniques for modelling the extruder. They experiment on a 38 mm diameter laboratory extruder, (17:1 L/D ratio) extruding low density polyethylene at an average screw speed of 18 r/ min. Except for the much lower screw speed used by Parnaby, the conditions are similar to those used in the experiments described in this thesis. Parnaby et al(1975) determine a time series model relating melt temperature at the die to screw speed input. Kochhar and Parnaby(1977) presents the same model (2.4) and one relating pressure at the die to screw speed (2.5).

$$T_t = \frac{(0.3248 + 0.1078Z^{-1} - 0.093Z^{-2})}{(1. + 0.4398Z^{-1} - 0.2155Z^{-2})} U_{t-1} +$$

$$\frac{(1. + 0.3343Z^{-1} - 0.2949Z^{-2})}{(1. - 0.5540Z^{-1} + 0.4499Z^{-2})} a_t \qquad (2.4)$$

$$P_t = \frac{(0.1072 - 0.0093Z^{-1})}{(1 - 0.5286Z^{-1} + 0.5198Z^{-2})} U_{t-K_p} +$$

$$\frac{(1 + 0.2876Z^{-1})}{(1 - 0.5879Z^{-1})} a_t \qquad (2.5)$$

$$0<K_p<1$$

Unfortunately, in both papers the authors fail to explain the significance of the models. There is no discussion explaining why the models are second order or what type of disturbances are the noise terms modelling.

The process sampling time is 12.5 s. The smallest system time constants are given as 5. s for pressure and 100. s for temperature.

One can analyze the structure of the models to determine what each of the model terms represents. Factoring Parnaby and Kochhar's transfer function model (2.4) gives roots $Z^{-1} = 2.52$ and $Z^{-1} = -1.38$ for the numerator and $Z^{-1} = 3.4$ and $Z^{-1} = -1.36$ for the denominator. The numerator/denominator pair of roots, -1.38 and -1.36, are very

close indicating that the transfer function was over-modelled. Removing these roots reduced (2.4) to (2.6).

$$T_t = \frac{(1 - 0.40Z^{-1})}{(1 - 0.29Z^{-1})} U_{t-1} + \frac{(1 + 0.3343Z^{-1} - 0.2949Z^{-2})}{(1 - 0.5540Z^{-1} + 0.4499Z^{-2})} a_t \qquad (2.6)$$

This transfer function models a system with an overshoot of 18% at the first sampling interval after a screw speed change, followed by a gradual decline to the steady state value. A response that is more indicative of the melt pressure not the melt temperature. The AR part of the noise model $(1 - 0.5540Z^{-1} + 0.4499Z^{-2})$ (roots $Z^{-1} = 0.62 \pm 1.36i$) can be shown to represent a damped sine wave with a frequency of 0.015 Hz (a period of approximately 60 seconds). One can see minor oscillations of this frequency in the steady state data for screw speed, die melt temperature and die melt pressure presented in Parnaby et al(1975).

The pressure transfer function in equation (2.5) has a second order dynamic term $(1 - 0.5286Z^{-1} + 0.5198Z^{-2})$. This has roots $Z^{-1} = 0.51 \pm 1.29i$, very close to the noise model for the

temperature. This also identifies a damped sine wave of 0.015 Hz frequency. The pressure data Parnaby and Kochhar(1977) show for the response to the PRBS test shows an almost instantaneous pressure response to screw speed changes. This particular sine wave starts at its maximum amplitude and then slowly decays as it oscillates. One can see a rapid response to a step with a slow sinusoid behavior in Parnaby and Kochhar's data. This second order term could probably be fit as part of the noise model. Parnaby and Kochhar use very short PRBS sequences. Sequences 15, 31 and 63 values long are mentioned but the authors do not specify the length of the series used to develop the models (2.4) and (2.5). However, all three possibilities are short series. Using short sequences of time series data can lead to models which satisfy all the diagnostic tests but which do not have the best overall structure.

Another problem with the pressure model (2.5) is that the parameter K_p is specified by Parnaby and Kochhar as being between zero and one ($0<K_p<1$). K_p represents the sampling periods of delay and must be an integer value greater than or equal to one. At least one

period is needed to represent the sample and hold used in all digital transfer function models. No explanation is given for this unusual value of K_p.

Both (2.4) and (2.5) should have been modelled with a $(1 - Z^{-1})$ term in the noise model denominator. This would allow the model to track any non-stationary disturbances and force integral action into the controller designed for this model. This $(1 - Z^{-1})$ term is often not necessary for the modelling stage as there may not be any non-stationary disturbances present. However, for practical reasons, integral action is generally needed by most controllers to eliminate any system offsets or long term drifts.

In a third paper, Kochhar and Parnaby(1978) compare various forms of stochastic identification techniques, including time series analysis, using the extruder melt temperature as the output variable. The same model (2.4) is presented in addition to models developed by using the same data with other identification techniques. Because of the short sequence of data used to develop the models, there are significant discrepancies between the various models.

In these papers Parnaby and his co-workers show the ability of the time series modelling technique to model the extruder. Unfortunately they did not use their models to gain a better understanding of the process and its noise. Without this understanding they could not appreciate what each individual term in the model represents or how to improve the structure of the model. No attempt was made to apply control schemes to the extruder, however, they do propose the use of screw speed

to control melt temperature and a die restrictor valve to compensate for changes in melt pressure and flow rate.

Patterson and his co-workers at Ecole Polytechnique discuss the use of PRBS tests and time series analysis for a 25 mm diameter extruder (120:1 L/D ratio), extruding low density polyethylene. This extruder is configured in a similar manner to the one used in this thesis. In their first paper, Patterson and de Kerf(1978) use screw speed as the manipulated variable. Later work (Patterson et al(1979)) makes use of a die constricting valve as manipulated variable. Melt temperature, melt pressure and the extrudate thickness are the measured variables. They report that the pressure responds almost instantaneously to screw speed changes. Thickness has a similar response, but with a 2 s transport delay due to the distance between the extruder and the photocell which is measuring the thickness. Temperature responds with a delay of 25 s and a time constant of 120 s. Step changes in valve position yield similar responses except the die melt temperature is unaffected by the change and the valve melt temperature shows an unexpected non-minimum phase response. This valve melt temperature response is postulated to be due to a rearrangement of the temperature profile caused by the change in flow rate. In both papers, time series models are not presented and control of the extruder is not attempted.

Chin(1979) performs some preliminary time series modelling of the same extruder used in this thesis. He models melt temperature as a function of screw speed and implements the corresponding minimum variance

controller. However, he samples too slowly to determine a model relating pressure to screw speed or to identify any significant temperature disturbances.

2.3 Extruder Disturbance Studies

Tadmor and Klein(1978), in their comprehensive book on plasticating extrusion classify extruder die pressure fluctuations according to frequency. The highest frequency fluctuations are those that occur at the same frequency as the screw rotations. This can be caused by the periodic changes in the feed rate due to the passage of the flight at the hopper opening. Disturbances of this type are rare and usually occur only when extruding at very low back-pressure. This can be caused by excessively cooled screws or screws with inadequate compression ratios.

Fluctuations at the frequency of the screw rotations can also be picked up by mispositioning of the pressure transducer. A transducer placed close to the tip of the screw will measure a fluctuation caused by the passing of the screw flight. However, this is a measurement problem and is not an actual change in the extruder pressure. These fluctuations would not be recorded by a transducer placed in the die.

The next class of disturbances is at intermediate frequencies, from 1 to 15 cycles per minute. Fluctuations in this frequency range are the main cause of poor product quality. They are caused by the periodic breaking up of the melt region, leaving large blocks of solid polymer which melt very slowly while they are immersed in the polymer melt. This variation in the length of the melt region causes a surging

effect in the extruder. Tadmor and Klein(1978) report that the breaking of the solid bed usually occurs at approximately the same point in the extruder each time. This is an inherent instability in the melting process having a fairly consistent frequency. This break up process is dependent on the polymer, pellet size and screw geometry and only to a small extent on the extruder steady state operating conditions. This means that the extruder will have surging of relatively constant frequency through its whole range of operation. However, the size of surges will depend on the operating level.

Maddock(1964) reports that these surges can be considerably reduced by cooling the screw. This stabilized the bed by creating a solid layer on the screw. A negative effect, however, is that the throughput is reduced (Fenner et al(1978)). Presently many extruders operate with their screws cooled in order to avoid these disturbances, thereby sacrificing throughput rate. Eliminating these fluctuations without cooling the screw will allow these extruders to achieve a higher level of productivity.

The last class of disturbances are very low frequency variations. These are usually caused by conditions external to the extruder. Possible examples include cycling in the heater power controllers, plant voltage fluctuations, water pressure variations or long term variations in feed polymer quality. As will be seen in Chapter 4, the extruder used in the experiments for this thesis experiences all three types of disturbances.

Maddock(1964) published a comprehensive analysis of extruder stability, concentrating on the effect of pressure on throughput.

To study the possible effect of variations in pressure on throughput, Maddock derived equation (2.7).

$$Q = BP^{1/1-m} \qquad (2.7)$$

where Q = volumetric flow rate, P = pressure and B = constant depending on the die resistance and on the polymer viscosity. For low density polyethylene, in high shear rate ranges, a typical value of m would be about 2/3. For this value (2.7) reduces to:

$$Q = BP^3$$

A 1% variation in pressure would yield a 3% variation in throughput and assuming a constant take up rate, a 3% increase in diameter. A 5% variation would yield a 16% increase in throughput and a 15% increase in diameter. Minor variations in pressure can cause considerably larger variations in thickness. The value of the pressure exponent can vary from 1.5 to 4.0 depending on the polymer and the shear rate used.

Any application where the extrudate is to be produced to close diameter tolerances must have pressure variations kept to a minimum. Maddock gives an example where a heavy wall cable is to be produced with a tight tolerance specified for the thickness. In this case, pressure surges of 48. kPa, in an average operating level of 7.1 M.P.a, produce borderline product. ± 21. kPa is established as an operating limit. These surges have a period of 20. to 30. s, an example of an intermediate frequency pressure fluctuation.

For this same example, Maddock observes high frequency variations of from 34 to 69 kPa, at the same frequency as the screw rotation, 39 r/min.

However, these fluctuations are too quick to have a noticeable effect on the finished product, and are otherwise ignored by Maddock for the rest of the discussion.

The high frequency type of pressure fluctuations would be expected to have little effect on the final product as these fluctuations would be too fast to appreciably change the thickness of the extrudate (Vlachopoulos(1981)). Unfortunately, except for the observations of Maddock, research on the dynamic effect of extruder pressure changes on die swell and thickness have yet to be undertaken especially in a practical system which includes a take-up mechanism.

Fluctuations in pressure can also be caused by a change in melt temperature. The temperature affects the viscosity, which in turn affects the pressure. Maddock presents data for various polymers giving the percent change in pressure for a 1°C change in temperature. For example, low density polyethylene will experience a change in pressure at the die of between 1.25% and 1.67% for each 1°C change in melt temperature.

Griffith and Tsai(1980) study the shape changes experienced by non-circular extrudate during its cooling and take up. They give typical current industrial tolerances for profile angles as 5°, for wall thickness, 10% and for cross-section dimensions of profile extrusion ± 0.25 mm or ± 1%, whichever is larger. Common causes of deviation from desired shape are listed as fluctuations in the quality and quantity of the melt delivered by the extruder, non-ideal flow and drawing conditions, uneven cooling in the water bath and stretching and contact with sizing dies, guides or other drag points along the drawing path.

In the experimental section, they compare various ratios of the profile dimensions and found a high correlation between these values. Therefore, one measurement can in general be used to size the entire extrudate profile. Another important conclusion is that the common industrial practice involving the use of metal guides or local cooling by small water streams, along the drawing path, have negligible effect on the thickness.

Unfortunately all the experimental data presented is for steady state conditions. There is no information on the size or frequency of the disturbances or the responses of the extrudate to changes in screw speed or take up mechanism rate. Griffith and Tsai conclude that feedback control for correct size is possible based on measuring one dimension.

CHAPTER THREE

EQUIPMENT AND INSTRUMENTATION

3.1 Minicomputer Facilities

The extruder is interfaced to the minicomputers of the Department of Chemical Engineering Control Laboratory. These computers were used for all data logging programs and control algorithms that were implemented on the extruders. A schematic of the system is presented in Figure 3.1.

This laboratory consists of twin Data General NOVA 1200 minicomputers. They share an inter-processor bus, a 1/2 M-byte fixed head disk and a Data Acquisition and Control Subsystem (DGDAC). The DGDAC consists of 48 A/D and 12 D/A channels, 32 TTL inputs and 32 TTL outputs, 32 contact sense lines and 16 relay outputs. These parts can be accessed by FORTRAN callable subroutines in library file AIO.LB (Harris(1979)).

One of the NOVA 1200's has a 10 M-byte moving head disk, a magnetic tape drive, an ADM-3A CRT, a Centronics line printer and a real time clock. This machine is configured for program development.

The other NOVA has a high speed paper tape punch and reader, hardware floating point processor, hardware multiple and divide, real time clock, a Data General dasher terminal and a teletype. It is used for the production runs and communicates with the teletype which is situated in the same room as the extruder. This allows the experimenter to be with the equipment at all times. Because they reduce computation time, the hardware floating point and multiple/divide allowed a much higher sampling rate to be used in the control experiments.

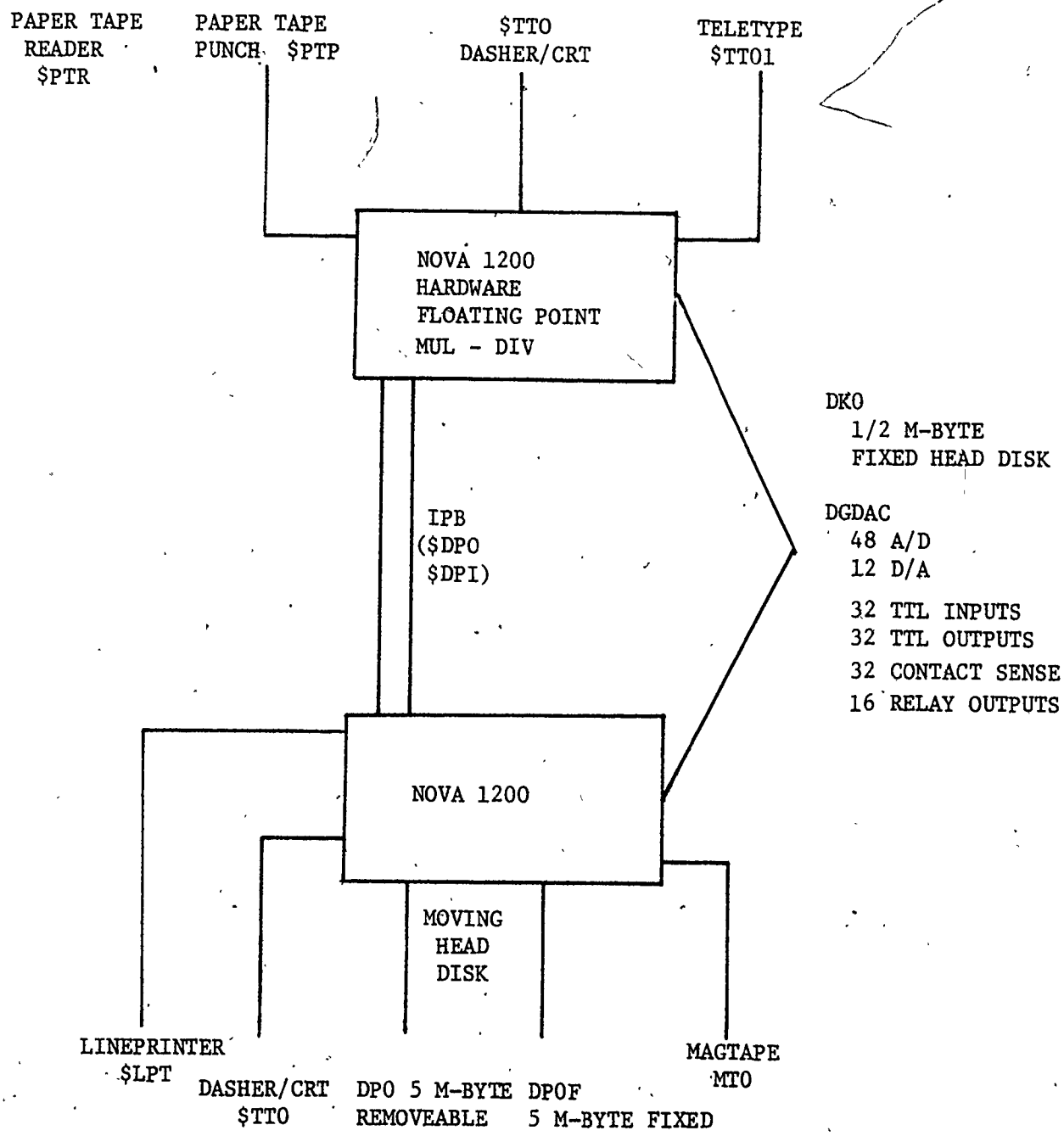

Figure 3.1 Schematic of the Computers and Peripherals

The computers use the RDOS operating system, revision 6.62. All process control programming is written using Real-Time Fortran. Appendix B provides the program listing used for the extruder data logging, PRBS testing and process control routines.

3.2 Extruder

The experiments were performed on a single-screw Killian 38 mm extruder having a length to diameter ratio of 24:1. This extruder is equivalent in size to many of the smaller scale extruders that are used in industry. Figure 3.2 gives the schematic of the extruder and its associated equipment.

The extruder barrel is made from Xalog-306 and is lined externally with asbestos. The extruder is fed through a hopper that is equipped with a shut-off slide and a drain chute for emptying.

The screw is machined from 4140 flame hardened steel and has 12 flights in the feed section and 6 flights each in the compression and metering sections. The extruder motor is a 10 horsepower DC Baldor motor. It is linked to the screw by a parallel type Dodge reducer, model no. TDT-415.

There are four heating zones along the barrel and one at the die. Each is controlled by Barbara-Colman PI controller. The four zones controllers are time proportional controllers with an on-off auxiliary output controlling a cooling air fan. The temperature is measured by J type thermocouples that are implanted in the barrel wall. The heat is supplied by means of electrical heating bands. The die controller is similar but it has no on-off auxiliary output or fan.

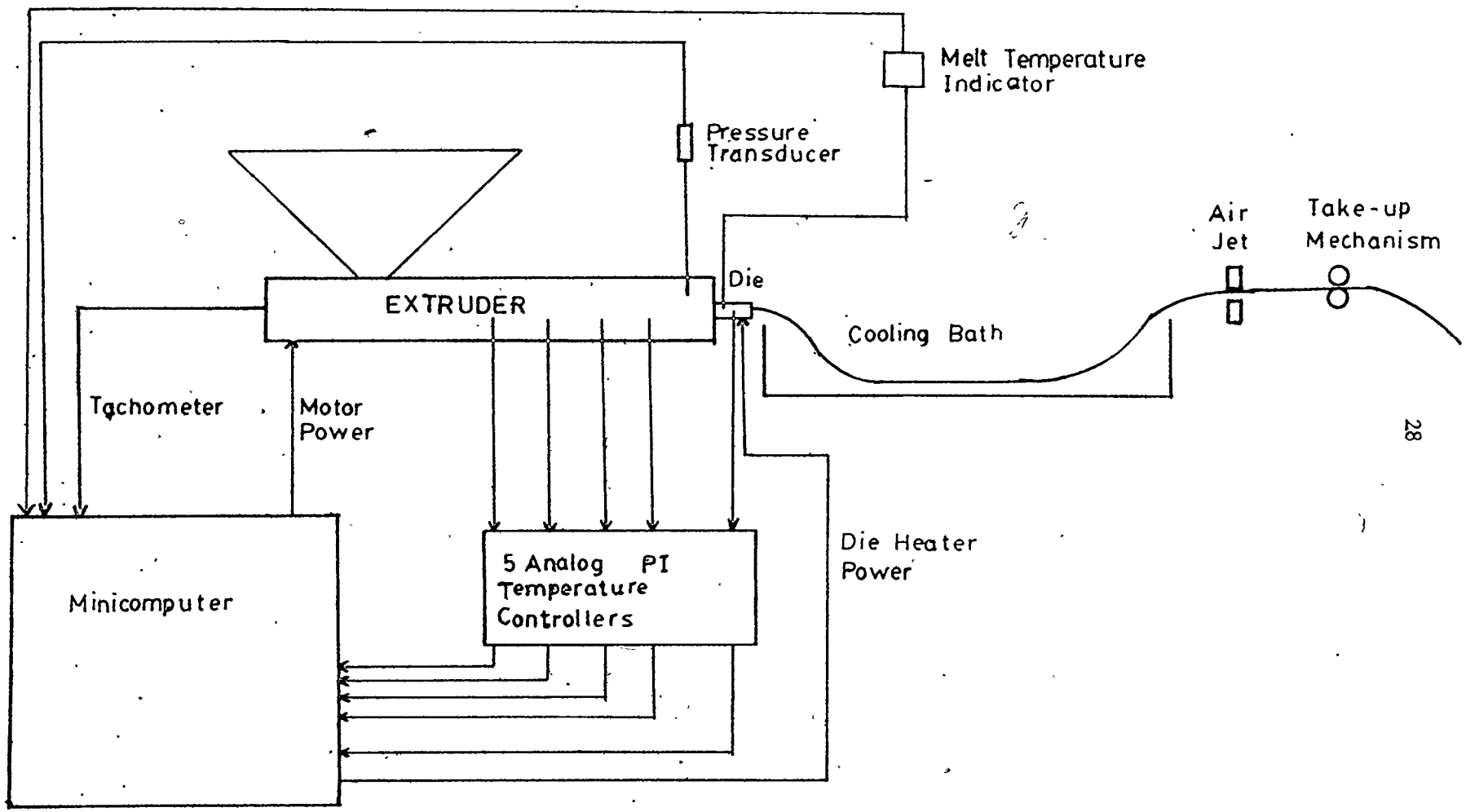

Figure 3.2 Schematic of Extruder and Associated Equipment

Each controller contains an amplifier and process signal conditioner that provides a linear value between 0 to 5 V corresponding to the process temperature. This signal is then buffered and amplified by a factor of two and sent to the computer. Table 3.1 details the controller setpoints. These were left unchanged during experiments unless otherwise noted.

There is also an additional J thermocouple that is used to measure the melt temperature. This thermocouple is immersed in the melt just prior to the die and its signal is sent to a Barbara Colman series DB 11 digital temperature indicator. The indicator has been modified to allow a temperature signal to be sent to the computer. This signal is first filtered and then amplified before it is sent to the DGDAC's. A schematic of the filter-amplifier circuit is given in Figure 3.3.

The melt pressure is measured by means of a Dynisco PT 402A, strain gauge type pressure transducer that is situated in the melt pumping region of the screw, upstream from the breaker plate and the adapter. This transducer is connected to a Dynisco PC 201 pressure controller. The pressure controller is not used to control the extruder and is only used as a signal amplifier and conditioner. This controller also has a linear process signal output which is then amplified and sent to the computer. The output of the controller is disconnected from the motor control unit. In its place a signal from the computer is used to run the extruder. A switch allows the operator to choose between manual and computer control. The computer output is clamped using a hardware circuit fixing the upper and lower limits of the extruder speed as approximately 90. r/min and 16. r/min respectively. Figure 3.4 shows

TABLE 3.1

NORMAL EXTRUDER OPERATING LEVELS

Wall Temperature Controllers Settings

Zone 1	:	162.8°C
Zone 2	:	162.8°C
Zone 3	:	168.3°C
Zone 4	:	168.3°C
Die	:	168.3°C

Extruder Screw Speed Operating Range	0 - 100 r/min
Lower Clamp Setting	16 r/min
Upper Clamp Setting	90 r/min
Normal Extruder Operating Point	50 r/min

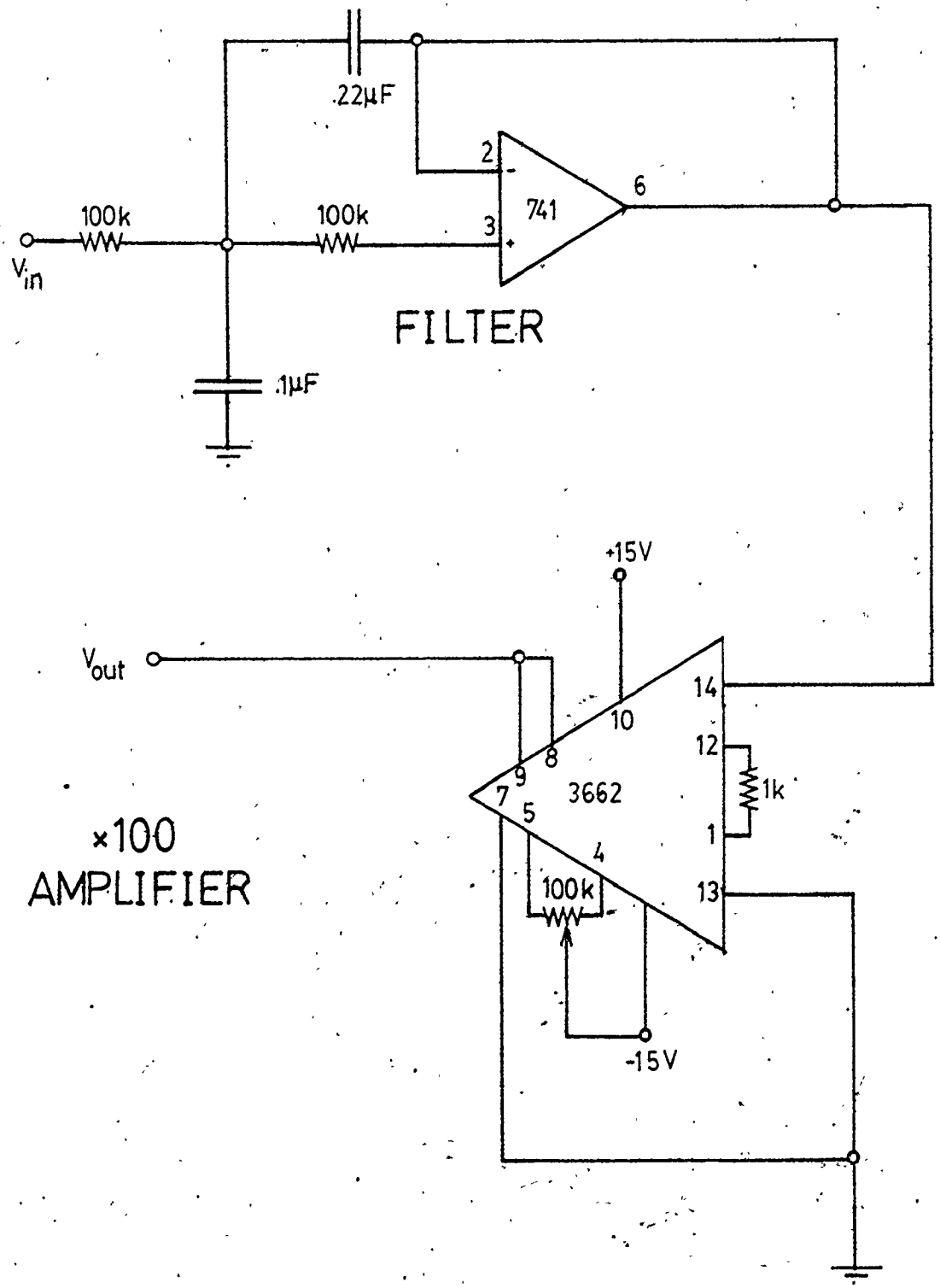

Figure 3.3 Filter-Amplifier Circuit for Melt Temperature

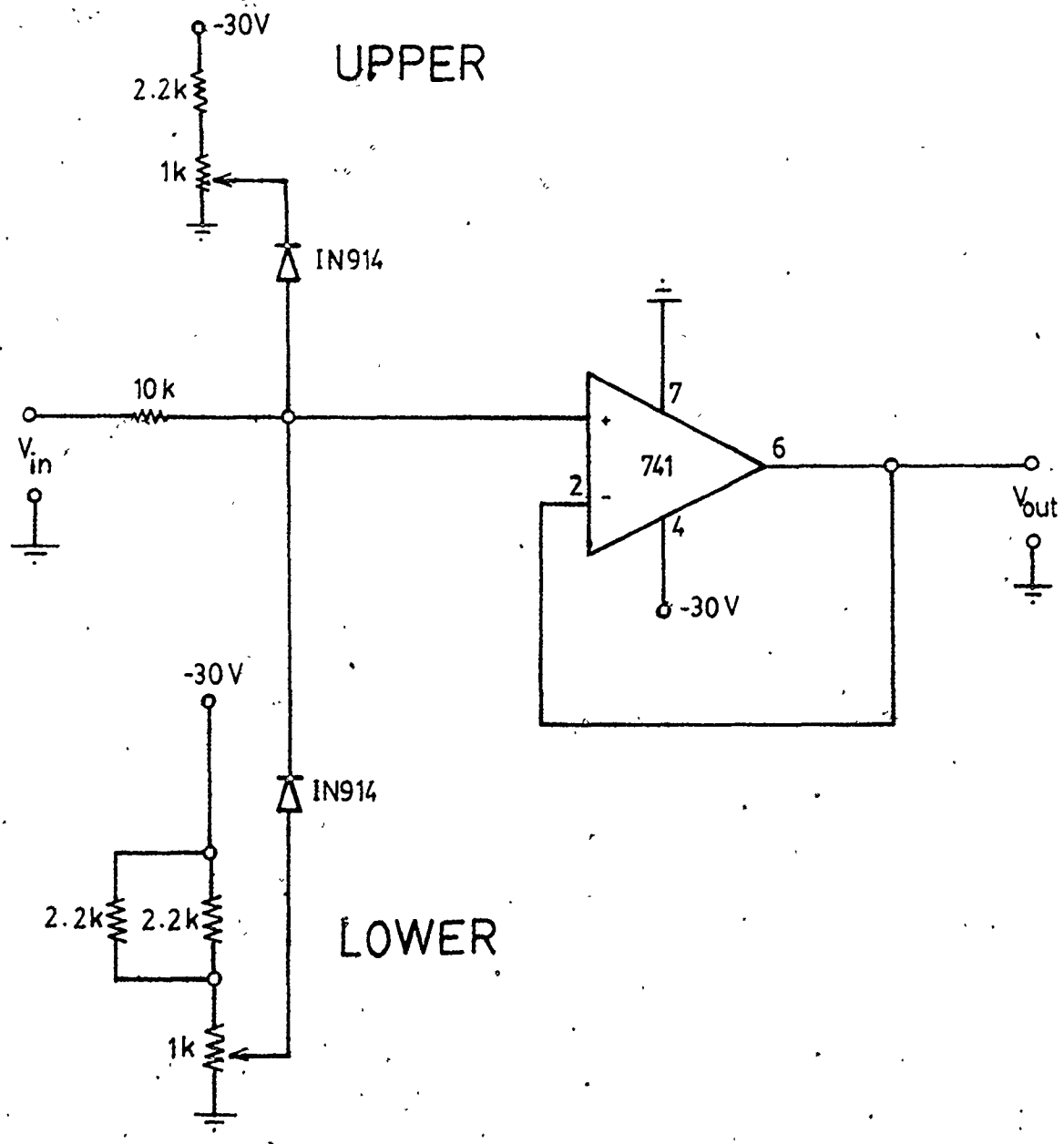

Figure 3.4 Clamp Circuit for Extruder Screw Speed

the schematic of the clamp circuit.

A measure of the extruder screw speed is also available to the computer. Calibration curves and procedures for all the measurements are presented in Appendix A. Operation ranges and normal operating levels are given in Table 3.1.

The computer is also able to control die heater power. When a relay is thrown, the die heater control switches from the PI controller to a Barbara Colman CB 41 single phase time proportioning controller whose input signal is from the computer.

The die produces cylindrical extrudate which drops into a cooling water bath. It is then dried in an air stream and then passed through the rollers of a take-up mechanism. The take-up mechanism is manufactured by Killian and uses a SECO 8504 motor control. At the time of this writing, the take-up mechanism and a thickness measurement device are being interfaced to the computer system. At the present moment, the take-up mechanism is run manually with no on-line indication of the thickness.

The polymers used in the experiments were donated by Union Carbide Co. of Canada. They are DNDY-2530, DFDY-6600 and DFDQ-4400 low density polyethylene. Table 3.2 lists their melt indices and densities.

Appendix C provides the startup and shutdown procedures for the extruder system.

TABLE 3.2

POLYETHYLENE POLYMER PROPERTIES

Polymer	Melt Index	Density
DFDQ 4400	2 g/min	917.5 kg/m^3
DFDY 6600	.03 g/min	920.0 kg/m^3
DNDY 2530	.17 g/min	920.0 kg/m^3

CHAPTER FOUR

STEADY STATE BEHAVIOR AND STEP TESTS

4.1 Steady State Behavior

Figure 4.1 (a) and (b) shows the steady state pressure behavior of the extruder for polymer DNDY extruded at approximately 50 r/min. This data was recorded in order to determine what type of disturbances are normally associated with the extruder. The extruder was preheated for over two hours and then run for almost an hour at the same operating point of 50 r/min to ensure steady state operation and to eliminate any effects of the startup. The disturbances in Figure 4.1 consist of oscillations at three different frequencies which are described in the following paragraphs.

Figure 4.2 presents the data of Figure 4.1 on an expanded time scale. This graph shows that the highest frequency oscillation has a period of approximately 1.2 s. The extruder operating screw speed of 50 r/min correlates with this frequency of noise.

As discussed in section 2.3, Tadmor and Klein(1978) indicate that a pressure transducer located at the tip of the screw would pick up a signal that is caused by the passing of the screw flight and is not part of the actual pressure measurement. The transducer is located at the screw tip (as described in section 3.2) and is therefore picking up a fluctuation due to the flight rotation. This fluctuation would not be measured by a transducer located in the die. Unfortunately, in the present extruder configuration, it is impossible to place the pressure

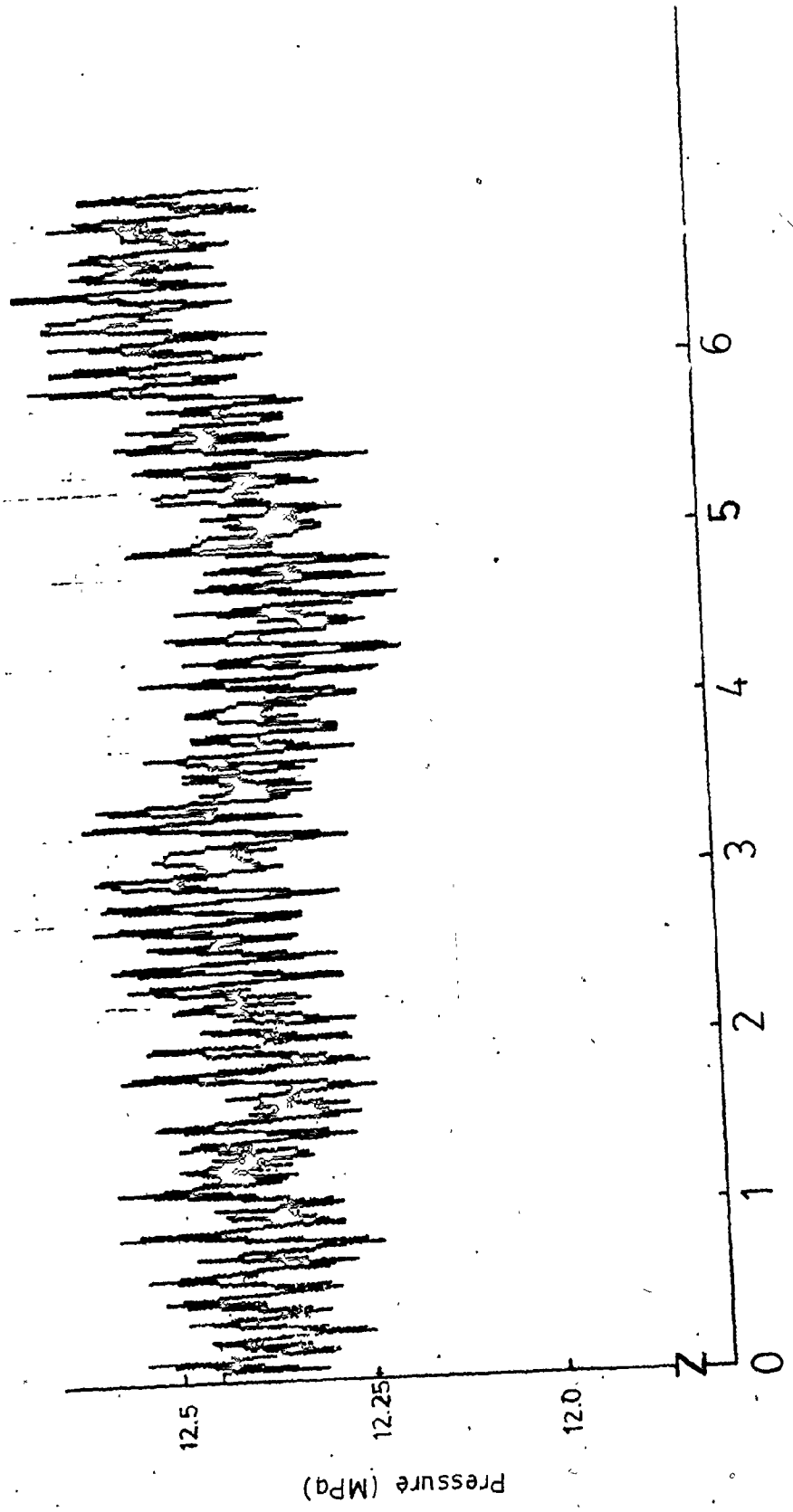

Figure 4.1(a) Extruder Steady State Melt Pressure Behavior

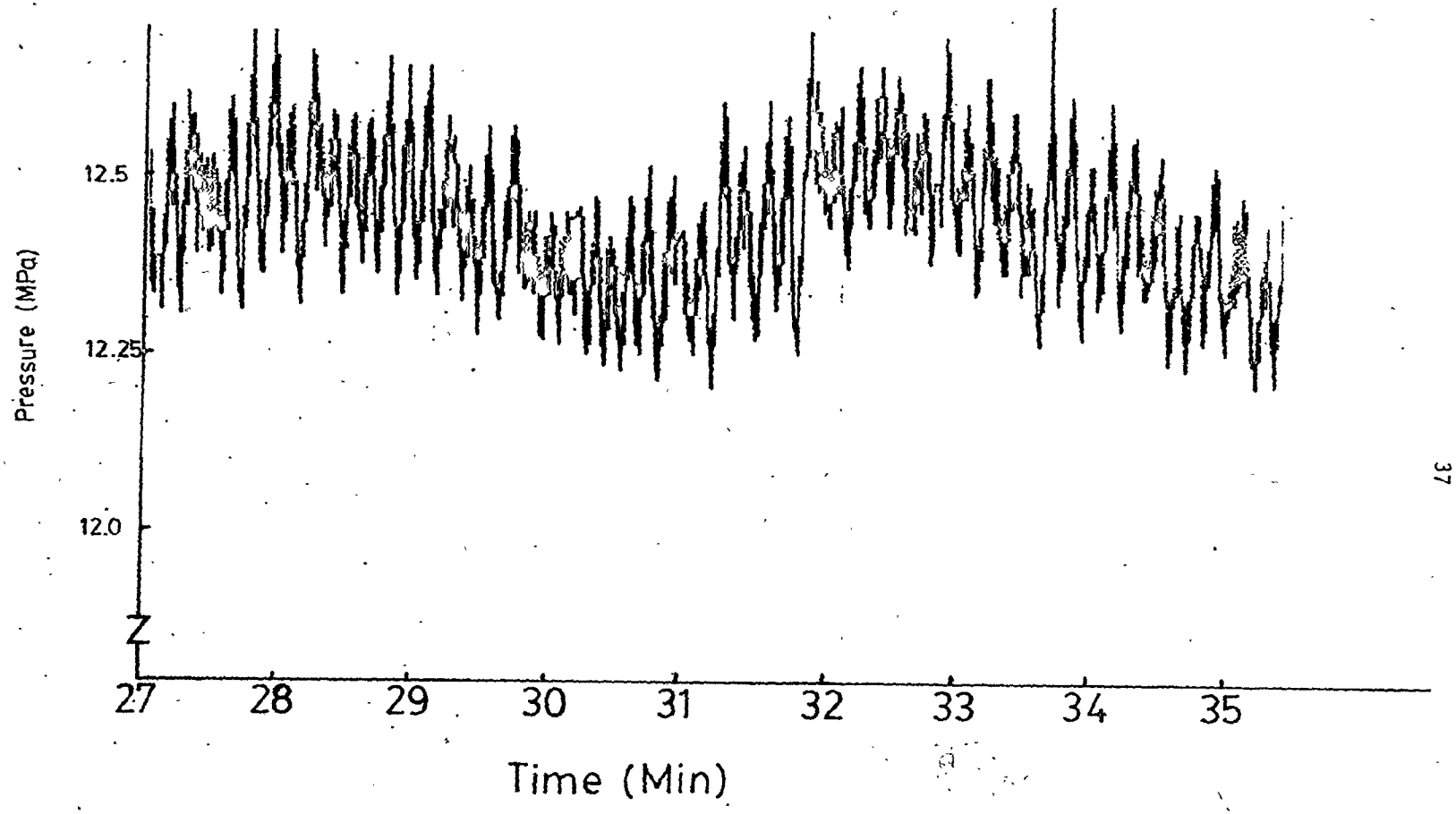

Figure 4.1 (b) Extruder Steady State Melt Pressure Behavior

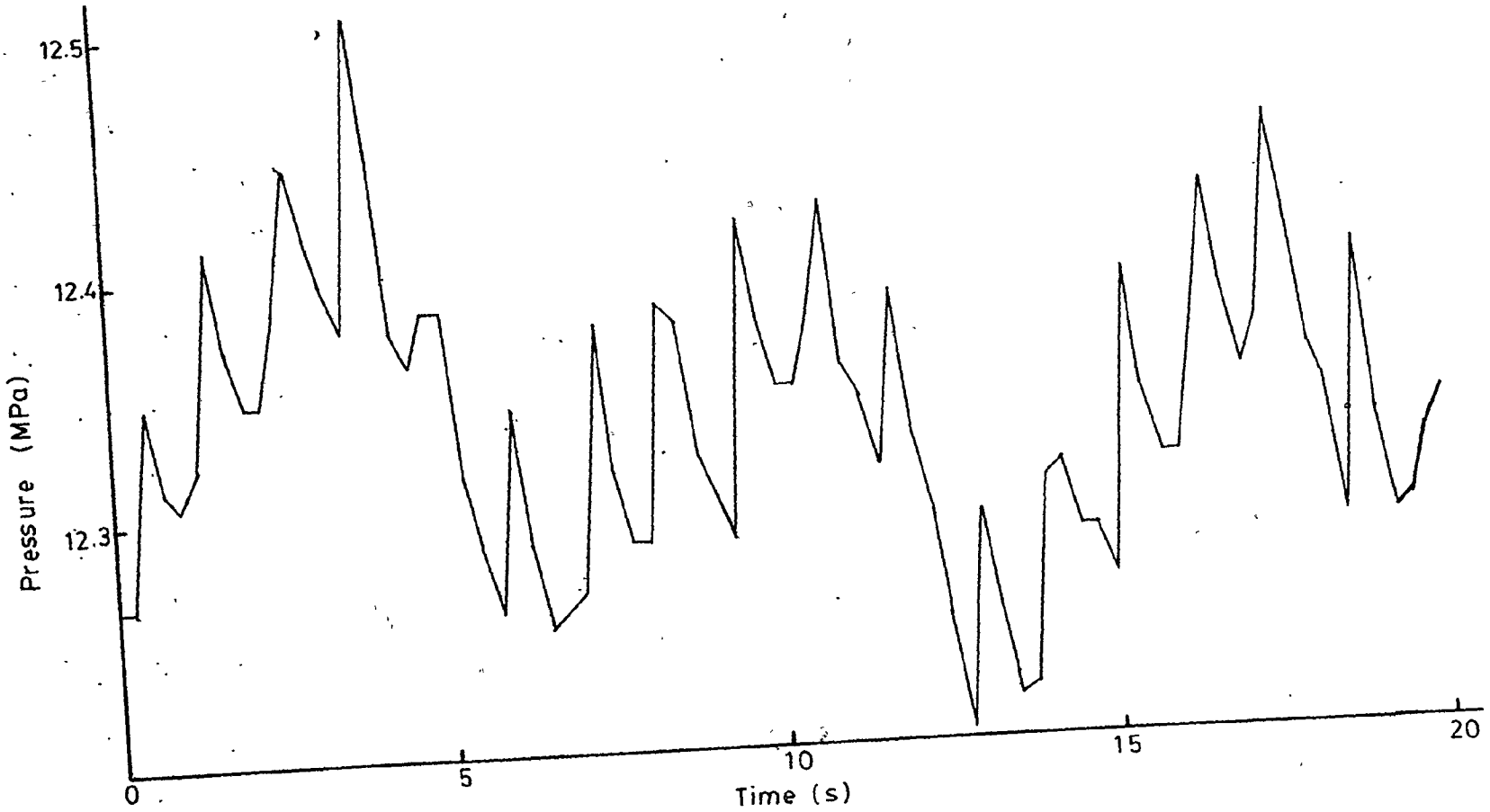

Figure 4.2 Extruder Steady State Melt Pressure Behavior, Expanded Time Scale

transducer in the adapter or the die, for this to be demonstrated. Chapter 5 and 6 will discuss various attempts to model and remove this signal.

Figure 4.3 shows the data of Figure 4.1 after it has been digitally filtered by a fourth order Butterworth low-pass filter with a cutoff frequency of 0.5 Hz. The filter removes the flight noise from the data and leaves a fluctuation in pressure with a period of approximately 8 s. These 8 s fluctuations are examples of the intermediate frequency pressure surges discussed in section 2.3. As was also mentioned in section 2.3, the period of the surging was found to be unaffected by the extruder screw speed or the type of polyethylene used. However, the amplitude of the disturbance was observed to depend on the operating region. This can be seen by comparing the data for step tests at different operating points (Figures 4.6 and 4.8) presented in the next section.

Finally there is a much longer term oscillation with a period of approximately 3.0 min. This is due to the cycling of the die temperature controller. Figure 4.4 shows the melt and the die temperatures for the same experiment as Figure 4.1. Originally it was thought that the problem was attributable to excessive tuning parameters on the analog PI controller. However, the die temperature cycled even with a detuned controller. Schott(1971) also reports problems with a cycling temperature controller. Figure 4.5 shows an experiment for polymer DFDQ at 50. r/min with the die controller turned off. There is still a small amount of cycling in both the melt temperature and the pressure. This is probably due to the cycling of

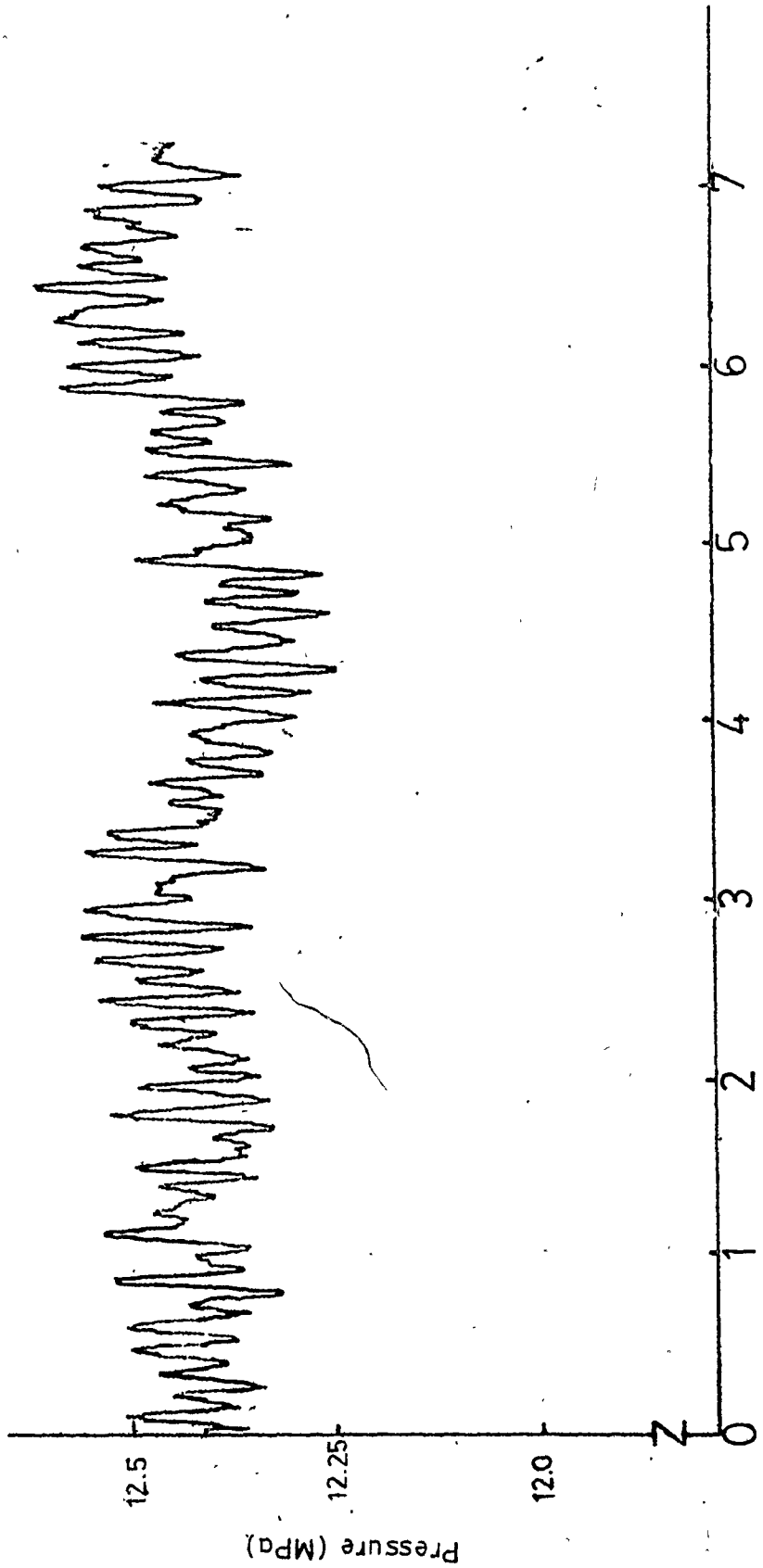

Figure 4.3 Extruder Steady State Melt Pressure Behavior, Low-Pass Filtered Data

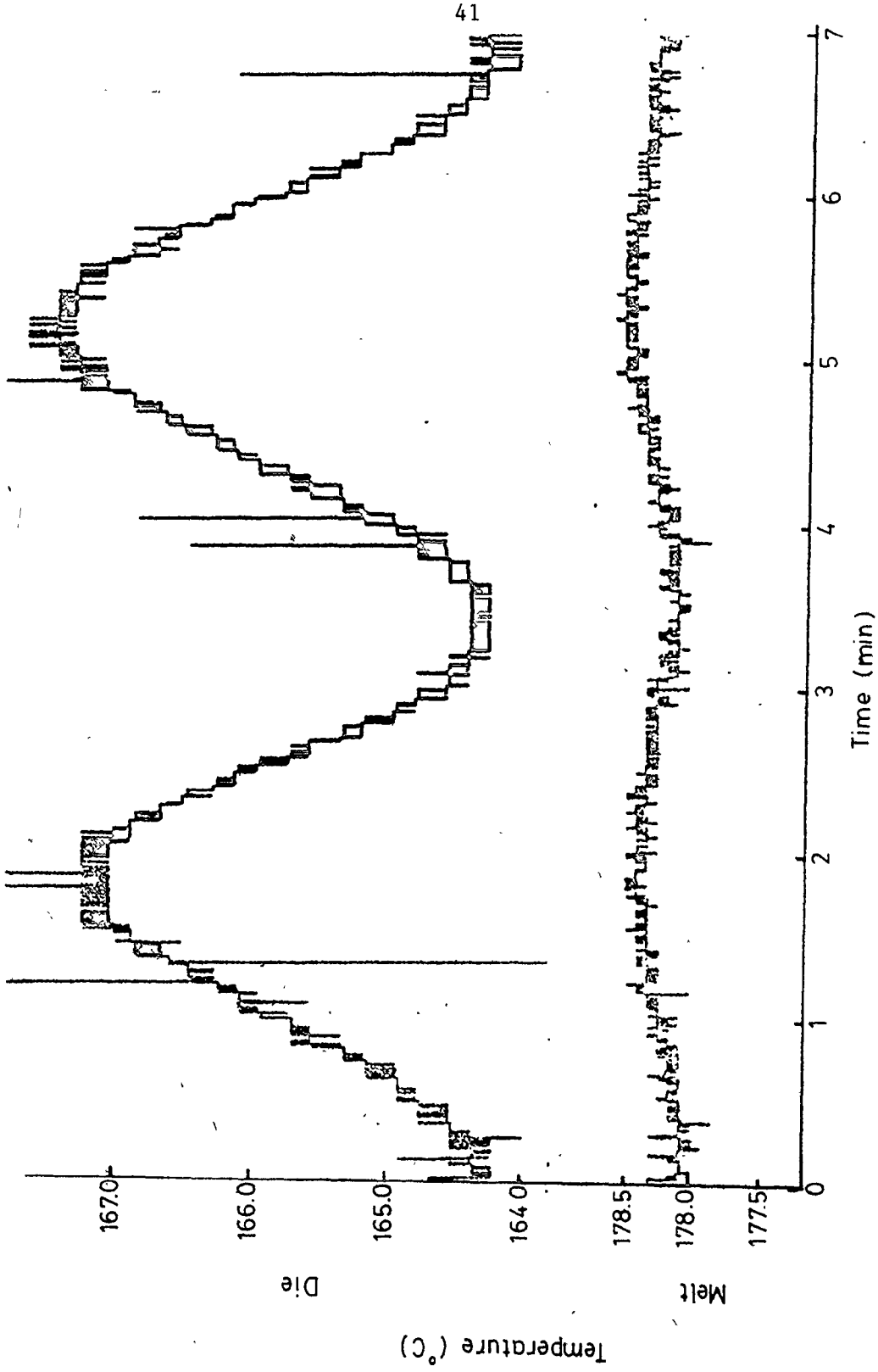

Figure 4.4 Die and Melt Temperatures Behavior

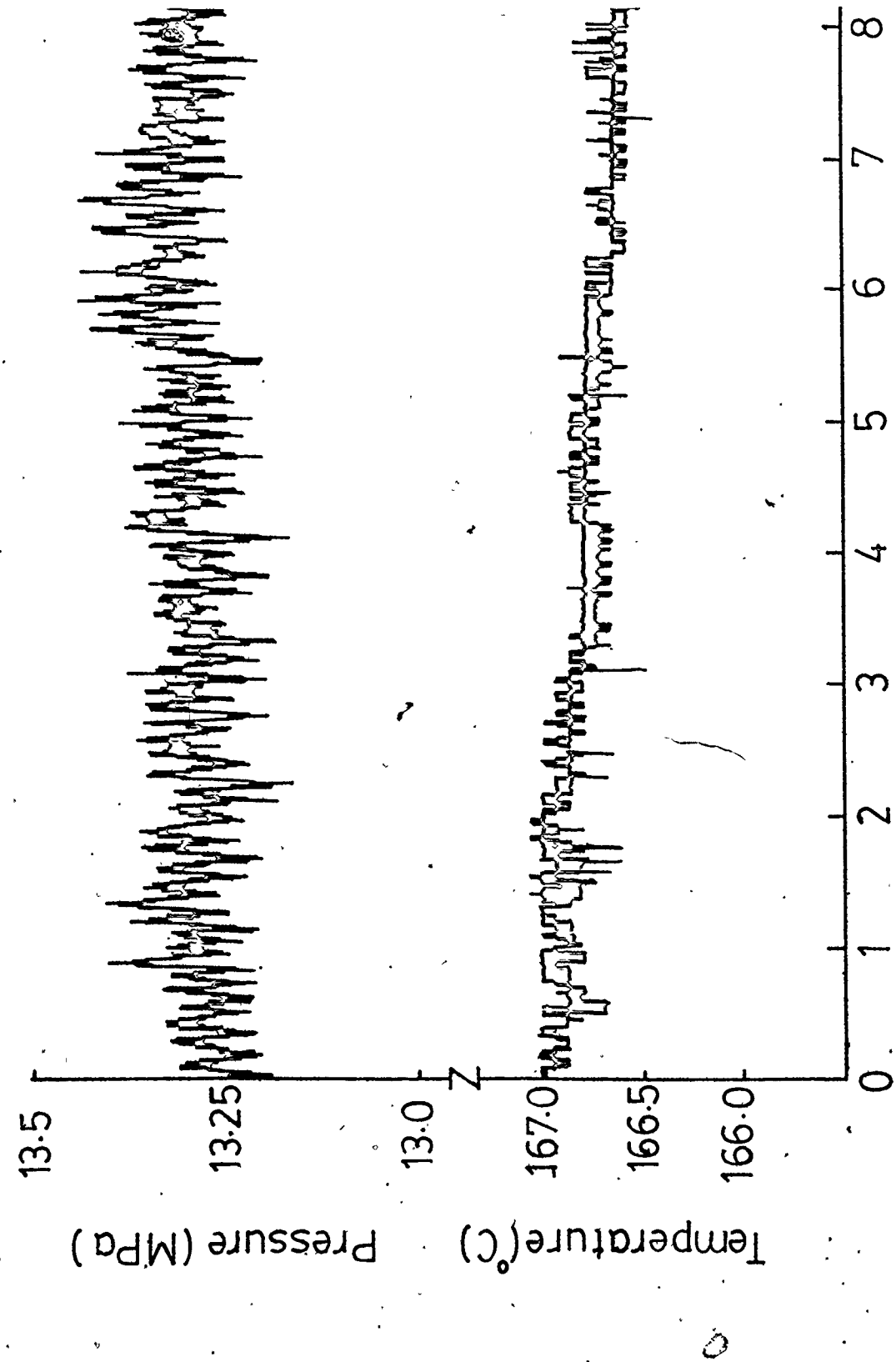

Figure 4.5 Steady State Melt Temperature and Pressure, No Die Temperature Controller

the barrel temperature controllers. There is a drift in the data due to the pressure and temperature not achieving steady state values. Without the die heater, the temperature decreases, and the pressure increases, as heat is removed from the die. These data were recorded after the die heater was off for approximately 20. min.

The melt temperatures shown in both Figures 4.4 and 4.5 show small deviations that appear to be at the same frequency as the 8 s pressure surging. This would be expected as the temperature and pressure are strongly interacting variables. The higher frequency temperature variations are due to quantization error in the temperature data read by the computer.

4.2 Step Tests

In order to estimate the process time constant and to determine the system linearity, numerous step tests were performed on the extruder. The step tests involve changes in the extruder screw speed. However, the actual manipulated variable is the signal from the computer sent to regulate the extruder motor power. The computer output signal is scaled between 0 and 100 to correspond to the extruder operating range of 0 to 100 r/min. This computer output is referred to as motor power (M.P.) throughout the rest of this thesis.

Figures 4.6 and 4.7 show a step change of 8. motor power (M.P.) (52 to 60 M.P.) for DNDY polymer. The screw speed change was approximately 9. r/min (49 to 58 r/min). There is a rapid pressure response (Figure 4.6) but no significant decay in pressure is seen as the temperature settles (Figure 4.7). The pressure response appears to be completed in one

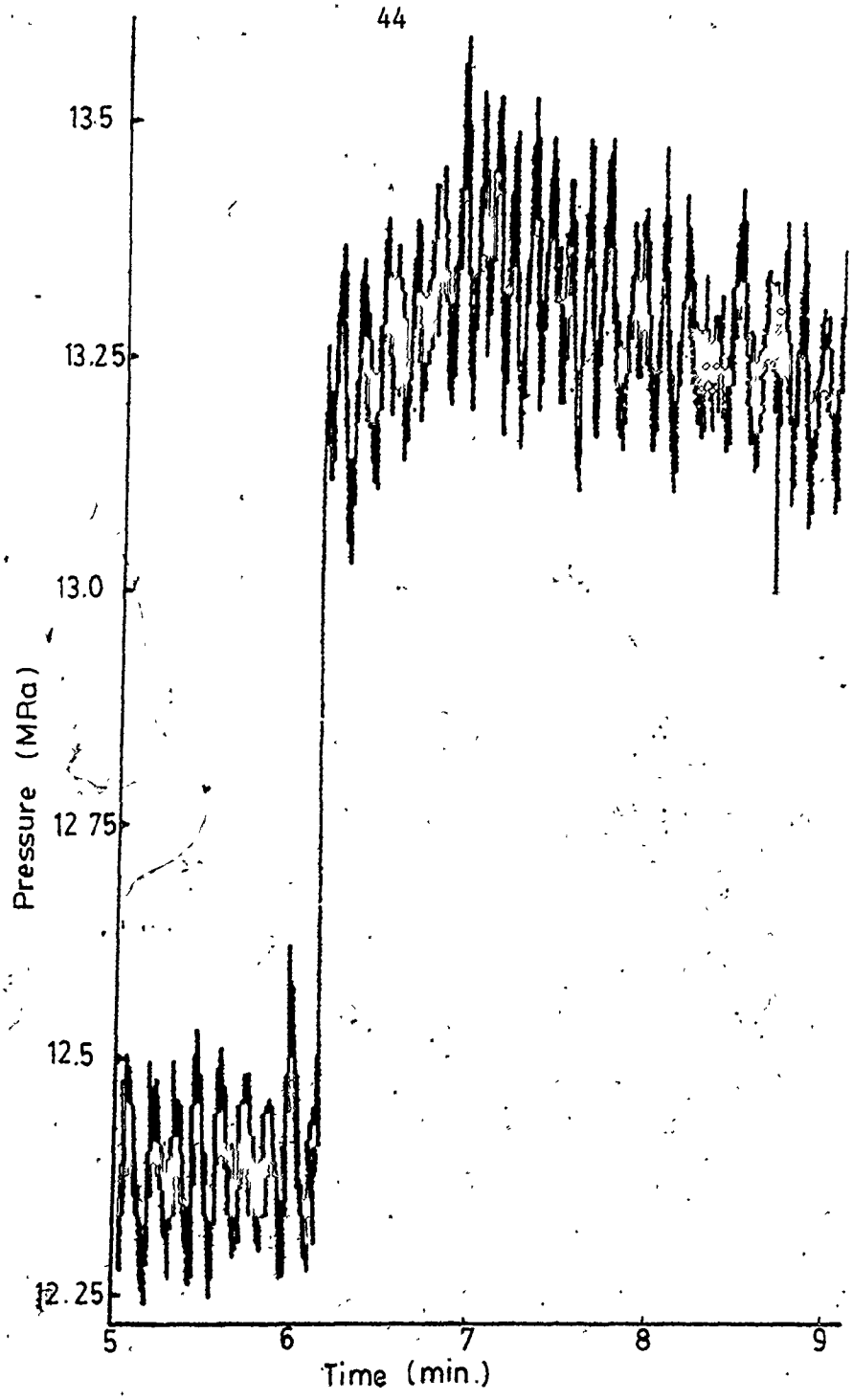

Figure 4.6 Pressure Response, Step in Motor Power 52 to 60 M.P., 49 to 58 r/min

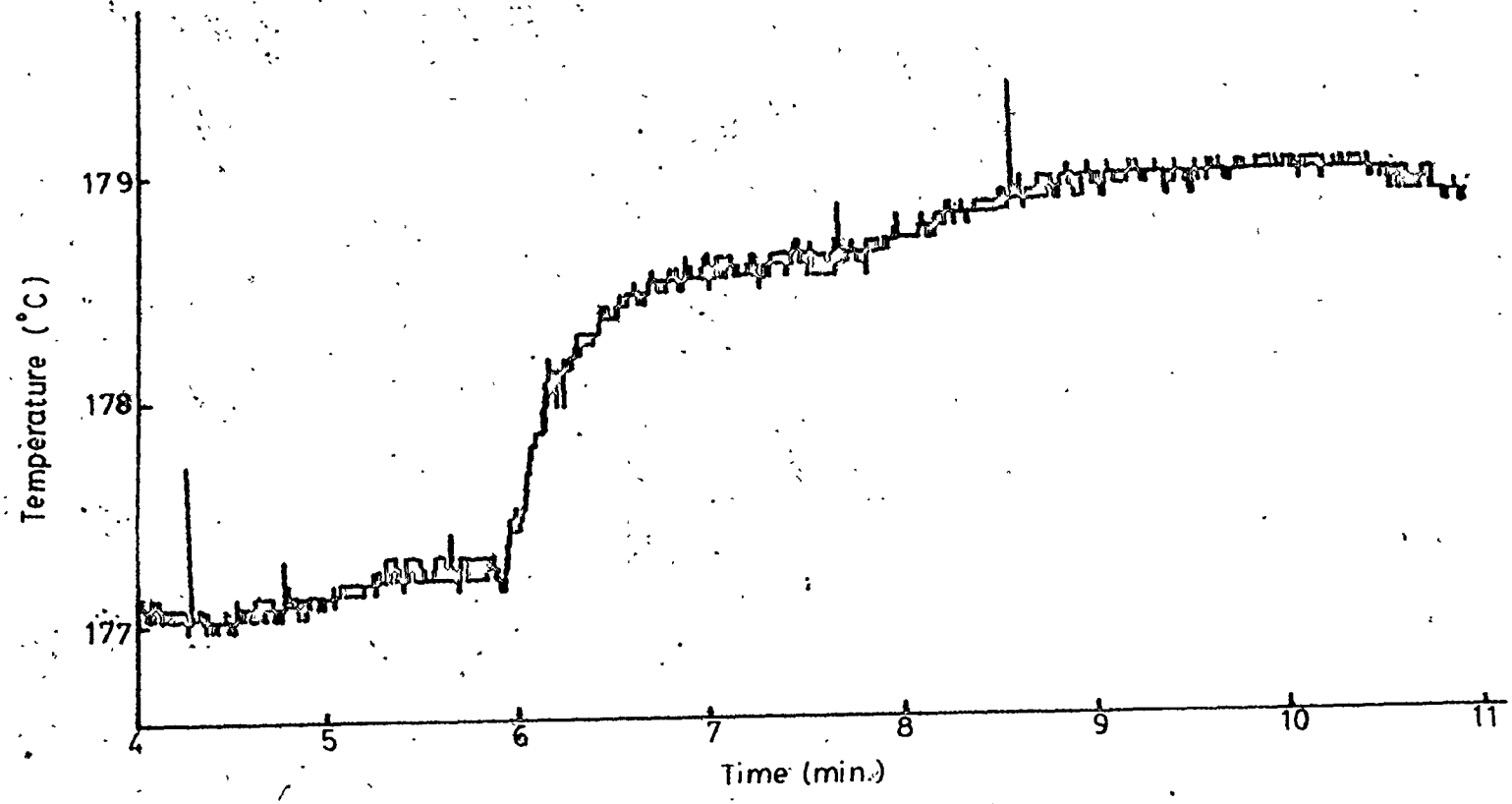

Figure 4.7 Melt Temperature Response, Step in Motor Power 52 to 60 M.P., 49 to 58 r/min

sampling interval. The time constant can be estimated as 0.2 s for pressure and 20 s for temperature, with gains, estimated by averaging the steady state values, of 110 kPa/M.P. and 0.28°C/M.P. The transfer functions are presented by equations (4.1)and (4.2):

$$P(s) = \frac{110.\ kPa/M.P.}{0.2s + 1} \quad U(s) \tag{4.1}$$

$$T(s) = \frac{0.28\ °C/M.P.}{20.s + 1} \quad U(s) \tag{4.2}$$

The data of Figures 4.6 and 4.7 are also presented in Appendix D over a much longer time period.

Figure 4.8 shows a similar step of 74 to 80 in motor power. Here the gains are reduced to 76. kPa/M.P. and 0.19°C/M.P. for pressure and temperature respectively. The screw speed changed approximately 6.5 r/min. The transfer functions for this case are presented in equations (4.3) and (4.4):

$$P(s) = \frac{76.\ kPa/M.P.}{0.25\,s + 1} \quad U(s) \tag{4.3}$$

$$T(s) = \frac{0.19°C/M.P.}{15\ s + 1} \quad U(s) \tag{4.4}$$

Another step test was taken from 80 to 86 motor power. This has a gain of 32. kPa/M.P. and 0.09°C/M.P. for pressure and temperature respectively. However the screw speed change was only 4.5 r/min. This region of operation is close to the point where the upper clamp was set. This probably restricted the size of the step. However, correcting

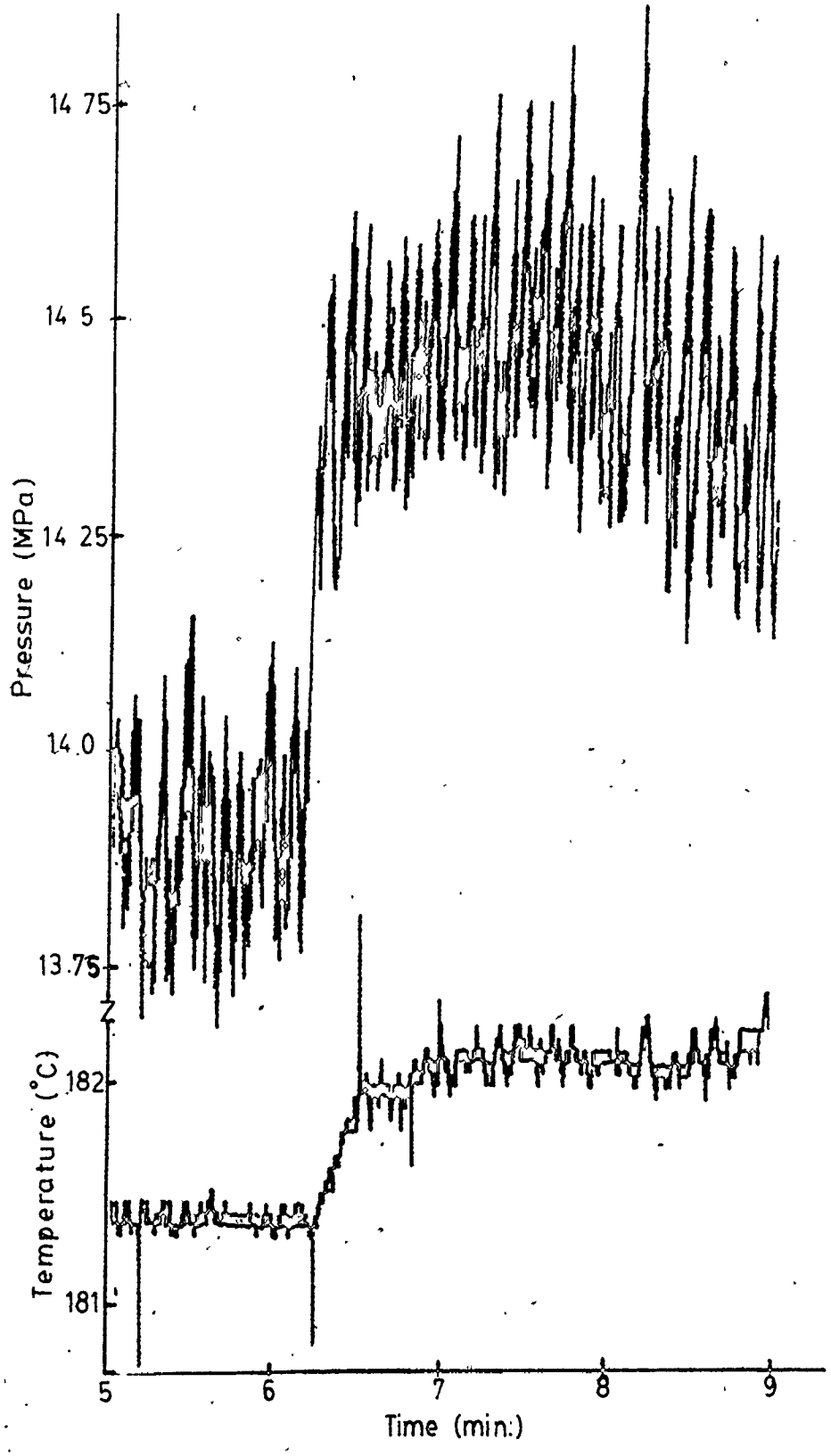

Figure 4.8 Melt Temperature and Pressure Response,
Step in Motor Power 74 to 80 M.P., 73 to 79.5 r/min

the gain for the reduced step (multiple by 6/4.5) still yields reduced gains when compared to transfer functions (4.3) and (4.4).

Observing the response of the temperature to screw speed steps, in Figures 4.7 and 4.8 and in Appendix D, shows that the mean temperature has moved to a new level. The die temperature controller is unable to maintain the melt temperature at a mean level in the face of screw speed disturbances. This phenomenon will be discussed further when the effect of closed loop control on the melt temperature is examined in Chapter 6.

Figures 4.9 and 4.10 show the linearity of pressure and melt temperature for motor power steps of ±2, ±4, ±6 and ±8 for polymer DFDQ at a mean operating level of approximately 50. r/min. These values were determined by averaging the results obtained after the responses reached steady state. Both figures indicate that the gains, 98. kPa/M.P. for pressure and 0.2°C/M.P. for temperature, are linear within this region. This is consistent with similar figures presented by Kochhar and Parnaby(1977).

The midpoint of the extruder screw speed operation is quite linear, however, this linear region becomes reduced as one reaches the upper levels of operation. As discussed previously, a step from 74. to 80. M.P. has gains of 76. kPa/M.P. and 0.19°C/M.P. whereas a step from 80. to 86. M.P. has a gain of 32. kPa/M.P. and 0.09°C/M.P. The change is quite significant for this short range of operation. Therefore, not only would any controller parameters determined for midrange operation have to be modified for operation at upper levels but this nonlinearity

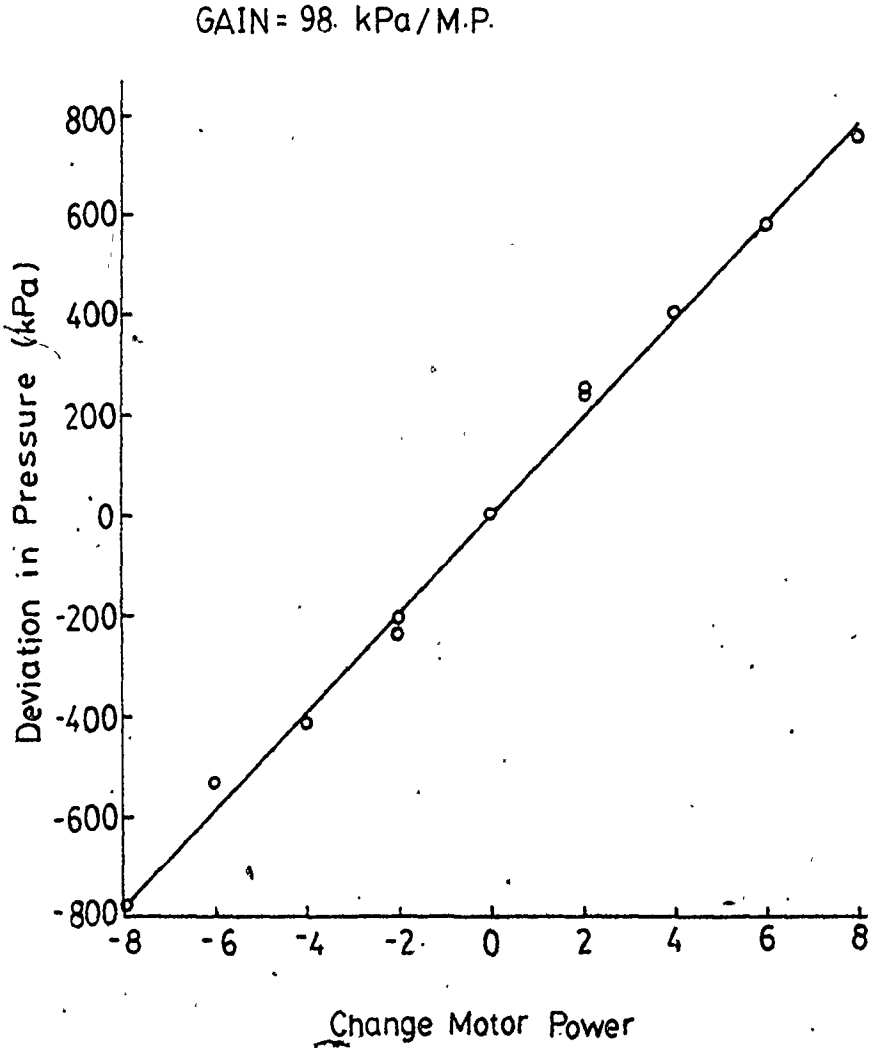

Figure 4.9 Linearity of Pressure Gain for Steps in Motor Power

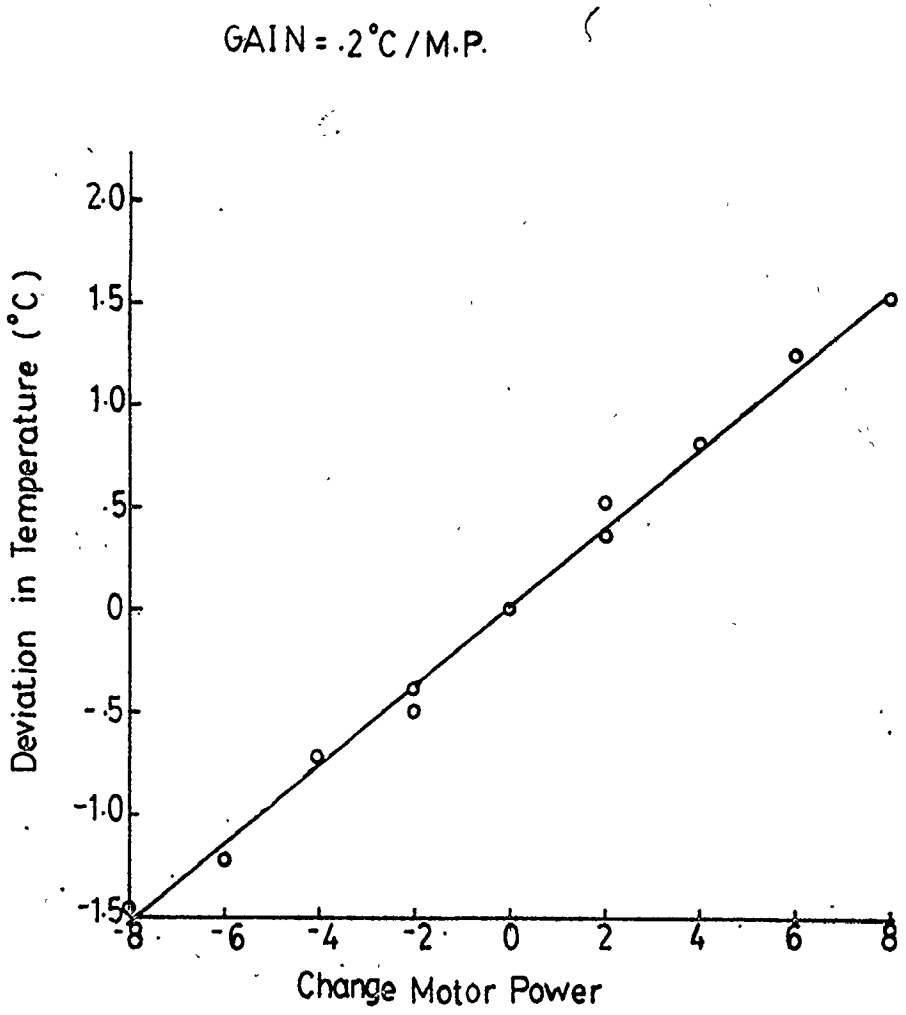

Figure 4.10 Linearity of Melt Temperature Gain for Steps in Motor Power

in this upper level of operation, will necessitate detuned controllers in order to maintain system stability. Changing the polymer quality might also necessitate retuning the controllers.

Because commercial polymers may have varying characteristics from batch to batch, or even within different bags of the same batch, it was decided to study the effect of polymer quality on the extruder performance. As a gross approximation to this phenomenon of varying quality, a step change in polymer feed type was introduced to the extruder. Figure 4.11 shows the results of a change from DFDQ to DFDY polymers. As can be seen in Table 3.1, the melt indices of the two polymers are very different, resulting in a very large disturbance. The pressure increased from 10.1 MPa to 15.7 MPa with a corresponding temperature increase of 5°C. By contrast a typical change of 8. in motor power with DFDQ will yield 1.0 MPa and 1.6°C changes. The shape of the disturbance response appears to be second order, as was also observed by Schott(1971) in similar experiments already described in section 2.1.

Performing the step in polymer type with two polymers with smaller property differences, will yield a similar shaped response. However, the magnitude of the changes in temperature and pressure will be reduced. Disturbances of this type can be seen under closed loop control in Chapters 6 and 7.

The experimental results presented in this Chapter match the previous experimental results, reviewed in section 2.1, in a quantitative sense. The only exception is the response of the pressure as the temperature increased during a step in screw speed. Fingerle(1978) and

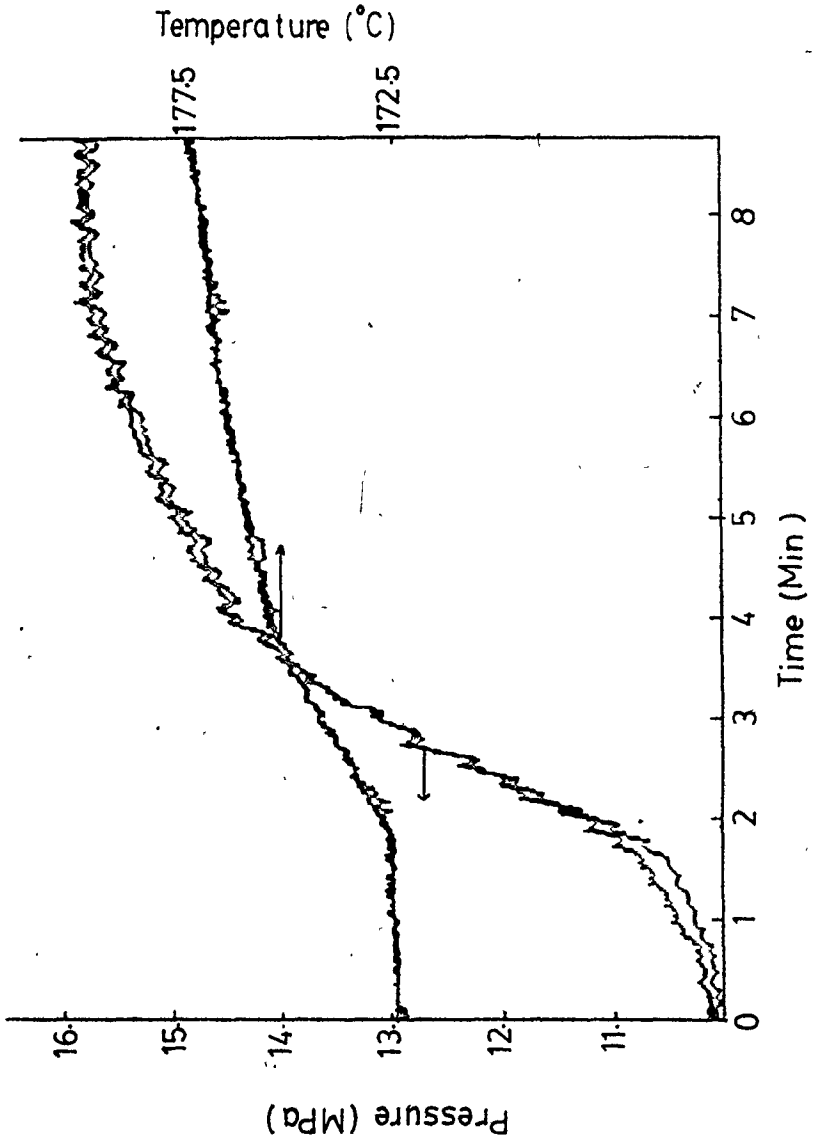

Figure 4.11 Melt Temperature and Pressure Response to a Change in Polymer Feed Quality

Fontaine(1975) reported that the pressure drifted downward as the temperature increased. This drift was not observed in the steps presented here, however, it is possible that a small downward drift was masked by the large pressure surges. In general, variations in the mean level of the pressure were observed as the melt temperature changed, especially during startup conditions.

The step test experiments match the simulation results of Tadmor et al(1974), discussed in section 2.3, except that the simulation temperature response has an overshoot and the experimental pressure response does not drift downward as the temperature increases. The simulation results of Brauner et al(1976) do not resemble the experimental change in polymer quality. The simulation shows a sharp change in pressure at the die when the new polymer reaches that section of the extruder, as opposed to the second order response observed here. It seems that the simulation does not account for any mixing of the polymers in the hopper or as they melt in the extruder. This possibly can account for the discrepancy between the model and the experiments.

In summary, this chapter shows step tests and steady state experiments performed on the extruder. The disturbances of the melt pressure were found to consist of long term oscillations of 3.0 min periods and a pressure surging of 0.125 Hz frequency. A signal noise at the same frequency as the screw speed was also observed. The dynamic model relating pressure to steps in extruder motor power was found to be first order with a time constant of approximately 0.2 s. The dynamic model relating melt temperature to steps in motor power was also found to be first order but with a time constant of approximately 20. s.

CHAPTER 5

TIME SERIES MODELLING

In the previous chapter it was shown that the transfer function for screw speed to pressure can be modelled adequately by a first order model with a very small time constant. Looking at a response such as Figure 4.7 one can see that the disturbances caused by the pressure surging can be almost as large as those caused by a step of 6 M.P. in the motor power. The data of Figures 4.1 and 4.6 also show significant pressure variations. When the process disturbances are such a large part of the overall process behavior, it is very important, that they be modelled. One can then determine the most effective control strategy that can eliminate these disturbances.

A serious defect in classical modelling techniques is that the noise is neglected. Both Fontaine(1975) and Wright(1978), as discussed in section 2.1, observed large pressure fluctuations, however, both chose to ignore this information. Fontaine modelled only the long term pressure level and Wright performed setpoint changes in desired screw speed without attempting to regulate the pressure.

The time series modelling approach, already introduced in section 2.2, models both a transfer function and a noise model. The noise model can then be used to predict the next value of the disturbance allowing for improved control. However, when one performs time series modelling, one must remember to use the knowledge obtained about the system from the steady state runs and step tests. This ensures that one arrives at a practical model of the process. Sometimes, it is possible to obtain

many models of the process with comparable fits (especially if one fits with a small amount of data). Selecting the best form of the model will depend on one's knowledge of the system. This was the major difficulty with the models presented by Kochhar and Parnaby (1977).

A PRBS (pseudo-random binary sequence described in section 2.2) was input to the extruder at 0.5 s intervals. The extruder produced DNDY polymer at a mean level of approximately 49. r/min with the motor power alternating by ±1 about the mean value. The implementation rate of 0.5 s was selected so that a reasonable extruder dynamic model could be determined without unduly straining the extruder motor. The PRBS test rate should also be the same as the planned control frequency. This eliminates the need to convert the model to a different sampling frequency when calculating the controller (see MacGregor(1976) for the conversion method). The system was sampled at 4.0 Hz so that the flight noise could be identified more accurately.

The data were modelled by equation (5.1)

$$\nabla_s P_t = \frac{\omega_0(1 - \omega_s Z^{-s} - \omega_{s+1} Z^{-s-1})}{1 - \delta Z^{-1}} U_{t-1} + \frac{(1 - \theta_1 Z^{-1} - \theta_2 Z^{-2})}{(1 - \phi_1 Z^{-1} - \phi_2 Z^{-2})} a_t \quad (5.1)$$

where the parameters and their 95% confidence bands are

ω_0 = 70.7 ± 3.4 kPa/motor power

ω_s = 0.711 ± 0.064

ω_{s+1} = 0.521 ± 0.065

δ = 0.281 ± 0.039

θ_1 = 1.134 ± 0.154

θ_2 = -0.295 ± 0.163

ϕ_1 = 1.722 ± 0.079

ϕ_2 = -0.869 ± 0.079

∇_s = $1 - Z^{-s}$

s = $60./TACH_t/T_s$

T_s = sampling time = 0.5 seconds.

The block diagram of (5.1) is given by Figure 5.1.

This model can be examined term by term to determine the physical significance of the equation. The flight noise has a period solely dependent on the screw speed. This period would be calculated as $(60./TACH_t)$ seconds. This noise can be modelled as a seasonal non-stationarity denoted by a $(1 - Z^{-s})$ term in the denominator of the noise model where s is the number of lags corresponding to the period of the noise. Because in this case, s is a non-integer value, this term was physically implemented by linearly interpolating between the sampled data which are available 0.25 seconds apart. The operator $(1 - \omega_s Z^{-s} - \omega_{s+1} Z^{-s-1})$ was used to approximate the ∇_s operator acting on the input series. The term $(\omega_s Z^{-s} + \omega_{s+1} Z^{-s-1})$ weights the input signals between values at s lags and s+1 lags, acting like a linear interpolation. A surprising result was that the sum $(\omega_s + \omega_{s+1}) = 1.232$, a value significantly higher than the expected value of 1.0 (1.0 is not included in the 95% confidence limits calculated by the maximum likelihood parameter fixing program). The replacement of ω_{s+1} by $(1 - \omega_s)$ caused a significant degradation in the fit of the model. This is probably due to some small inaccuracies in the noise model which are partially compensated by ω_s and ω_{s+1}.

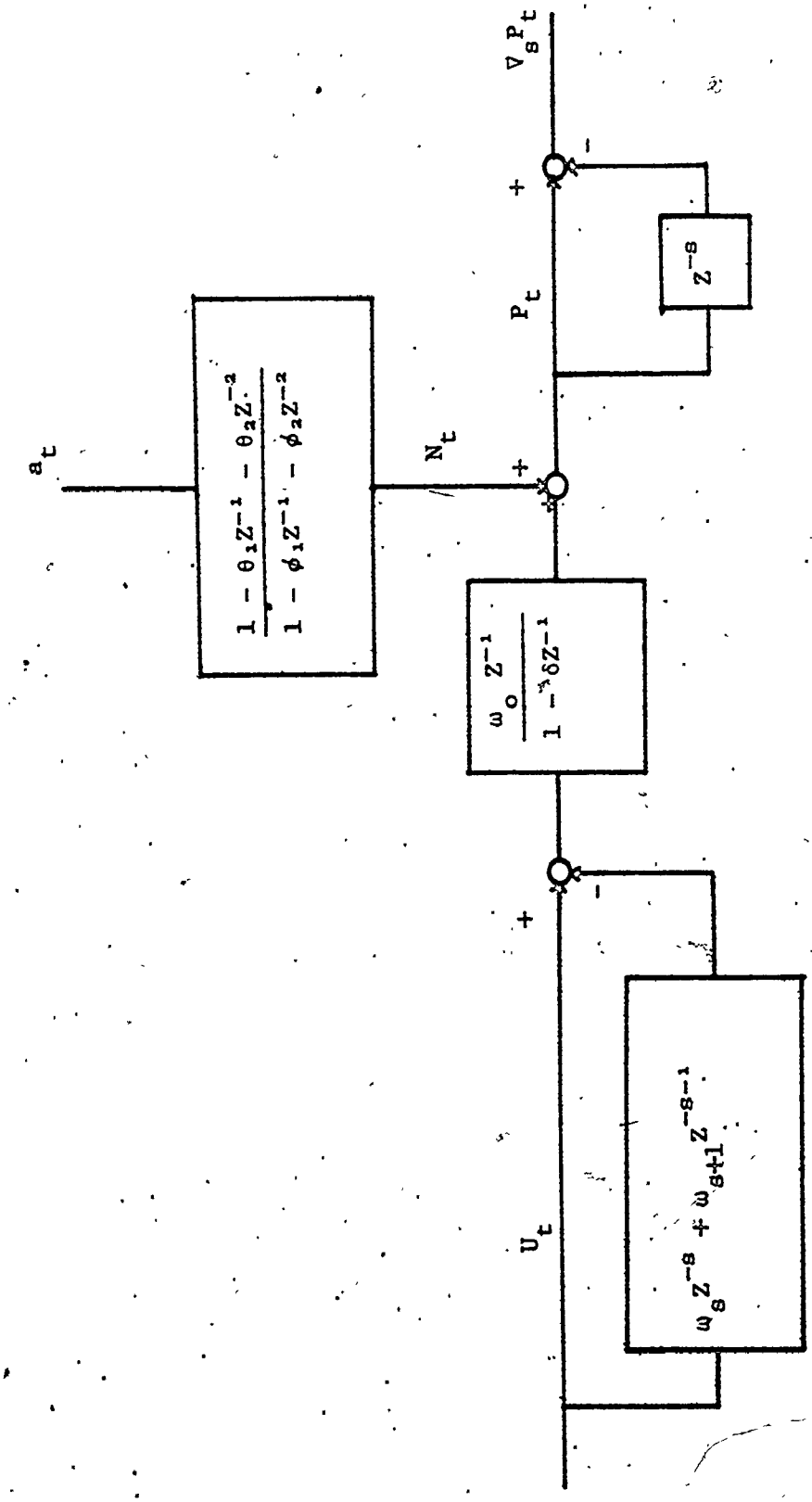

Figure 5.1 Block Diagram of Model

Box and Jenkins(1976) give equations relating the transfer function model to the continuous system. The system time constant is given by:

$$\zeta/T_s = -1/\ln\delta$$

For the values in equation (5.1), ζ = 0.39 seconds. The process gain is given by replacing Z^{-1} by one in the transfer function giving g = 121. kPa/M.P. The terms $(1 - \omega_s Z^{-1} - \omega_{s+1} Z^{-s-1})$ are neglected in this calculation because they are cancelling the ∇_s term, part of the noise.

The noise model is on ARMA(2,2) (second order in both denominator and numerator of the noise model). An AR(2) (second order in the denominator) will model damped sinusoidal behavior when its roots are imaginary $(\phi_1^2 + 4\phi_2 < 0)$ as is the case for equation (5.1). Box and Jenkins give the frequency and damping factors as:

$$d = \sqrt{-\phi_2}$$

$$f_0 = 2\pi T_s \cos^{-1}\left(\frac{|\phi_1|}{2\sqrt{\phi_2}}\right)$$

For (5.1) the damping factor is 0.93 and the frequency is 0.125 cycles/sec (period of 8.0 sec).

The time series modelling matches well with the parameters for the gain (121. kPa/M.P. versus 110. kPa/M.P.), time constant (0.39 s versus 0.2 s) and surging period (8. s for both) approximated from the steady state and step test analysis given in Chapter 4. This is convincing evidence of the good fit for the data determined by this model.

Figure 5.2 shows the actual data used (0.5 s apart) versus the one step ahead prediction values. Model (5.1) was developed using only the first 250 data points of Figure 5.2. For the last 250 values, the model is predicting values that were not used to fit the model. Besides the first 25 or so points, while the routine is initialized, the model predicts the data well.

In summary, this chapter presents a time series model relating the extruder pressure to the motor power. The model identifies the system time constant and the frequencies of the major system disturbances very accurately. The extruder model is an improvement over the previous models presented in the literature.

FIGURE 5.2 ONE STEP AHEAD PRESSURE FORECAST

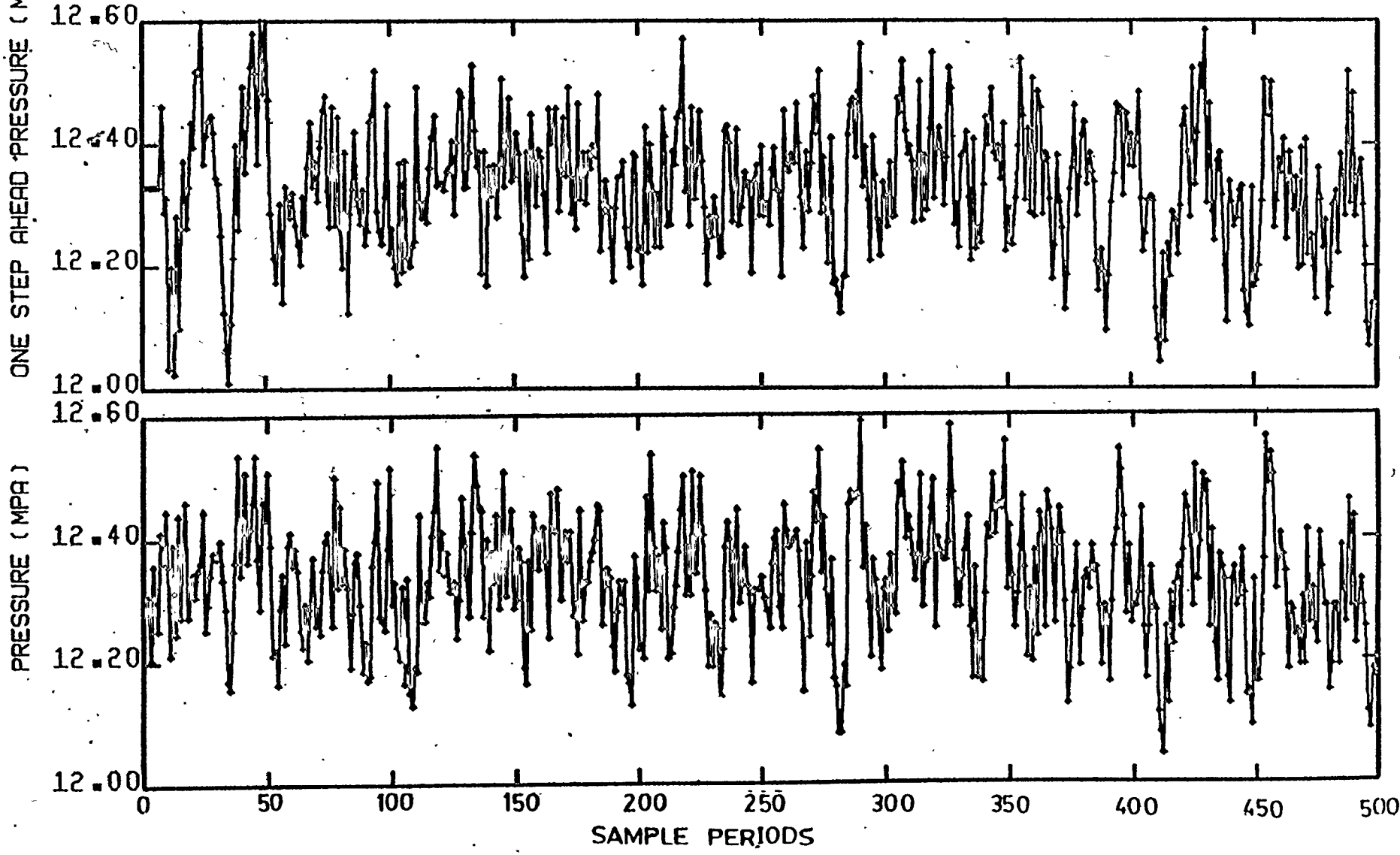

CHAPTER 6

PROCESS CONTROL USING A DIGITAL PI ALGORITHM

6.0 Introduction

As discussed in Chapter Two, there have been many attempts to construct dynamic models between melt pressure output and screw speed manipulations input. However, none of the authors test their models or control schemes by attempting to regulate an actual extruder. Dormeier(1980) does briefly describe an analog control system similar to the analog pressure controller on the extruder used in the experiments for this thesis. However, all other authors stopped at the modelling stage and did not implement their recommended control schemes.

The previous two chapters discussed the modelling of the extrusion process. In particular, the most significant noise was divided into two categories. The first category consisted of a pressure surging with an 8 s period due to the breakup of the extruder solid zone. The second category was a signal noise caused by the screw flight passing the tip of the pressure transducer. This chapter describes the first attempt to control an extruder for pressure surging while the pressure signal is affected by flight noise.

The first experiment in this chapter implements a digital PI controller on the extruder. This is compared to later experiments which use the PI algorithm in combination with various digital filters. The digital filters are used in an attempt to improve the control by removing the signal noise.

The various filters considered are: the low-pass filter, filters derived from seasonal time series models, the bandstop filter and a filter formed from a transfer function that combines two poles and two zeroes to make a simple bandstop filter.

6.1 PI Controller and Unfiltered Pressure Data

The first control algorithm applied on the extruder was the digital PI algorithm. This was used as a base case for comparison to the other control schemes tested in this thesis. It was originally intended to use the analog pressure controller to provide this base case. Unfortunately, the analog pressure controller could not be used for control purposes due to a malfunction. However, digital and analog controllers often give comparable results making the digital PI a reasonable second choice for the base case. The algorithm implemented was the velocity form of the digital PI algorithm, equation (6.1) (Smith(1972)).

$$\nabla U_t = K_c((e_n - e_{n-1}) + T_s/T_I \; e_n)$$

$$\text{where} \quad e_n = P_{set} - P_t \qquad (6.1)$$

$$\text{and} \quad \nabla = \text{The difference operator } (1-Z^{-1})$$

The tuning parameters K_c and T_I were tuned on-line by trial and error.

Figure 6.1 (a) and (b) shows a typical example of the control action and pressure response of a digital PI controller applied on the extruder. No control was taken during the first five minutes. The PI controller was then started with initial tuning parameters, $K_c = 5.8 \times 10^{-3}$ M.P./kPa and $T_I = 1.$ s. The control and sampling rates were kept constant at 2 Hz throughout the experiment. The controller was then tuned for elimination of the 8 second surging with the final

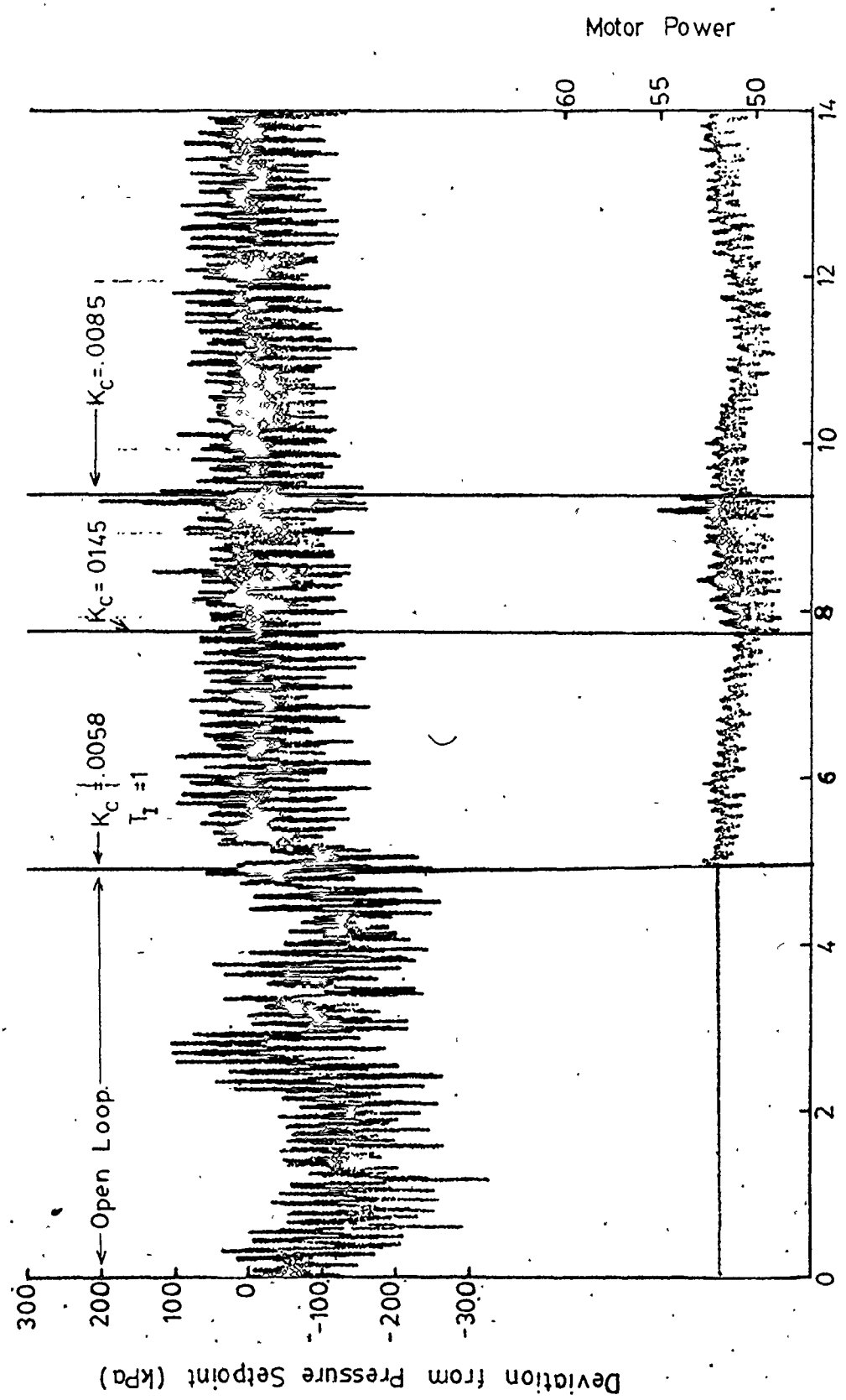

Figure 6.1 (a) Digital PI Control of Pressure

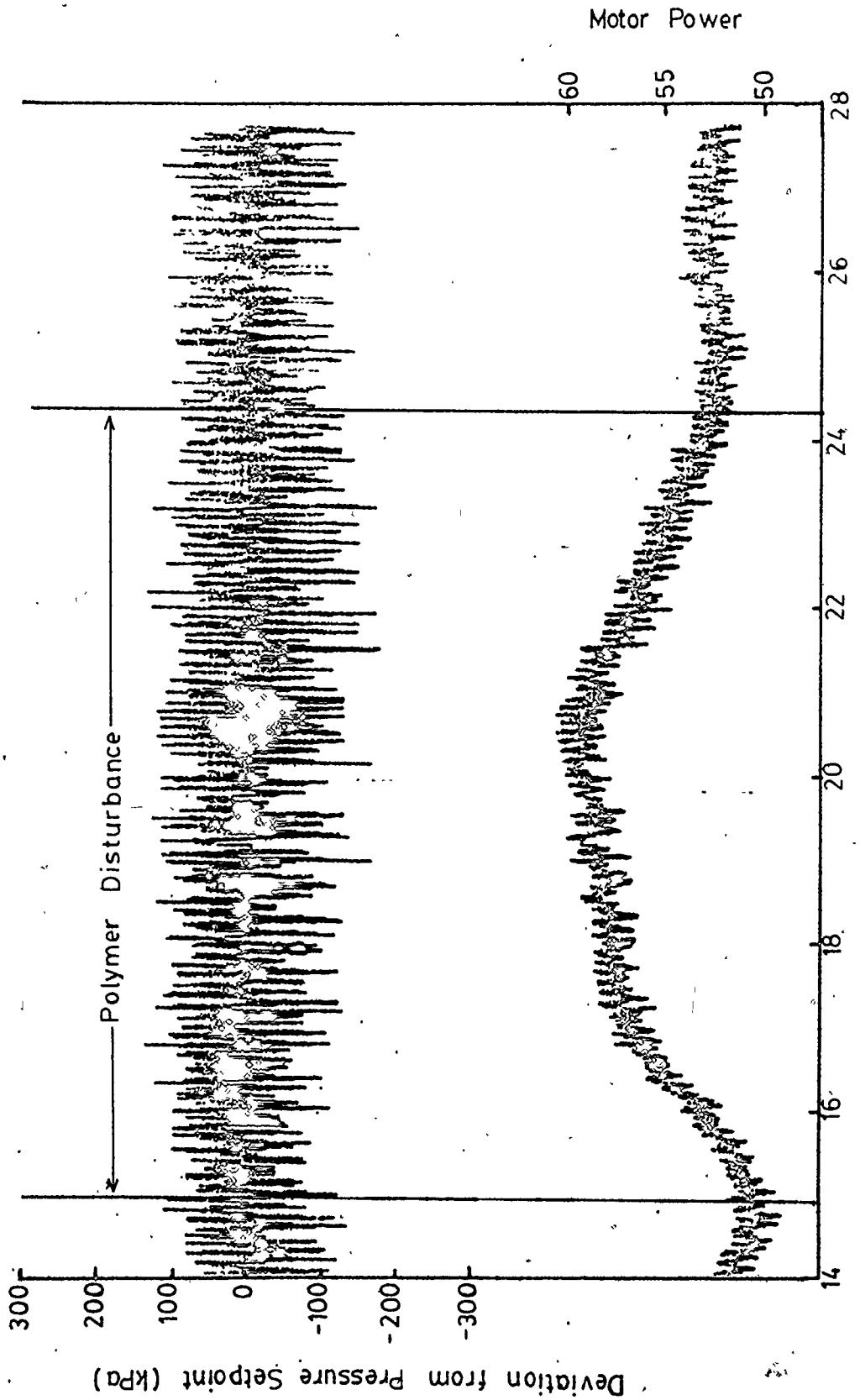

Figure 6.1 (b) Digital PI Control of Pressure

control parameters selected as K_c = 8.7 x 10^{-3} M.P./kPa and T_I = 1. s. The tuning in other similar runs varied. The parameter values varied as much as ±100% about those selected for this experiment, showing some drift in the process.

The algorithm is then tested for its effectiveness in the face of both the pressure surges and a disturbance in product quality. The product quality disturbance consists of a pulse change in polymer from DNDY to DFDQ. As can be seen in Figure 6.1 (b), the controller completely eliminates any offsets or long term drifts. The second order response to the change in polymer has been eliminated by a corresponding action of the manipulated variable. Looking at the control actions, one can see that any drifts or cycles in pressure have, under closed loop conditions, become drifts or cycles in the control action level.

The control objective is to regulate the pressure for both the pressure surging and for a disturbance in product quality. It is also desired that the controller take as little action as possible in response to the signal noise caused by the flight. However, because the flight noise is a large percentage of the surging and is at a higher frequency, no control setting was found that eliminated the 8 s surges without taking control action based on the signal noise. In most cases the flight noise was amplified by the controller.

The controller was very effective in eliminating any long term drifts and the changing polymer disturbance. However, the algorithm was much less successful in eliminating the 8 s surging. The high frequency control actions concentrate almost exclusively on the flight noise.

This can be observed more clearly in Figure 6.2 (a) and (b). This figure shows the pressure data given in Figure 6.1 digitally filtered off-line by an eighth order Butterworth low-pass filter with a cut-off frequency of 1/3 Hz. The high frequency pressure response was too rapid to significantly affect the extrudate (see section 2.3). It is therefore more important to examine only the lower frequencies of the pressure data in order to see what the true effect the controller will have on the product. In Figure 6.2 (a) and (b), the PI controller has removed the offset and the longer term cycling however, the 8 second surging has only been partially removed. The amplitude appears to be approximately half that of the open loop value. The control deteriorated during the polymer disturbance. The variance of the pressure increased by 20% as compared to the controlled data before the disturbance. These variances are calculated for a number of sequences of data, each 150 samples long. The increased variance was due to the process changing as the extruder moves to a new operating level. The new polymer can also have a different noise model and transfer function. At this point, the PI controller would require new tuning settings. Because it was desired to find a controller that needs a minimum of attention by plant personnel, the controllers, in this and subsequent experiments, were not retuned during a polymer quality disturbance. This tests how robust the controllers were for various ranges of extruder operation and for various polymer qualities.

Another experiment with control and sampling frequencies of 4 Hz yielded comparable results. In this case, the effect of the flight noise was even more pronounced. This is due to the ability of the

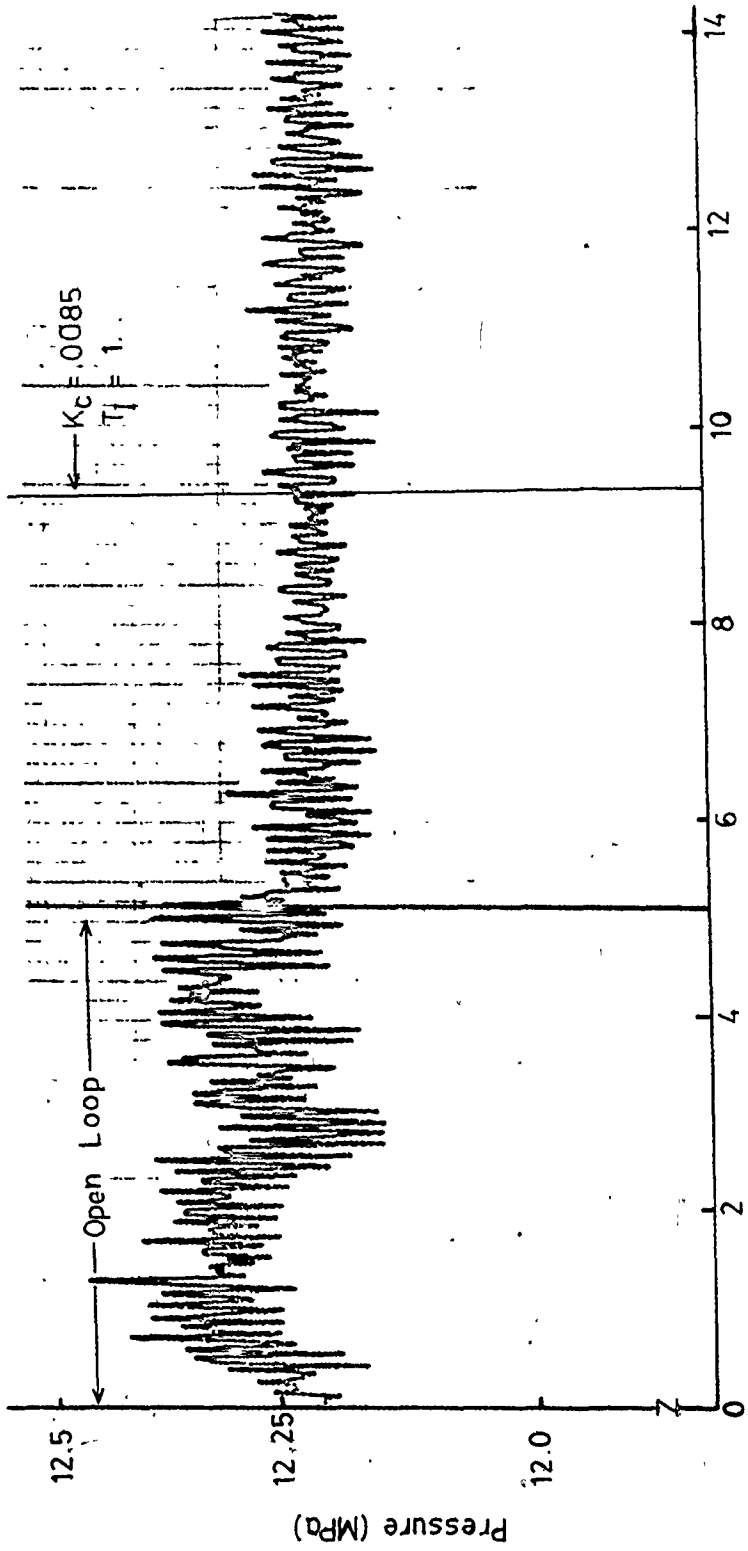

Figure 6.2 (a) Pressure Data of Figure 6.1 Filtered Off-Line

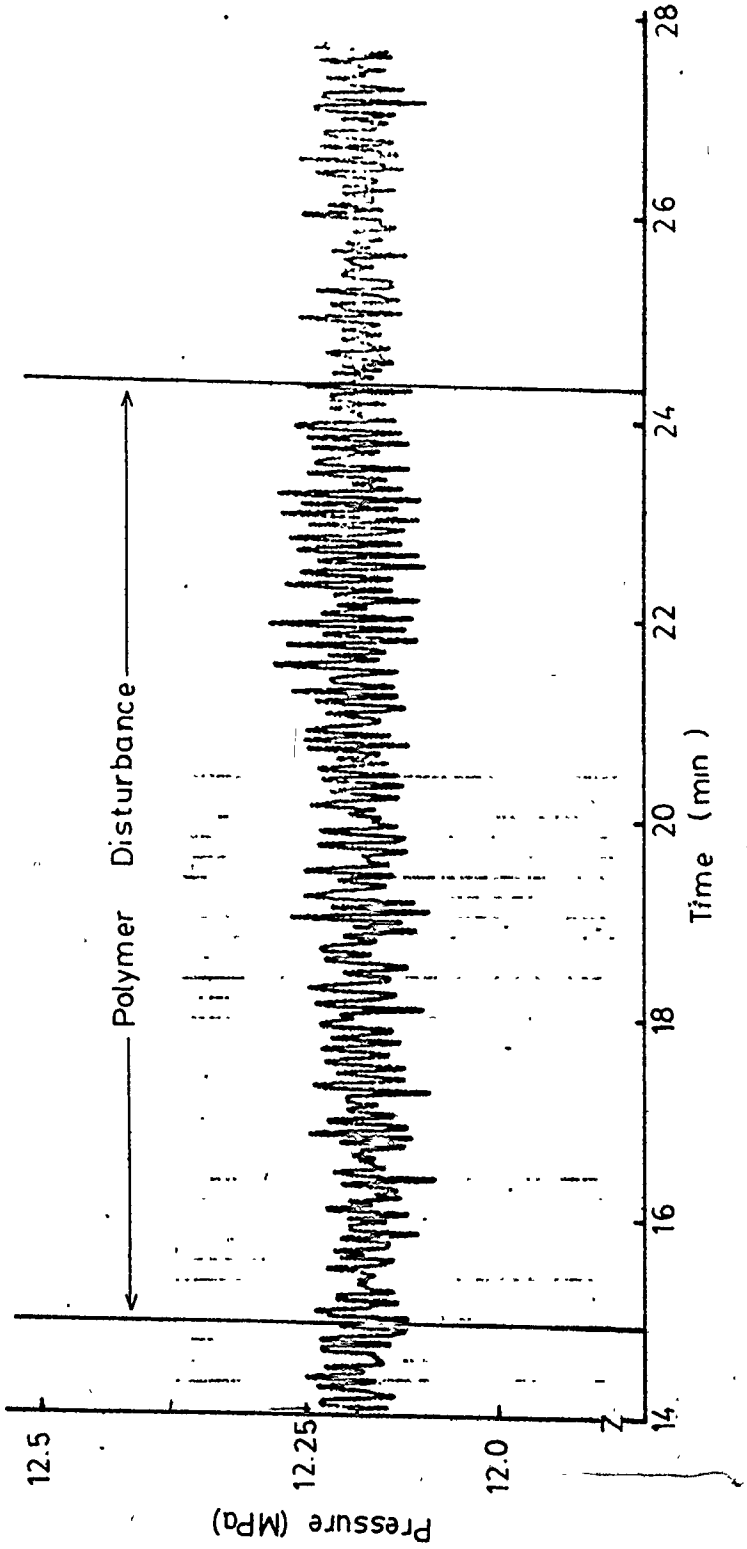

Figure 6.2 (b) Pressure Data of Figure 6.1 Filtered Off-Line

controller to identify more of the flight noise and take more rapid control actions based on this information.

6.2 PI Controller and Low-Pass Filtering

In the previous section, it was observed that the digital PI controller was unable to effectively regulate the 8 s surging disturbance because the pressure signal was corrupted by the flight noise. The controller concentrated its efforts in attempting to control the flight noise without controlling effectively the pressure surging.

In an attempt to remove the flight noise, it was decided to test various filters. The first filter studied was a low-pass Butterworth filter. Butterworth filters are characterized by a flat bandpass region, with unity gain and a constant rolloff which has slope determined by the order of the filter.

The equations for the Butterworth polynomial are given by Franklin and Powell(1980). For even orders:

$$H(s) = \frac{1}{\prod_{k=1}^{n/2} (s^2/\omega_o^2 + 2(\cos \theta_k)\, s/\omega_o + 1)} \qquad \theta_k = \Pi/2n\ (2k - 1) \qquad (6.2)$$

ω_o = cutoff frequency (i.e. when the amplitude = .707) in rad/s.

A fourth order filter was selected because of its reasonable number of parameters and its rapidly decreasing amplitude in the bandstop region. The cutoff frequency was selected as ω_o = 0.5 Hz, to be far from the surging frequency of 0.125 Hz and to give adequate attenuation for values near 1. Hz, the flight noise frequency. For these values (6.2) becomes:

$$H(s) = \frac{1}{(s^2/\omega_o^2 + 1.84776\ s/\omega_o + 1)\ (s^2/\omega_o^2 + 0.76536\ s/\omega_o + 1)} \tag{6.3}$$

To discretize (6.3) one uses the bilinear transformation (6.4)(Franklin and Powell(1980)):

$$s \rightarrow 2/T_s\ \frac{(1 - Z^{-1})}{(1 + Z^{-1})} \tag{6.4}$$

T_s, the sampling interval was selected as 50 ms. This is approximately the highest sampling rate attainable using the multiple/divide and floating point hardware on the NOVA 1200 computer system.

The digital version of (6.3) becomes (6.5):

$$H(Z^{-1}) = \frac{(1 + 2Z^{-1} + Z^{-2})^2}{(533.8 - 1016.6Z^{-1} + 486.8Z^{-2})(520.0 - 1016.6Z^{-1} + 500.6Z^{-2})} \tag{6.5}$$

(Note that $H(Z^{-1})$ denotes the digital version of H(s) and not that Z^{-1} replaces s). This filter was implemented as two cascaded second order equations, in order to minimize quantization problems. A sketch of the Bode diagram for this filter is shown in Figure 6.3.

Figures 6.4 and 6.5 shows the pressure response and control actions respectively for a PI controller using data filtered by (6.5). The initial section consists of open loop data with the flight noise removed. As soon as the control commenced, the system became unstable. The initial parameters used are the same as in Figure 6.1, the unfiltered PI, $K_c = 5.8 \times 10^{-3}$ M.P./kPa and $T_I = 1.s.$ Various tuning settings were attempted but gains above 4.4×10^{-3} M.P./kPa resulted in process instability. The best tuning was selected as $K_c = 2.9 \times 10^{-3}$ M.P./kPa and $T_I = 4.s.$ These values were so detuned that there was practically no control of the pressure surging.

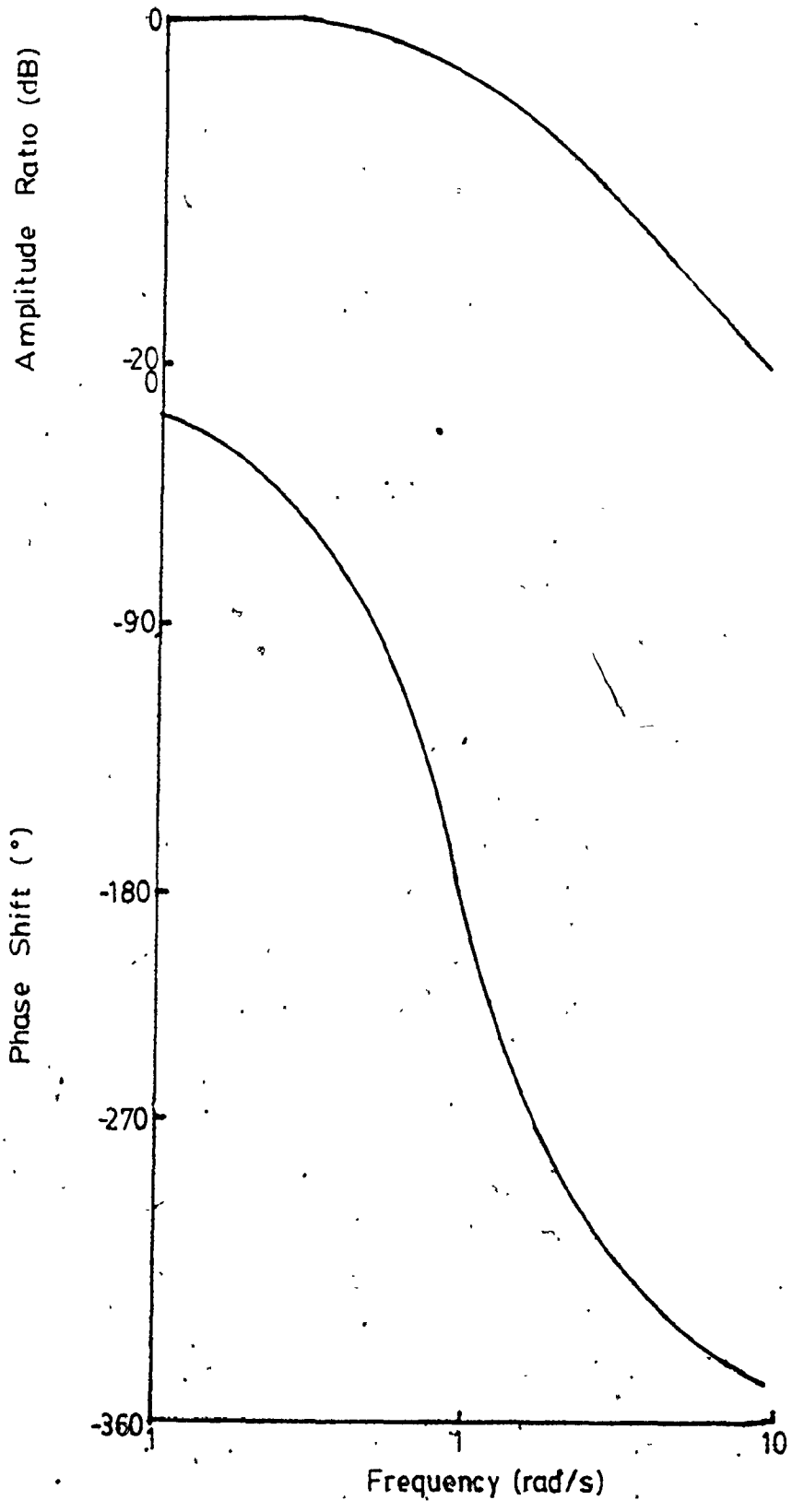

Figure 6.3 Bode Plot for Fourth Order Butterworth Low-Pa

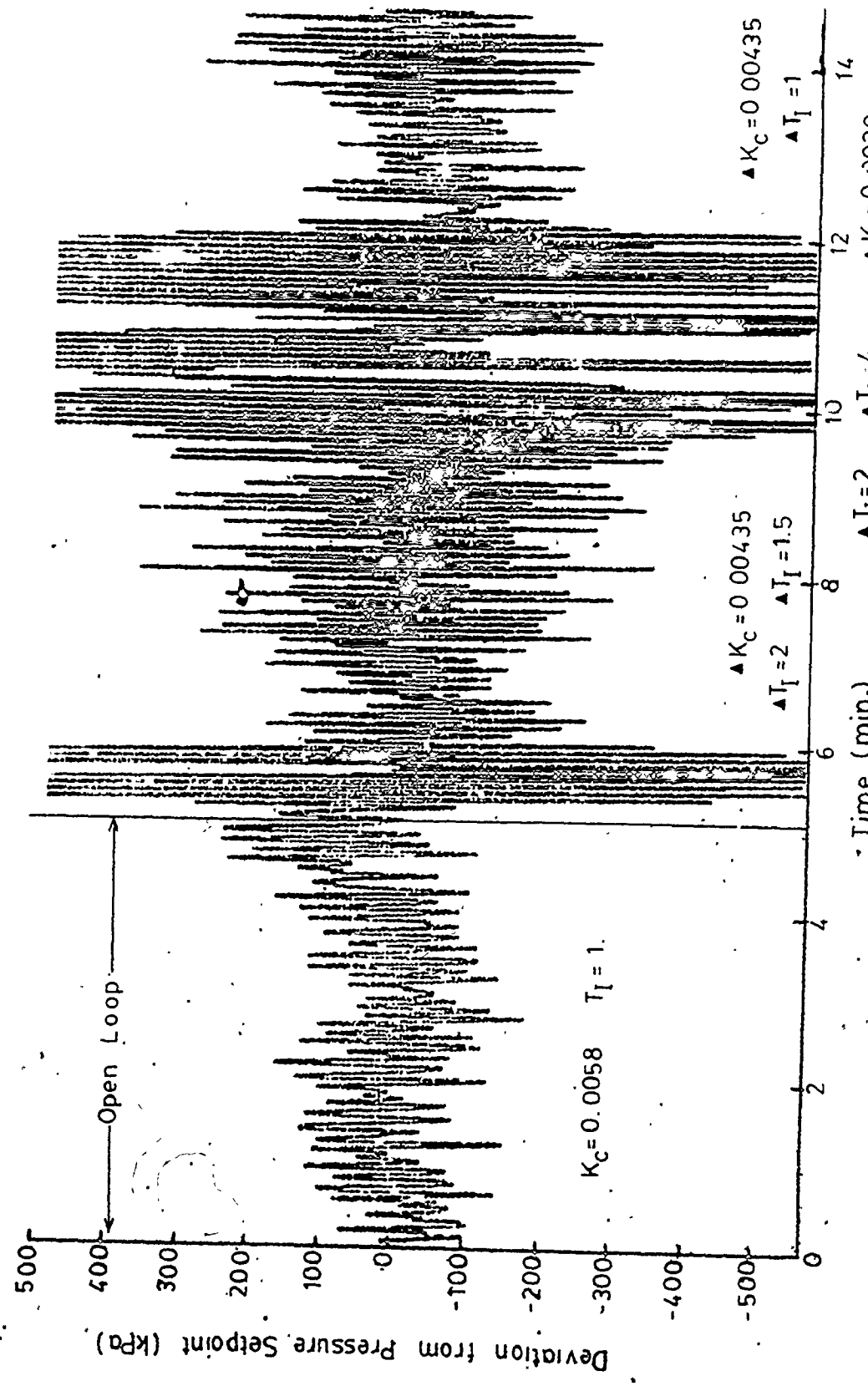

Figure 6.4 Pressure Response, Digital PI Algorithm and Low-Pass Filter

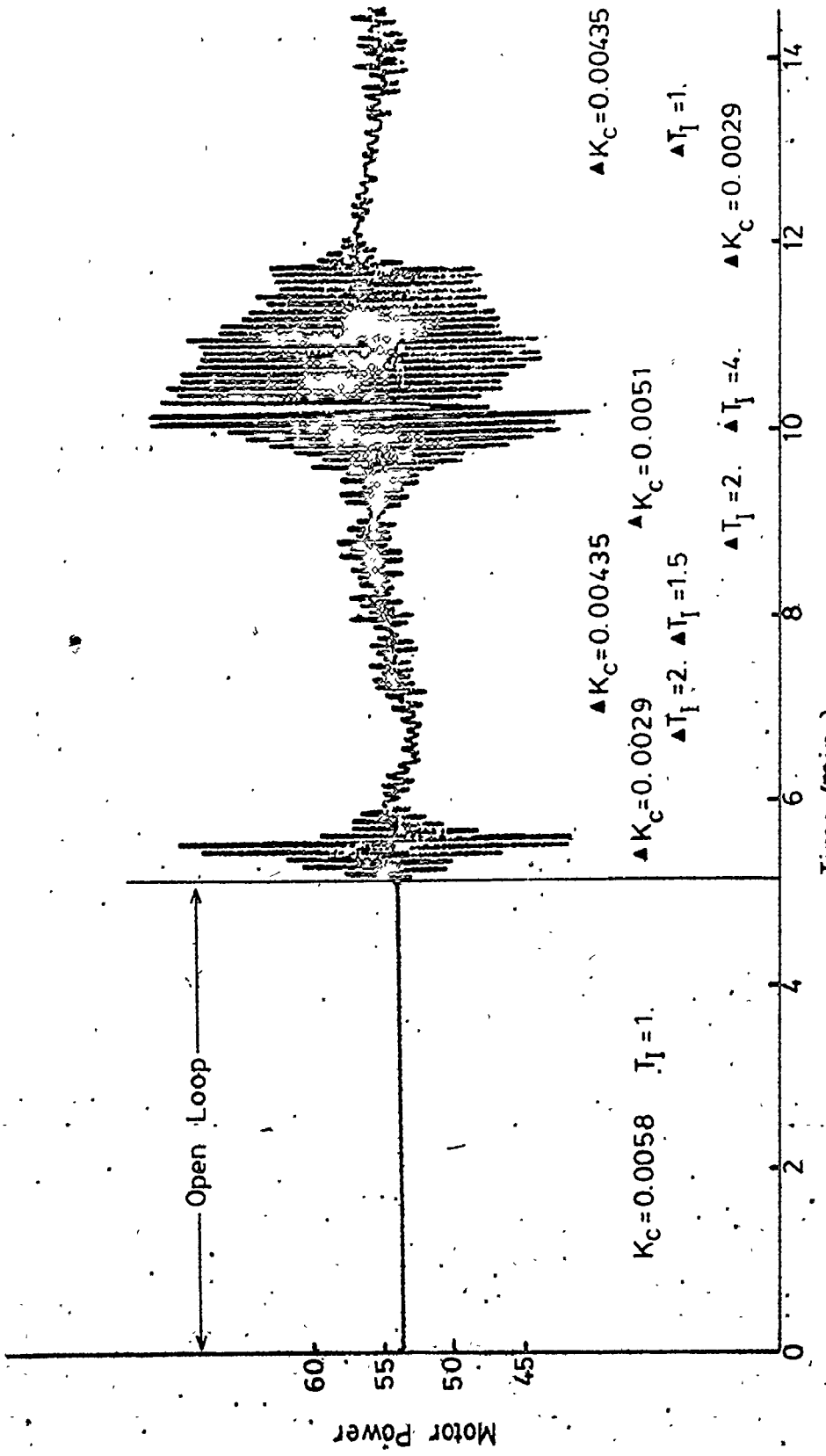

Figure 6.5 Control Action, Digital PI Algorithm and Low-Pass Filter

The instability is caused by the addition of the filter to the loop. The same settings of control parameters were stable for the unfiltered case. The system instability at high tuning was due to the filter reducing the system phase and gain margins. As can be seen in Figure 6.3, the filter can still introduce near -180° phase lag in the pass band.

In normal practice, a low-pass filter is implemented when one wishes to remove a noise that has a frequency much higher than the natural frequency of the plant and the control rate. These two frequencies would then be well within the flat unity gain region of the filter. The filter would then have no noticeable effect on the process transfer function and would not reduce the system phase and gain margins as described above.

In the case shown in Figures 6.4 and 6.5 both the plant and control frequencies are significantly higher than the filter cutoff point. The filter would then certainly affect the process transfer function because it would filter frequencies normally present in the process.

Equation (6.6) gives a time series model for the extruder extruding polymer DNDY-6600 at 50 r/min. The data were filtered by a fourth order Butterworth filter. The PRBS test was implemented at 1. Hz.

$$P_t = \frac{(\omega_0 - \omega_1 Z^{-1} - \omega_2 Z^{-2})}{(1 - \delta Z^{-1})} U_{t-1} + \frac{(1 - \theta Z^{-1})\, a_t}{(1 - Z^{-1})(1 - \phi_1 Z^{-1} - \phi_2 Z^{-2})} \qquad (6.6)$$

where

ω_1 = -112. ± 4.0 kPa/M.P.

ω_2 = -59.2 ± 6.7 kPa/M.P.

δ = -0.4268 ± 0.0812

θ = 0.8648 ± 0.0501

ϕ_1 = 1.387 ± 0.048

ϕ_2 = -0.8731 ± 0.0584

The term $(1 - \phi_1 Z^{-1} - \phi_2 Z^{-2})$ models a damped sinusoid, damping factor 0.93 and frequency 0.117 Hz (period of 8.6 s). The noise is similar to that found in equation (5.1). The system gain is 128.6 kPa/M.P., close to the one found in (5.1). However, the transfer function has become non-minimum phase, with only a small dependence on the value of U_{t-1} at lag one. ω_0 is small in comparison to ω_1 indicating that the filter is removing the dependence of values 1. s apart, adding phase lag in the form of dead time.

A similar result was found for polymer DNDY 2530 at 40 r/min in equation (6.7).

$$P_t = \frac{(\omega_0 - \omega_1 Z^{-1} - \omega_2 Z^{-2})\ U_{t-1}}{(1 - \delta Z^{-1})} + \frac{a_t}{(1 - Z^{-1})(1 - \phi_1 Z^{-1} - \phi_2 Z^{-2} - \phi_3 Z^{-3} - \phi_4 Z^{-4})} \qquad (6.7)$$

where

ω_0 = 13.8 ± 1.3 kPa/M.P.

ω_1 = -107. ± 1.8 kPa/M.P.

ω_2 = -46.7 ± 4.6 kPa/M.P.

δ = -0.2976 ± 0.0544

ϕ_1 = 0.1732 ± 0.0817

ϕ_2 = -0.1599 ± 0.0238

$\phi_3 = -0.339 \pm 0.0716$

$\phi_4 = -0.347 \pm 0.0806$

The term $(1 - \phi_1 Z^{-1} - \phi_2 Z^{-2} - \phi_3 Z^{-3} - \phi_4 Z^{-4})$ has roots at $0.83 \pm 0.80i$. These roots correspond to a damped sinusoid, damping factor 0.87, and frequency 0.122 Hz (period of 8.2 s). The system gain is 129.1 kPa/M.P. Again the noise model and system gain compared very reasonably with those obtained from equation (5.1). The transfer function, like equation (6.6) is non-minimum phase with a small value of ω_0 when compared to ω_1.

The filter has caused the replacement of the first order plant model of equation (5.1) with the transfer functions given in models (6.6) and (6.7) which are determined by the dynamics of the filter. This creates a non-minimum phase system which is much harder to control than a normal first order plant.

This section shows that the low-pass filter reduces the system phase and gain margins. This destabilizes the system under closed loop control. The filter also considerably changes the system time series model.

6.3 Theory of Seasonal Models as Filters

In the previous section, the low-pass filter was shown to cause poor closed loop behavior. In order to improve the system control it was decided to reexamine the system block diagram and model, in an attempt to more optimally remove the signal noise. This section presents various models and seasonal time series filters designed to remove the flight noise. This approach is introduced by examining some generalized block diagrams of the extruder process.

Figure 6.6 (a) shows the block diagram of the individual model

nts in the the

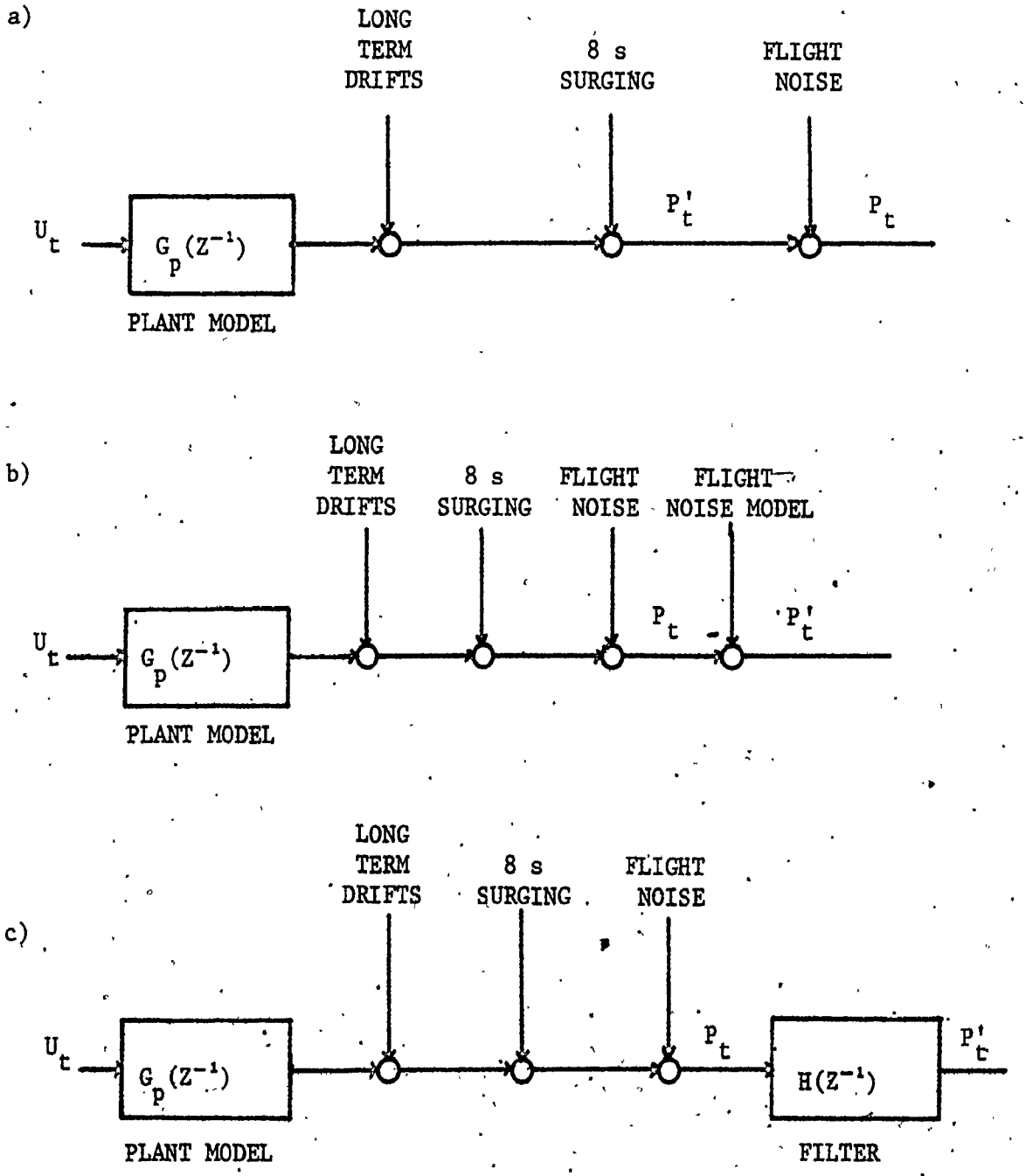

Figure 6.6 Simplified System Block Diagrams

drifts, the 8 s surging and the flight noise. This figure assumes that these processes are additive and do not interact. This is expected because the sources of the noise, as discussed in section 2.3, are independent.

One would like to use the P_t' of Figure 6.6 (a) as the controlled variable. This is the pressure before the addition of the flight noise. The only way to actually obtain P_t' would be through the manipulations used in either Figure 6.6 (b) or (c).

In Figure 6.6 (b), the flight noise is cancelled by a deterministic model of the noise subtracted from the pressure data. The flight noise can be considered as a deterministic disturbance modelled by a constant amplitude sawtooth wave, with frequency determined by the screw speed. The amplitude and starting values are selected as the model parameters. Unfortunately, it is impractical to use this method on-line for control as the model parameters may vary with different operating levels. More importantly, the value of the model is very dependent on accurate screw speed information. Since the offset in the sawtooth is dependent on all past screw speeds, errors could build up. On-line initialization of the parameters could also prove difficult.

Models, using this deterministic sawtooth model of the flight noise, to replace the seasonal difference operator of equation (5.1), yielded a poor fit. Attempts to use models of this form were abandoned.

Figure 6.6 (c) shows the more standard approach of constructing a filter $H(Z^{-1})$ to remove the noise. In the previous section it was shown that a standard low-pass filter performed poorly, causing instability. The next approach after using the low-pass filter was to

reexamine the Box and Jenkins noise model of equation (5.1) and the block diagram Figure 5.1, concentrating on the flight noise terms.

The noise model developed by time series modelling can be considered as a filter which selects certain frequencies of the white noise sequence, a_t, and produces a coloured noise series, N_t. This property of time series models can be used to modify the measured signal instead of modelling a noise sequence.

The Box and Jenkins noise models can be separated, as in equation (6.8), into terms due to the periodic signal noise and terms due to other process disturbances

$$P_t = \frac{\omega(Z^{-1})}{\delta(Z^{-1})} U_{t-b} + \frac{\theta(Z^{-1})}{\nabla^d \phi(Z^{-1})} \quad \frac{\theta_f(Z^{-1})}{\phi_f(Z^{-1}) \nabla_s^d} \quad a_t \qquad (6.8)$$

where $\frac{\theta_f(Z^{-1})}{\phi_f(Z^{-1}) \nabla_s^d}$ represents the periodic behavior. This term can then be used to modify equation (6.8) to remove this noise from the process measurement. Equation (6.8) becomes:

$$P'_t = \frac{\omega(Z^{-1})}{\delta(Z^{-1})} \frac{\phi_f(Z^{-1})\nabla_s^d}{\theta_f(Z^{-1})} U_{t-b} + \frac{\theta(Z^{-1})}{\nabla^d \phi(Z^{-1})} a_t \qquad (6.9)$$

where P'_t is the filtered measured variable:

$$P'_t = \frac{\phi_f(Z^{-1})\nabla_s^d}{\theta_f(Z^{-1})} P_t$$

In equation (6.9) the filter has modified the process transfer function. In effect the $\frac{\phi_f(Z^{-1})\nabla_s^d}{\theta \quad Z^{-1})}$ term has been removed from the

noise model and become the $H(Z^{-1})$ of Figure 6.6 (c). The filter becomes part of the loop transfer function relating P'_t to U_t. However, because the $\frac{\phi_f(Z^{-1})\nabla_s^d}{\theta_f(Z^{-1})}$ filter is calculated by time series analysis, it is an optimal filter. This means that it attenuates the noise as much as possible, with the least possible effect on other frequencies present in the noise model.

In the most common modelling method, $\theta_f(Z^{-1})$ and $\phi_f(Z^{-1})$ have terms only in orders of integer powers of s, where s is greater than one. For example $\theta_f(Z^{-1})$ might be:

$$\theta_f(Z^{-1}) = 1 - \theta_{f_1} Z^{-s} - \theta_{f_2} Z^{-2s} \ldots$$

The other method (discussed in more detail later in this section) involves modelling the periodic disturbance as a sinusoid. For example, both equations (6.10) and (6.11) will remove a sinusoidal disturbance with a period equal to 12 times the sampling period.

$$(1 - \sqrt{3}Z^{-1} + Z^{-2})\, U_t = a_t \qquad (6.10)$$

$$(1 - Z^{-12})\, U_t = a_t \qquad (6.11)$$

where U_t is the input series and a_t is the white noise output. Figure 6.7 shows the location of the zeroes for these two processes. Both have zeroes at $e^{\pm(i\, 2\pi/12)}$ which will remove a sinusoid with a period equal to 12 times the sampling period.

(6.11) is a comb filter and (6.10) is the inverse of a digital resonator (Rader and Gold(1972)). The frequency response of these

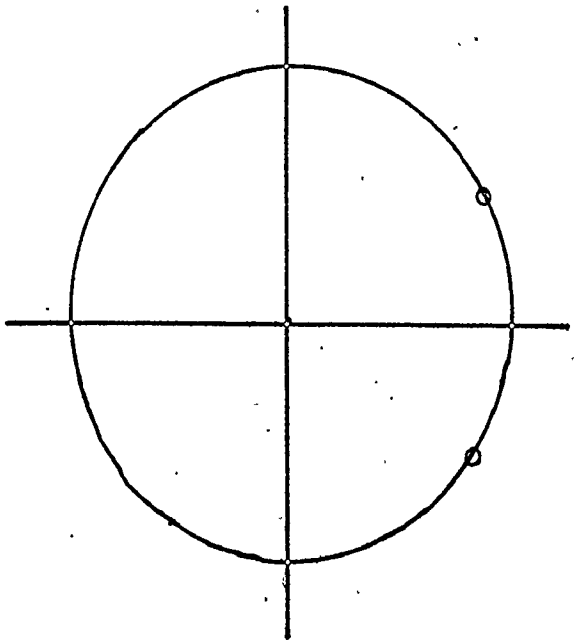

a) Zeroes of $(1 - \sqrt{3}\ Z^{-1} + Z^{-2})$, $= e^{\pm(i\ 2\pi/12)}$

Equation (6.10)

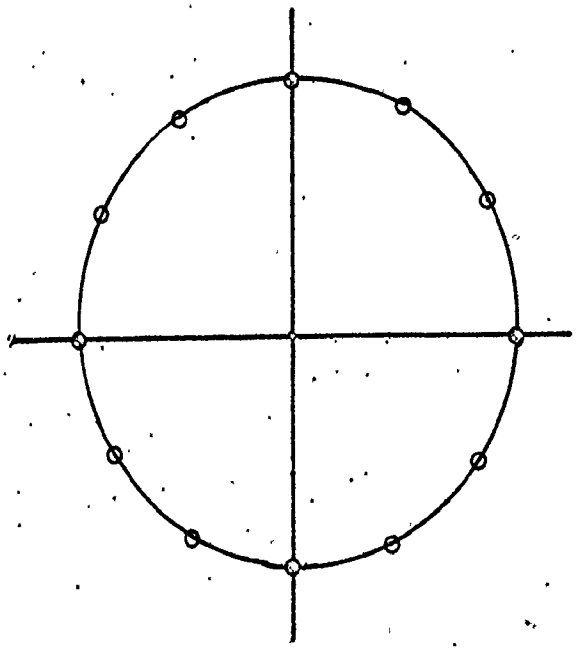

b) Zeroes of $(1 - Z^{-12})$, $= e^{i(2\pi\ K/s)}$ $K = 0,1\ldots,s-1$

Equation (6.11)

Figure 6.7 Plot of Zeroes for Equations (6.10) and (6.11)

filters can be studied by examining the Bode plots for these systems. For the seasonal difference filter $(1 - Z^{-s})$, Figures 6.8 and 6.9 give the amplitude and phase ratios plotted experimentally for $1 - Z^{-6}$. These plots were developed by filtering digital sine waves of various frequencies and then comparing the inputs and outputs.

The plots run from 0 to $\omega_s/2$ frequency where ω_s is the sampling frequency. This is because responses for frequencies higher than $\omega_s/2$ will be transformed to lower frequencies by the effect of aliasing (Franklin and Powell(1980)). Figure 6.8 shows the amplitude ratio Bode plot which has s/2 lobes with zero amplitude ratio at the frequencies which correspond to the zeroes of $1 - Z^{-s}$. These are located at ω_s/n $n = 1,2,\ldots,s/2$ for s even and $n = 1,2,\ldots,(s-1)/2$ for s odd. The midpoint between the zeroes has an amplitude ratio of 2. These are intuitively sound results. From the zeroes one can see that the seasonal difference operator would eliminate all sinusoids of frequency ω_s/s and their harmonics. However, for frequencies of $\omega_s/(2n + 1)$ s/2, one would be subtracting values with 180° of phase shift. These values would reinforce instead of eliminate, leading to an amplitude of 2 at these locations.

Many control texts on sampled data systems (Jury(1958), Tou(1959), Lindorff(1965) and Kou(1977)) recommend transforming digital equations from the Z-domain to the W-domain in order to study the system frequency response. This can be accomplished by using the bilinear transformation (6.12) when mapping the Bode diagram. This involves setting:

$$Z = \frac{1 + W}{1 - W} \qquad (6.12)$$

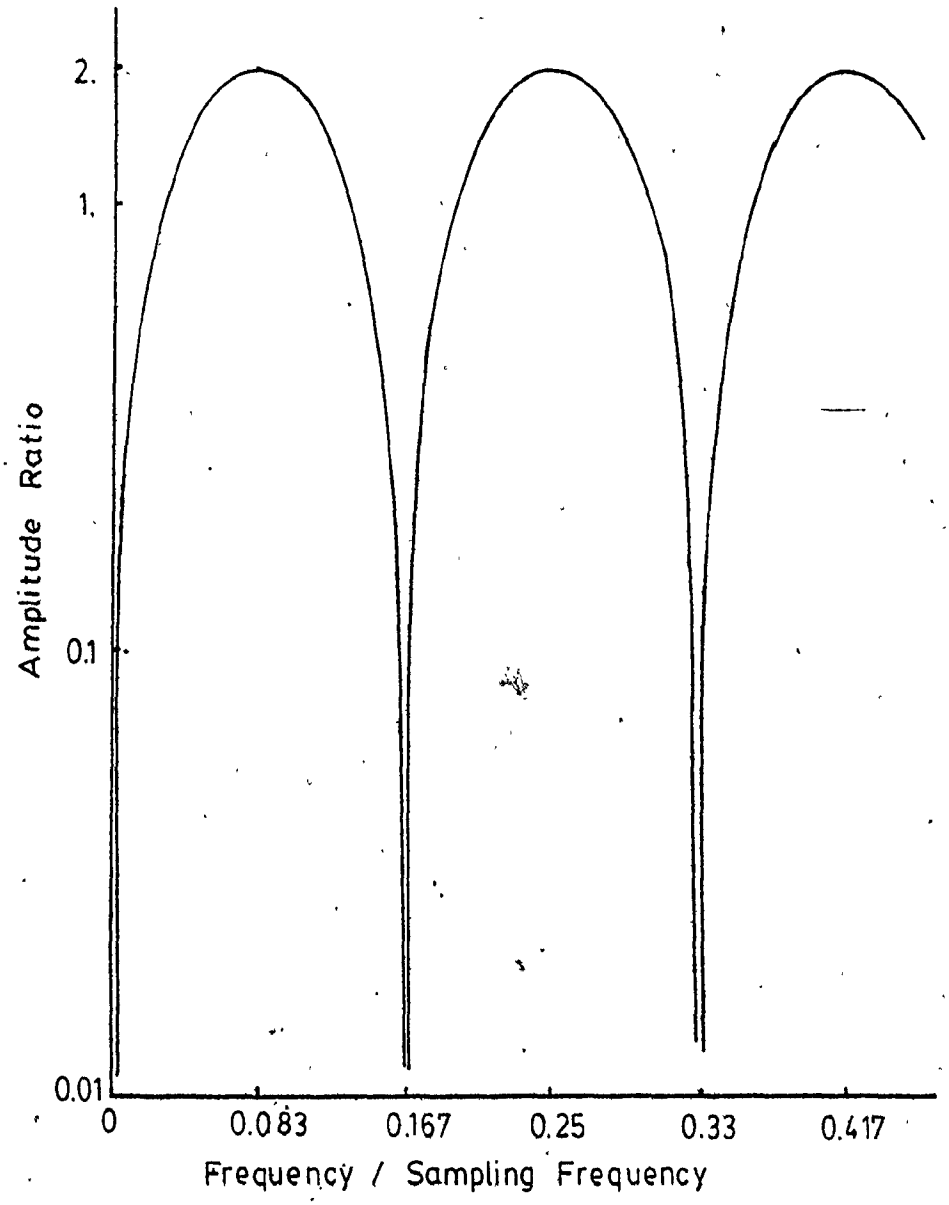

Figure 6.8 Amplitude Ratio, Seasonal Filter $(1-Z^{-6})$

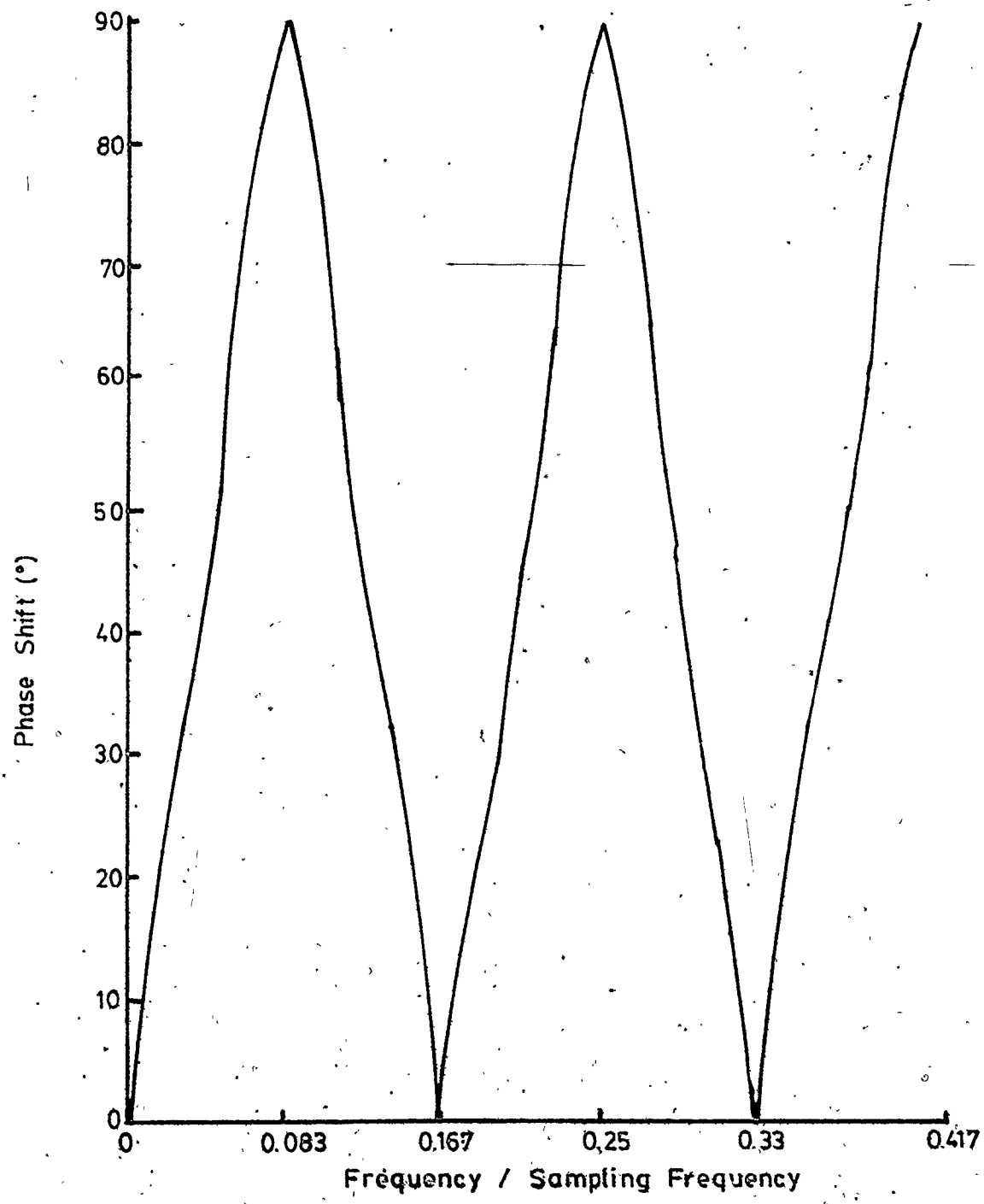

Figure 6.9 Phase Shift, Seasonal Filter $(1-Z^{-6})$

TABLE 6.1

W - TRANSFORM FOR SEASONAL FILTERS

Filter Order - s	Filter	W - Transform
1	$1 - Z^{-1}$	$\frac{2W}{1 + W}$
2	$1 - Z^{-2}$	$\frac{4W}{(1 + W)^2}$
3	$1 - Z^{-3}$	$\frac{6W\ (1 + 1/3\ W^2)}{(1 + W)^3}$
4	$1 - Z^{-4}$	$\frac{8W\ (1 + W^2)}{(1 + W)^4}$
5	$1 - Z^{-5}$	$\frac{10W\ (1 + 1/0,513\ W^2)(1 + 1/19.49\ W^2)}{(1 + W)^5}$
6	$1 - Z^{-6}$	$\frac{12W\ (1 + W^2/3)(1 + 3W^2)}{(1 + W)^6}$

and plotting the Bode plot in the W-plane. Frequencies in the W-domain can be matched to the real frequencies by

$$\omega_W = j \tan\left(\frac{\omega T_s}{2}\right)$$

Frequencies in the W domain go from 0 to infinity, whereas the actual frequencies ω take values from 0 to $\omega_s/2$. Table 6.1 shows the resulting transforms for different seasonal filters. By drawing the Bode plot for the cases listed, one can see that only the first and second order filters match an actual Bode plot like Figure 6.8. Other authors analyze the frequency response directly by setting $Z = e^{j\omega T_s}$ (Oppenheim and Schafer(1968) and Harris(1980)). Saucedo and Schiving(1968) shows that these two methods are equivalent in the W-domain. However, Bode plots in the W-domain do not actually conform to the system performance for the real frequencies. This is probably due to the bilinear transformation being an approximation for $Z = e^{sT_s}$ (the true definition of a Z-transform) causing some warping at high frequencies.

The frequency response for $1 - Z^{-6}$ can be calculated as follows:

$$Z = e^{j\omega T_s}$$

$$1 - Z^{-6} = 1 - e^{-6j\omega T_s}$$

$$= 1 - \cos 6\omega T_s + j \sin 6\omega T_s$$

$$AR = \sqrt{(1 - \cos 6\omega T_s)^2 + \sin^2 6\omega T_s}$$

$$= \sqrt{1 - 2\cos 6\omega T_s + \cos^2 6\omega T_s + \sin^2 6\omega T_s}$$

$$= \sqrt{2 - 2\cos 6\omega T_s}$$

The amplitude calculated above matches the response shown in Figure 6.8.

The seasonal filters are very effective at removing one frequency, however they have many features that are unacceptable for control purposes. The DC value, along with all the harmonics are lost and all other frequencies experience amplitude and/or phase changes. By losing the DC value, the controller will not be able to account for long term drifts or offsets meaning that the process may move to a new level without the controller seeing the change. In addition, Figure 6.10 shows the poor impulse response of the filter. An impulse introduced to the filter will never die away but will create a response with the frequency that the filter is designed to remove. Figure 6.11 shows the filter step response, an impulse of s sampling periods duration.

Another possible filter is $(1 + Z^{-s/2})$ which needs values of the signal noise s/2 lags apart to be equal and opposite in sign. Replacing ∇_s in (5.1) by $(1 + Z^{-s/2})$ gave a significantly poorer result. Most periodic disturbances, such as a sawtooth wave, will not have opposite signs s/2 periods apart and will not be removed effectively.

The other filter discussed are filters of the form:

$$(1 - 2\cos\theta\ Z^{-1} + Z^{-2}) \qquad (6.13)$$

where θ is the frequency of the noise to be removed. Again replacing Z with $e^{j\omega T_s}$ gives an amplitude ratio described by equation (6.14).

$$AR = \sqrt{(1 - 2\cos\theta\ \cos\omega T_s + \cos 2\omega T_s)^2 + (2\cos\theta\ \sin\omega T_s - \sin 2\omega T_s)^2} \qquad (6.14)$$

This gives values of $AR = 2 - 2\cos\theta$ for $\omega T = 0$, $AR = 0$ for $\omega T_s = \theta$ and $AR = 2 + 2\cos\theta$ for $\omega T_s = \pi$. These values match the Bode plot developed by simulation in Figure 6.12.

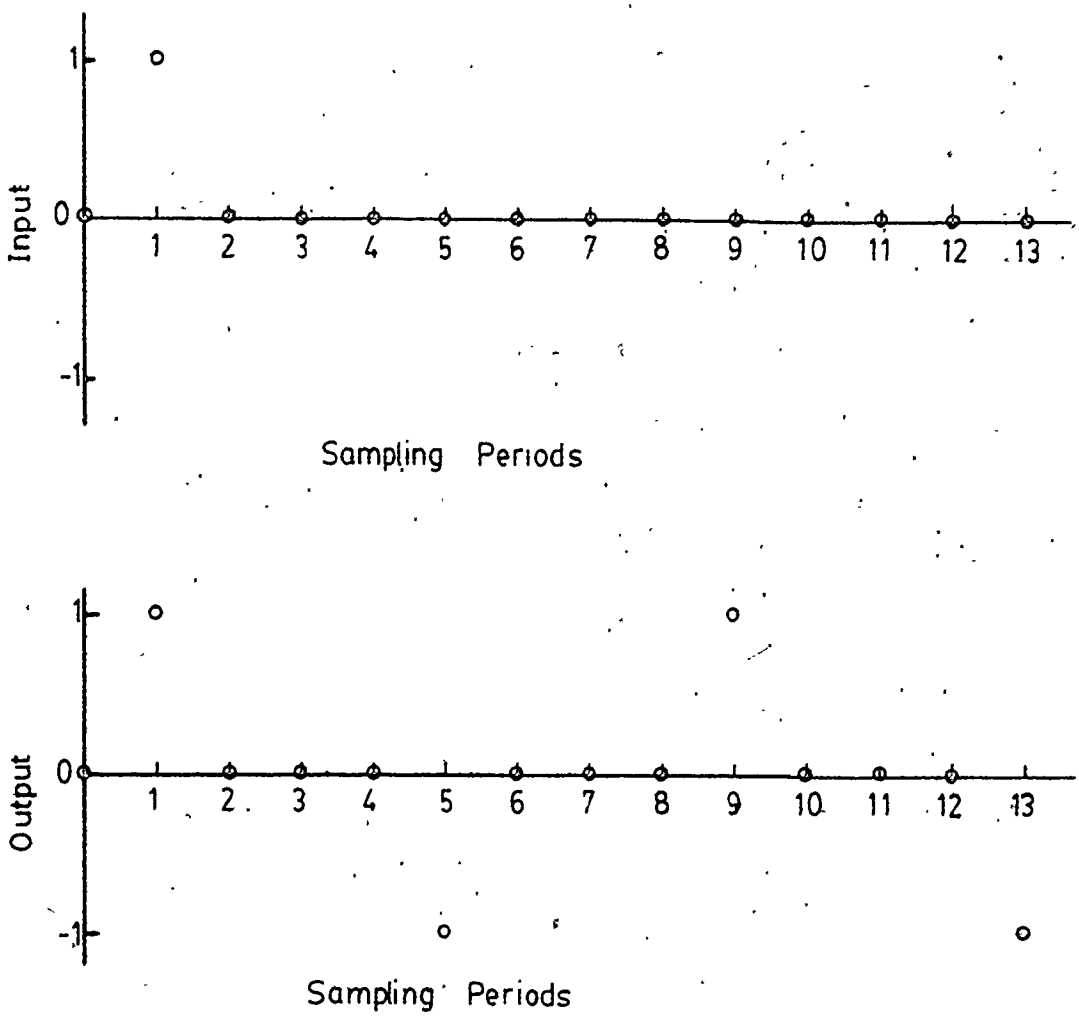

Figure 6.10 Seasonal Filter (Frequency 1/4 x Sampling Rate), Impulse Response

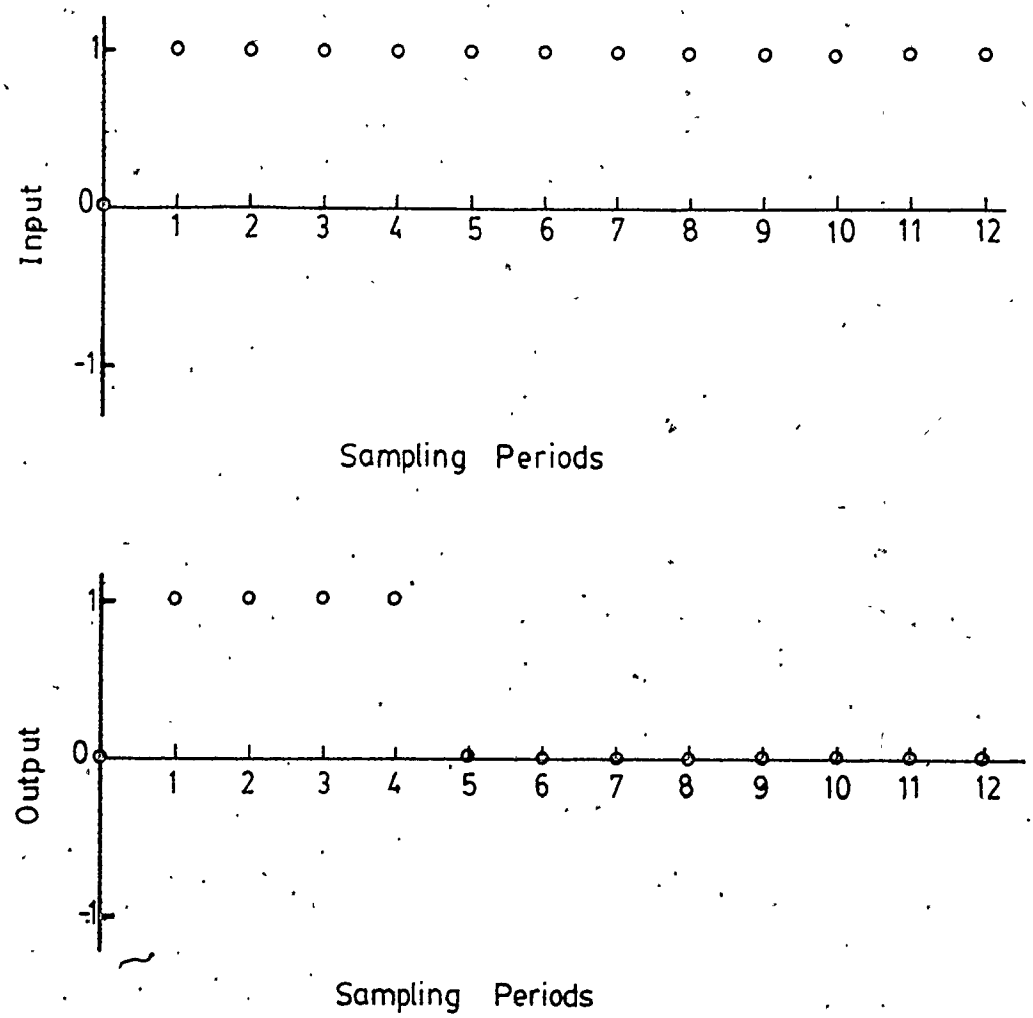

Figure 6.11. Seasonal Filter (Frequency 1/4 x Sampling Rate), Step Response

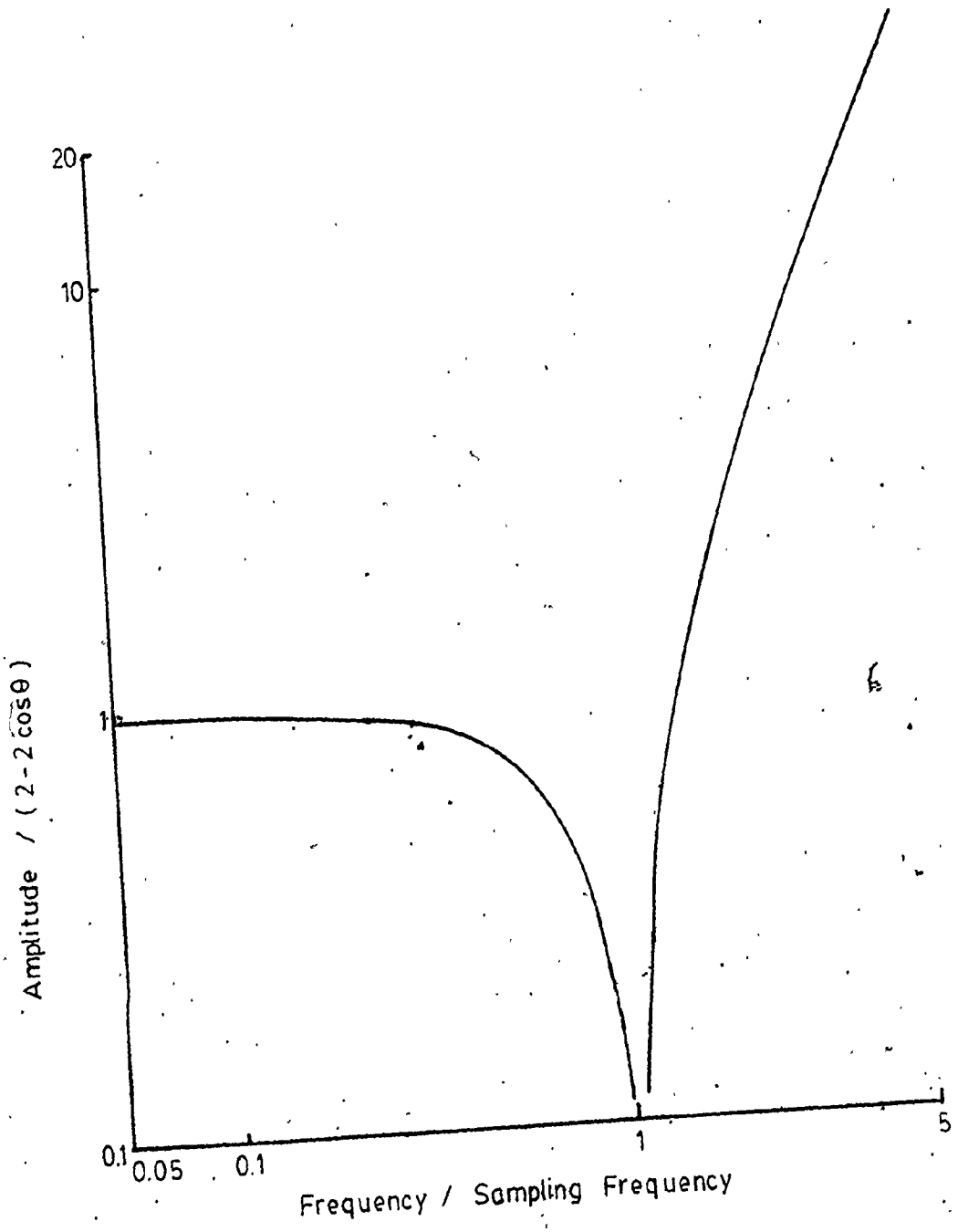

Figure 6.12 Amplitude Response, Sinusoidal Filter

Filters of this type amplify frequencies which lie above $\omega T_s = \theta$. This amplification can be removed by selecting compensating poles. Filters of this type will be discussed further in the next section. These are actually a form of the bandstop filters that can be transformed from low-pass filters.

In summary, in this section, various models and block diagram manipulations are studied in an attempt to remove the signal noise. Most importantly, Box and Jenkins seasonal noise models are examined for their applicability as filters. Two main models are studied; the seasonal difference operator, for example equation (6.11) and the sinusoidal operator presented in equation (6.13). The seasonal filter was found to be a poor filter. The DC value of the data was lost and all other frequencies experienced amplitude and/or phase changes. The sinusoidal type filter is much better with a flat response for low frequencies. However, the high frequencies are amplified.

The seasonal difference operator and the sinusoidal operator are compared in the next section to the more standard digital signal processing approach of bandstop filtering.

6.4 PI Control With a Bandstop Filter

The previous section shows attempts to use Box and Jenkins seasonal models as filters to remove one particular frequency of noise. This corresponds to the more standard signal processing technique of bandstop filtering. This involves constructing a filter that, in its ideal form, removes all frequencies in a specified stop band and does not affect any other frequencies outside the stop band. Both Figures

6.8, the Bode plot of the seasonal difference filter, and 6.12, the Bode plot of the sinusoidal filter, show a narrow stop band region about $\omega T_s/2\pi = 1$. However, these Box and Jenkins filters do not meet the band-stop criteria of not affecting the amplitude of frequencies outside the stop band. The seasonal difference operator has a comb shape and the sinusoidal filter amplifies the high frequencies.

Signal processing text books (for example Rabiner and Gold(1975)) construct bandstop filters from lowpass filters by using the transformation given by (6.15).

$$s \rightarrow \frac{s\,(\Omega_u - \Omega_e)}{s^2 + \Omega_u * \Omega_e} \tag{6.15}$$

where Ω_u = upper cutoff frequency (.707 amplitude ratio) rad/s and Ω_e = lower cutoff frequency (.707 amplitude ratio) rad/s. To use the transformation (6.15), the low-pass filter must be normalized to have a cutoff frequency of $\omega_o = 1$ rad/s.

A bandstop filter can now be constructed by taking the fourth order Butterworth lowpass filter already developed in section 6.2 (equation (6.3)) and setting $\omega_o = 1$ rad/s and $d = \Omega_u * \Omega_e$ and $c = \Omega_u - \Omega_e$. Filter (6.3) is transformed to (6.16):

$$H(s) = \frac{(s^2+d)^2}{(s^2c^2 + \alpha_1\, cs(s^2 + d) + (s^2+d)^2)} \cdot \frac{(s^2+d)^2}{(s^2c^2 + \alpha_2\, cs(s^2+d) + (s^2+d)^2)} \tag{6.16}$$

where $\alpha_1 = 1.84776$ and $\alpha_2 = 0.76536$

Filter (6.16) has twin zeroes at $\pm\sqrt{d}\,i$. These zeroes will eliminate a sinusoidal behavior of frequency $\sqrt{d}$. By using pole-zero mapping (Franklin and Powell(1980)) a zero at $\pm\sqrt{d}\,i$ in the s-plane

will correspond to a zero at $e^{\pm i\sqrt{d}\,T_s}$ on the unit circle in the Z plane. This corresponds to the digital model (6.17)

$$(1 - 2\cos\sqrt{d}\,T_s Z^{-1} + Z^{-2}) \tag{6.17}$$

Equation (6.17) is the same equation as the sinusoidal filter (6.13) discussed in the previous section (where $\sqrt{d}\,T_s = \theta$). (6.16) has a fourth order zero that removes the offending frequencies.

The filter is discretized using the bilinear transformation (6.4). A sampling time of 50 ms, same as for the low-pass filter, was chosen. The cutoff frequencies were chosen as $\Omega_e = (1/3)\ 2\pi$ rad/s (20 r/min) and $\Omega_u = (1.5)\ 2\pi$ rad/s (90 r/min). These frequencies correspond to the operating region of the extruder. At these values, no prewarping was required (Kaiser(1972)). The digital version of (6.16) is:

$$H(Z^{-1}) = \frac{(2.623\,555\,1 \times 10^6 - 1.023\,844\,1 \times 10^7 Z^{-1} + 1.523\,600\,7 \times 10^7 Z^{-2} - 1.023\,844\,1 \times 10^7 Z^{-3} + 2.623\,555\,1 \times 10^6 Z^{-4})^2}{(3.587\,063 \times 10^6 - 1.195\,073 \times 10^7 Z^{-1} + 1.506\,405\,6 \times 10^7 Z^{-2} - 8.526\,153\,2 \times 10^6 Z^{-3} + 1.831\,997\,8 \times 10^6 Z^{-4})(3.073\,024\,5 \times 10^6 - 1.094\,771\,1 \times 10^7 Z^{-1} + 1.506\,405\,6 \times 10^7 Z^{-2} - 9.529\,172\,1 \times 10^6 Z^{-3} + 2.346\,036\,1 \times 10^6 Z^{-4})} \tag{6.18}$$

The large number of significant figures used in the filter are required to maintain the accuracy and the stability of the filter.

This filter has twin zeroes at both (0.9743 ± 0.2191i) and (0.9770 ± 0.2197i) and poles at (1.100 ± 0.1148i), (1.227 ± 0.3084i), (1.009 ± 0.4720i) and (1.021 ± 0.1071i). The magnitude of the zeroes are very close to unity, with the error due to roundoff. These zeroes

remove a sinusoidal disturbance with a frequency of 0.72 Hz, which is very close to $\sqrt{d}/2\pi$ = 0.71 Hz, the frequency removed by the continuous version of the filter (6.16). Figure 6.13 gives the Bode plot of the continuous filter (6.16). Note that the figure shows considerable phase lead at certain frequencies due to the zeroes of the filter.

The amplitude response of Figure 6.13 closely matches that of the sinusoidal filter given in Figure 6.10. However, the bandstop filter has a flat amplitude in the high frequency range, whereas the sinusoidal filter amplifies the high frequency. The poles of the bandstop filter, not present in the sinusoidal filter, are flattening this region.

Figures 6.14 and 6.15 show the pressure response and control actions respectively for control using the bandstop filter, equation (6.18). The initial section shows filtered open loop data. The flight noise has been eliminated. The initial control is poor. However, attempts to increase the gain and the integral action resulted in system instability. Gains above $K_c = 5.8 \times 10^{-3}$ M.P./kPa caused instability. This is very similar to the settings that caused instability in the case using the low pass filter.

The instability must be caused by adding the filter to the loop. As shown in Figure 6.13, the filter will add 180° phase lead in the regions of the passband. In addition, the filter will modify the system transfer function similar to the effect of the low-pass filter has on equation (6.6) and (6.7). Especially serious would be the 180° phase lead at the corners of the filter where the amplitude is still near unity. A 180° phase lead in a closed loop system could cause instability because, in a similar case to a 180° phase lag, the control action will reinforce the oscillations instead of cancelling them out. The tuning parameters must therefore be reduced to increase

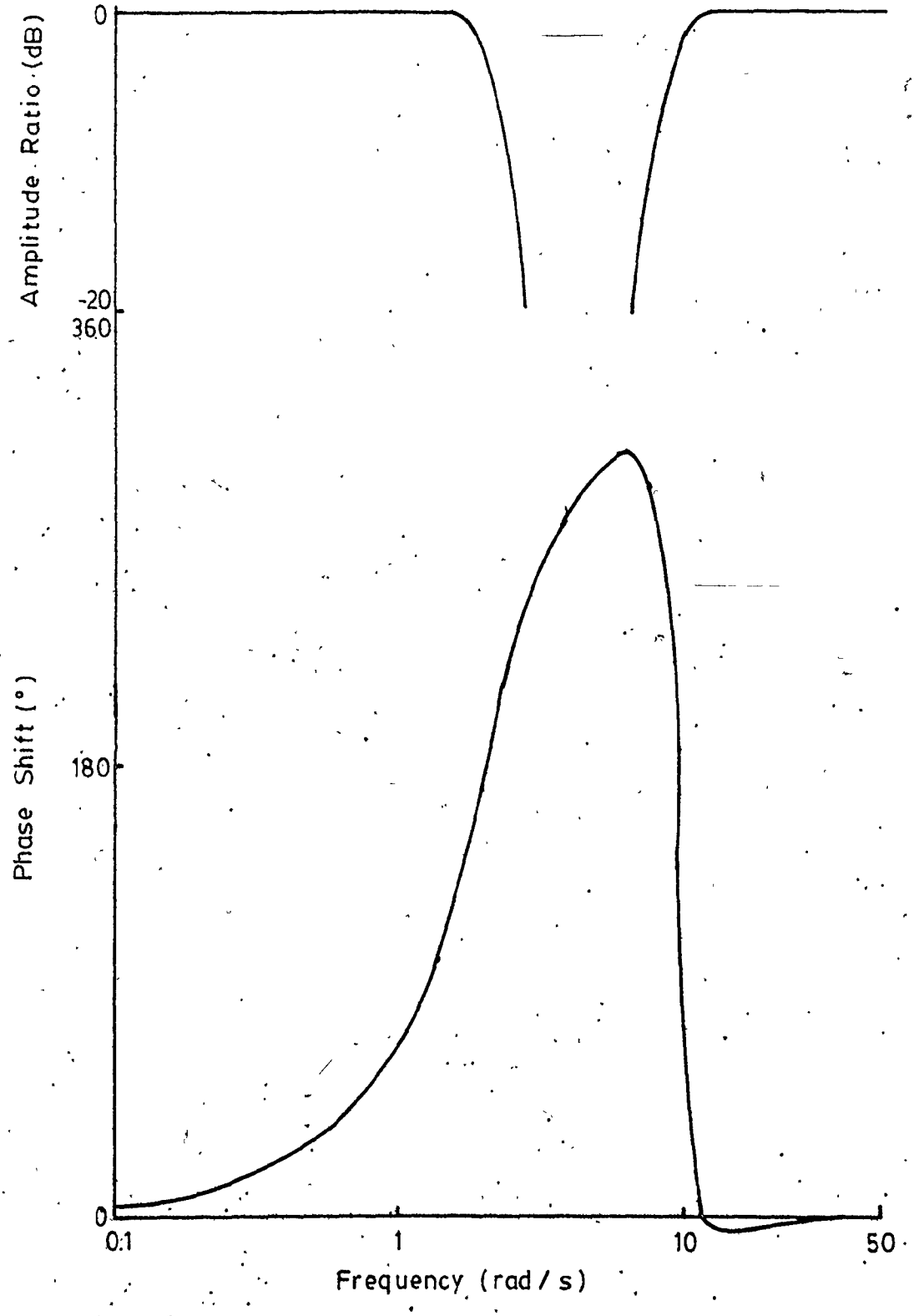

Figure 6.13 Bode Plot for Fourth Order Butterworth Bandstop Filter

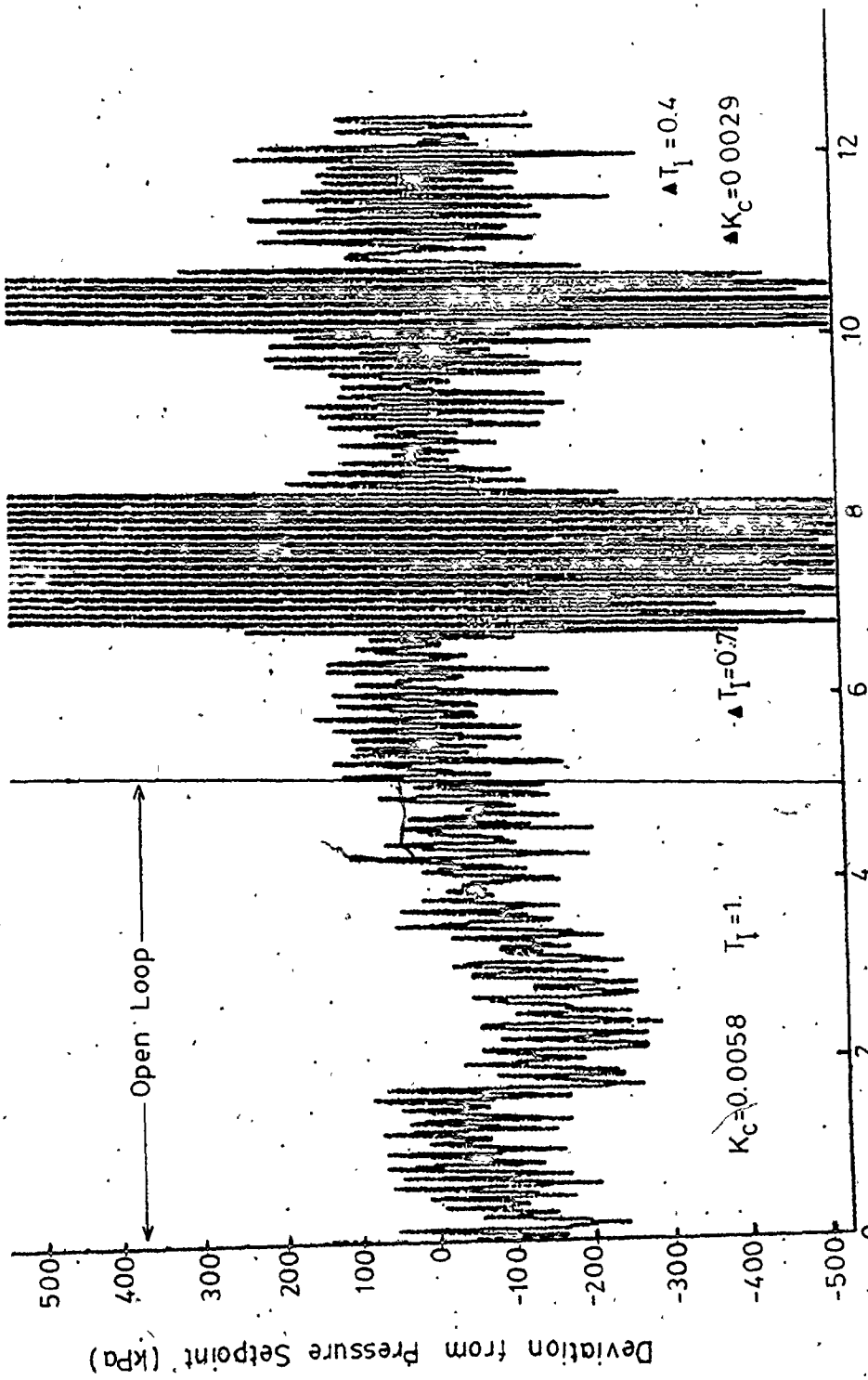

Figure 6.14 Pressure Response, Digital PI Algorithm and Bandstop Filter

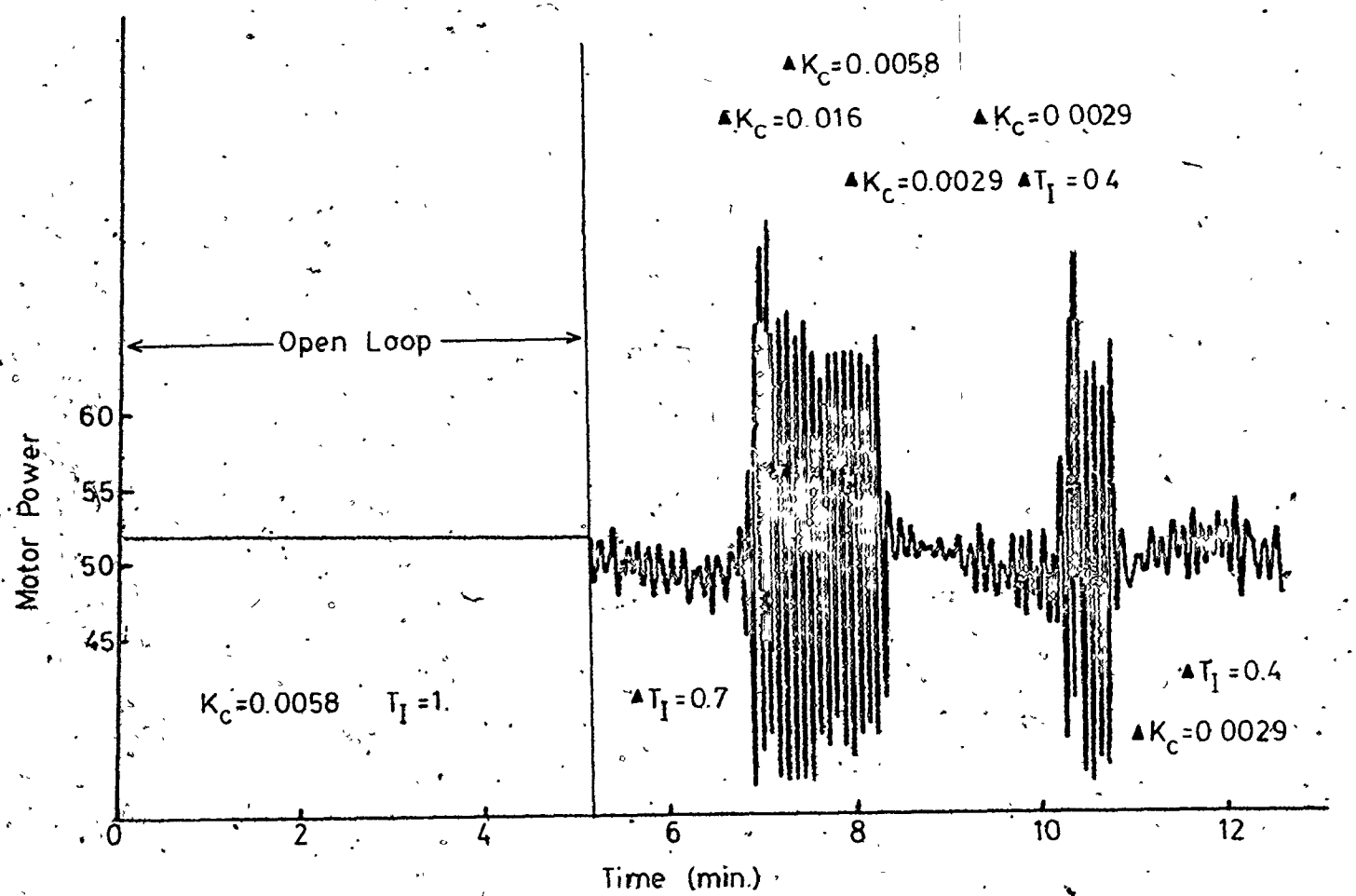

Figure 6.15 Control Action, Digital PI Algorithm and Bandstop Filter

the system gain and phase margins. This increases the stability of the system but lessens the ability of the controller to regulate the process.

Other order bandstop filters were also implemented in the extruder control loop. A second order Butterworth bandstop filter also has 180° phase lead in the bandpass region and was unstable. A first order Butterworth filter was also implemented. This filter did not introduce 180° phase into the system, however, it was found to be of too low order to remove much of the noise. The control achieved with this filter was little improvement over the unfiltered case.

6.5 PI Control and 2 Pole/2 Zero Filter

The previous section discusses the standard method for constructing bandstop filters. It was shown that these filters added too much phase lead to the system for effective control. However, a simpler bandstop filter, with a frequency response as given in Figure 6.16 (a), can be constructed by a transfer function consisting of 2 poles and 2 zeroes given by equation (6.19):

$$H(s) = \frac{(s + \sqrt{ab})^2}{(s+a)(s+b)} \qquad (6.19)$$

The amplitude in decibles at $\sqrt{ab}$ will be approximately $\log(2.) - 1/2 \log\left(\left(\sqrt{\frac{ab}{a}}\right)^2 + 1\right)$. b and a are the upper and lower cutoff frequencies in rad/s. Figure 6.16 (b) shows the construction of the phase response for this filter. It has a possible maximum and minimum phase shift of +90° and -90° respectively. If one does not worry about a non-unity amplitude in the high frequency section, one can construct

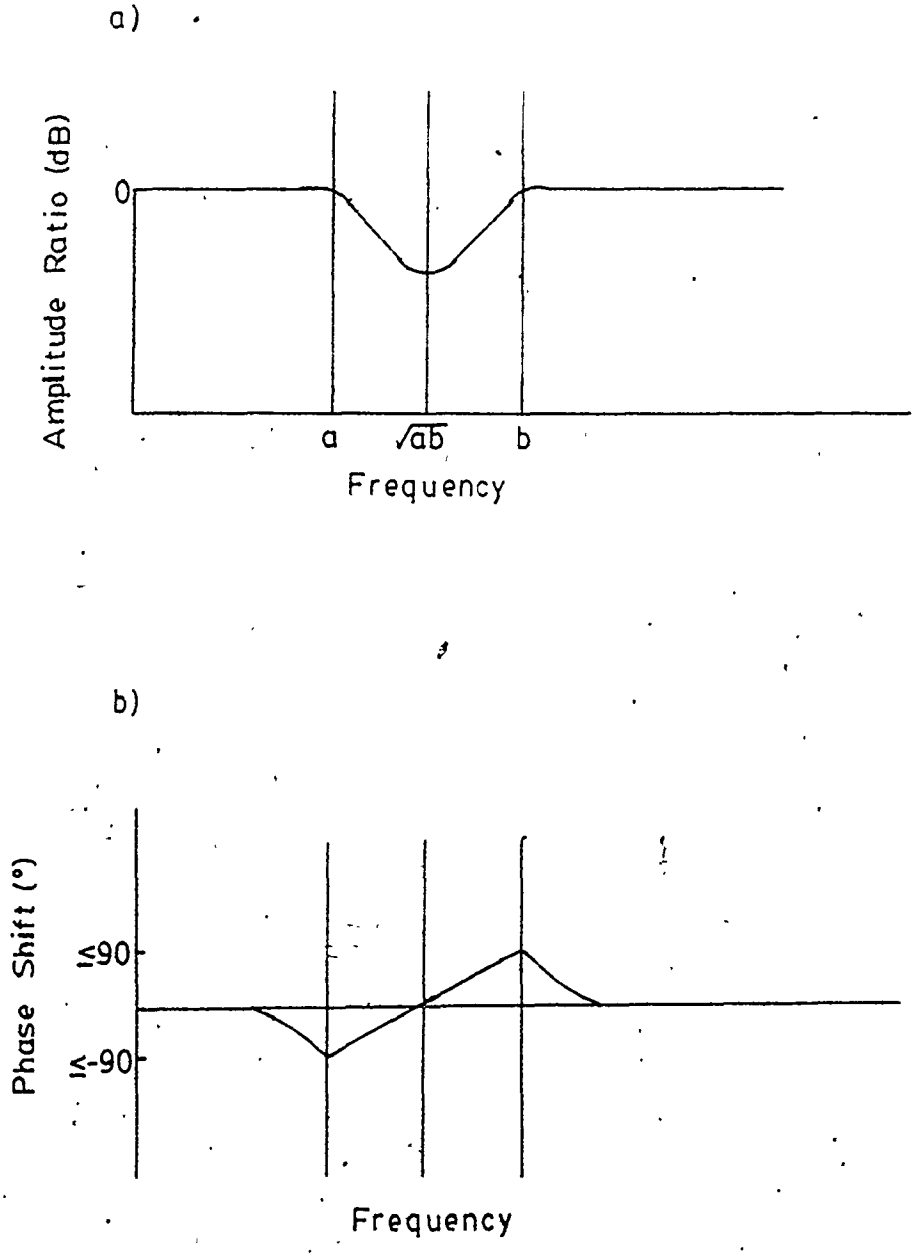

Figure 6.16 Bode Diagram for Various 2 Pole/2 Zero Filters (a) and (b)

(Note: Log-log scale)

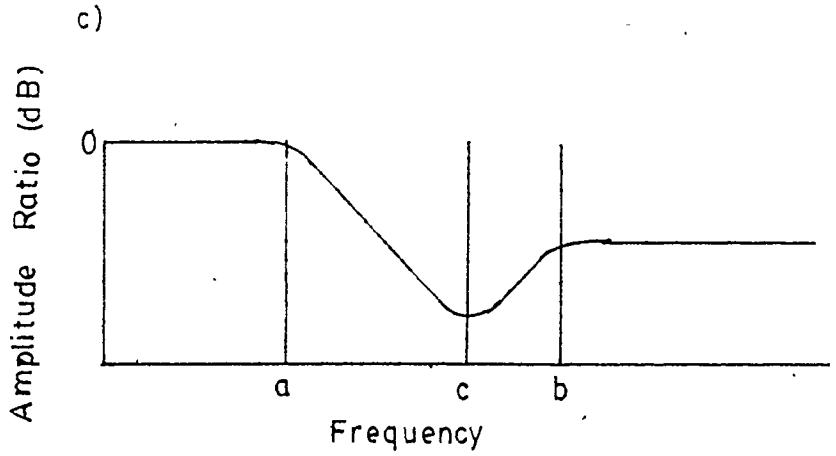

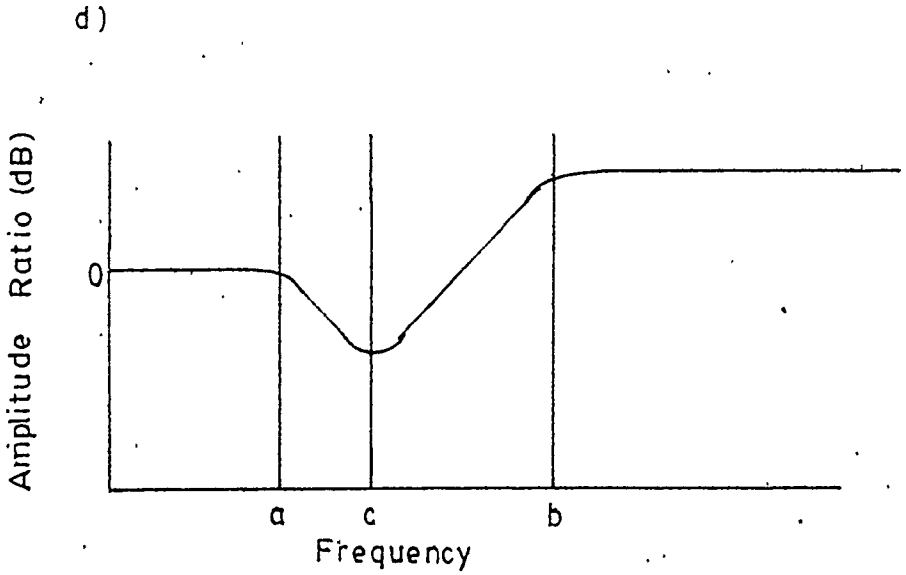

Figure 6.16 Bode Diagram for Various 2 Pole/2 Zero Filters (c) and (d)

(Note: Log-log scale)

narrower filters such as those shown in Figure 6.16 (c) and (d) by replacing the $\sqrt{a\,b}$ term in equation (6.19) with c. c is the center frequency of the filter allowing another degree of freedom in specifying the filter. These types of filters, are similar to lead-lag compensators commonly used by electrical engineers (see for example DiStefano et al(1967)).

For the extruder system, a narrow stop band is desired, between 0.3 Hz and 1.5 Hz (corresponding to 20 r/min and 90 r/min, the operating region of the extruder). A shape like 6.16 (c) was selected with $c = 1.\ (2\pi)$ rad/s. The amplitude at 2. Hz, the control frequency, is 0.45. The filter was digitallized using the bilinear transformation, equation (6.4). The amplitude at 1. Hz was still large, 0.48, so the filter was cascaded with itself to give a filter: $H(s) = (s + c)^4 / ((s + a)^2(s + b)^2)$. This gives an amplitude of 0.23 at 1. Hz. Because of the narrowness of the filter, the amplitude at 2. Hz is only 0.20.

Figure 6.17 (a) and (b) shows the control results for the PI algorithm in combination with the cascaded 2 pole/2 zero filter. The pressure data has been filtered by the 2 pole/2 zero filter. This filtered pressure shows a much smaller deviation from setpoint, due to either the flight noise or the 8 s pressure surging, as compared to Figure 6.1, the PI controller on unfiltered pressure data. However, the important pressure data to examine is the actual pressure that has had the high frequencies removed. Figure 6.18 (a) and (b) shows the actual pressure data after it has been filtered off-line using the same low-pass filter as used for the data of Figure 6.2. Figure 6.18 (b) also includes the actual unfiltered pressure data for comparison.

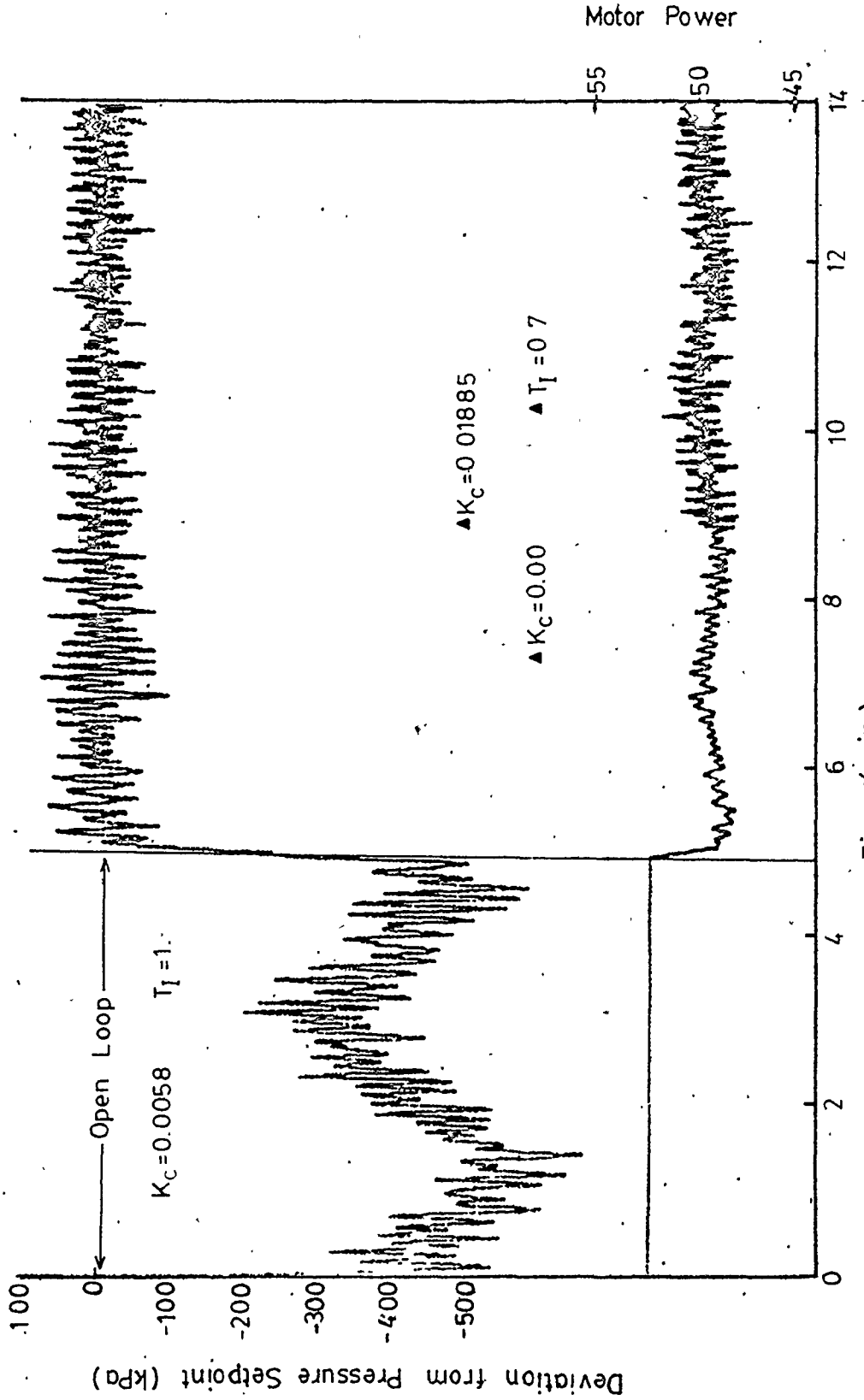

Figure 6.17 (a) Digital PI Control of Pressure, 2 Pole/2 Zero Filter

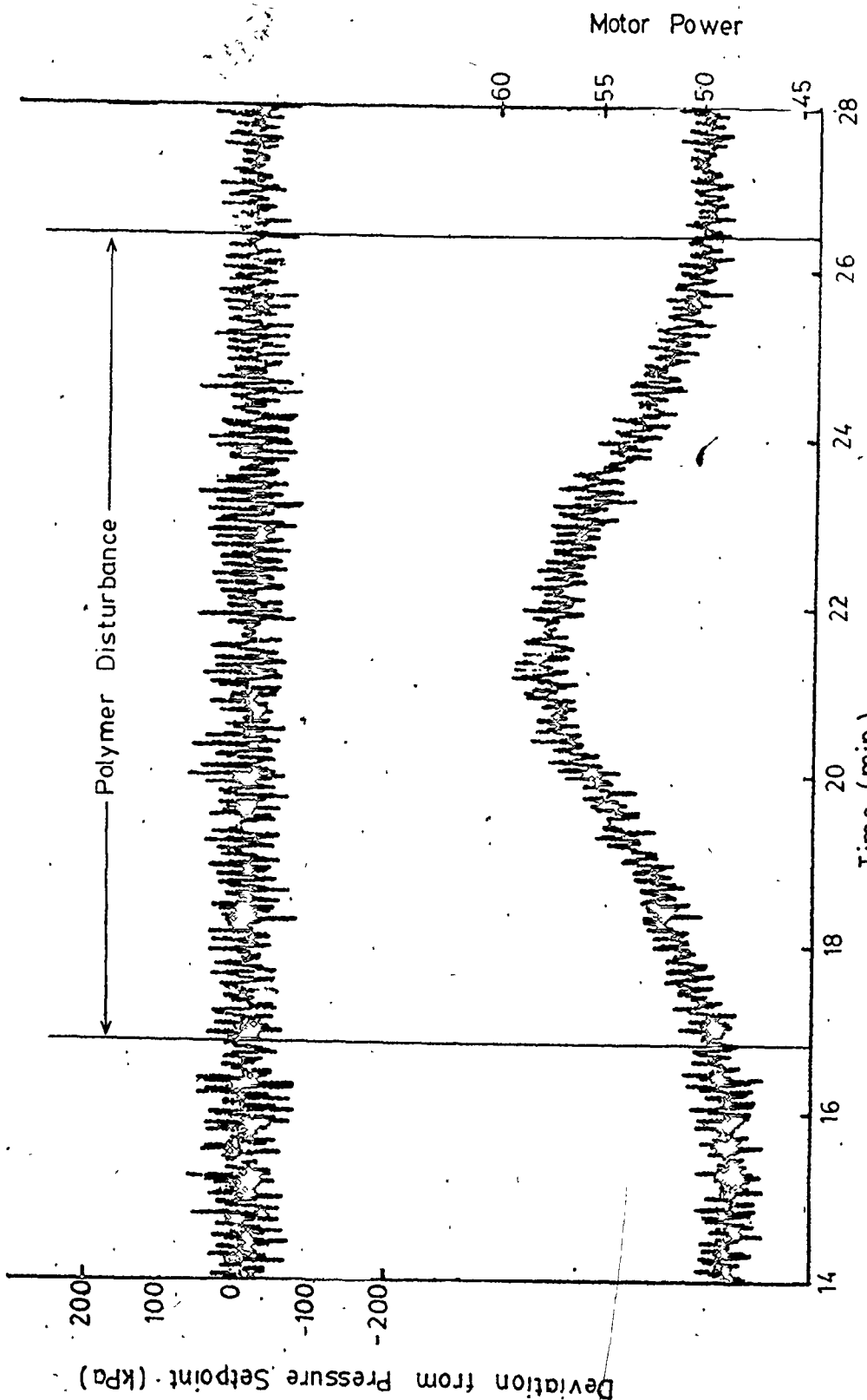

Figure 6.17 (b) Digital PI Control of Pressure, 2 Pole/2 Zero Filter

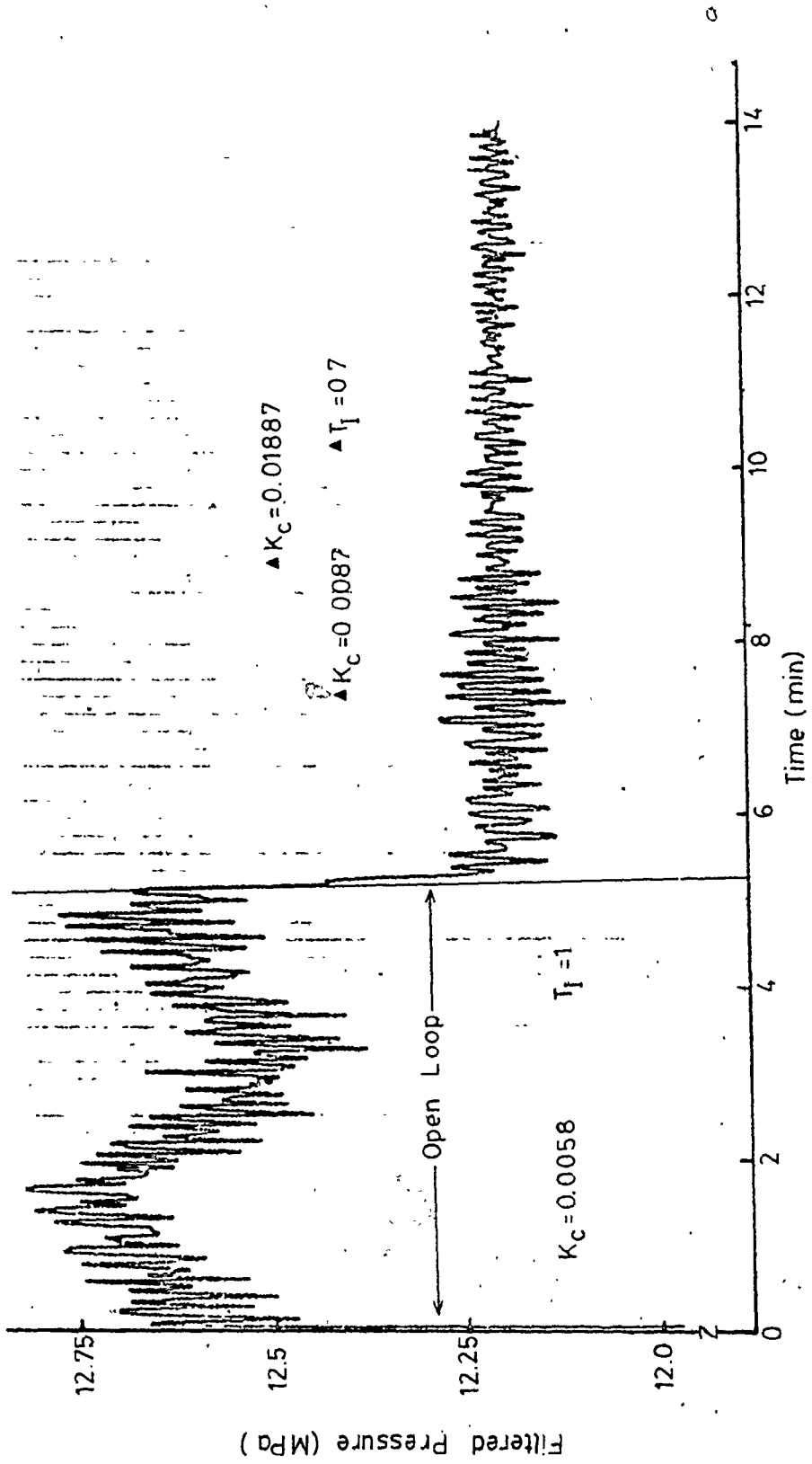

Figure 6.18 (a) Actual Pressure Data of Figure 6.17, Filtered Off-Line

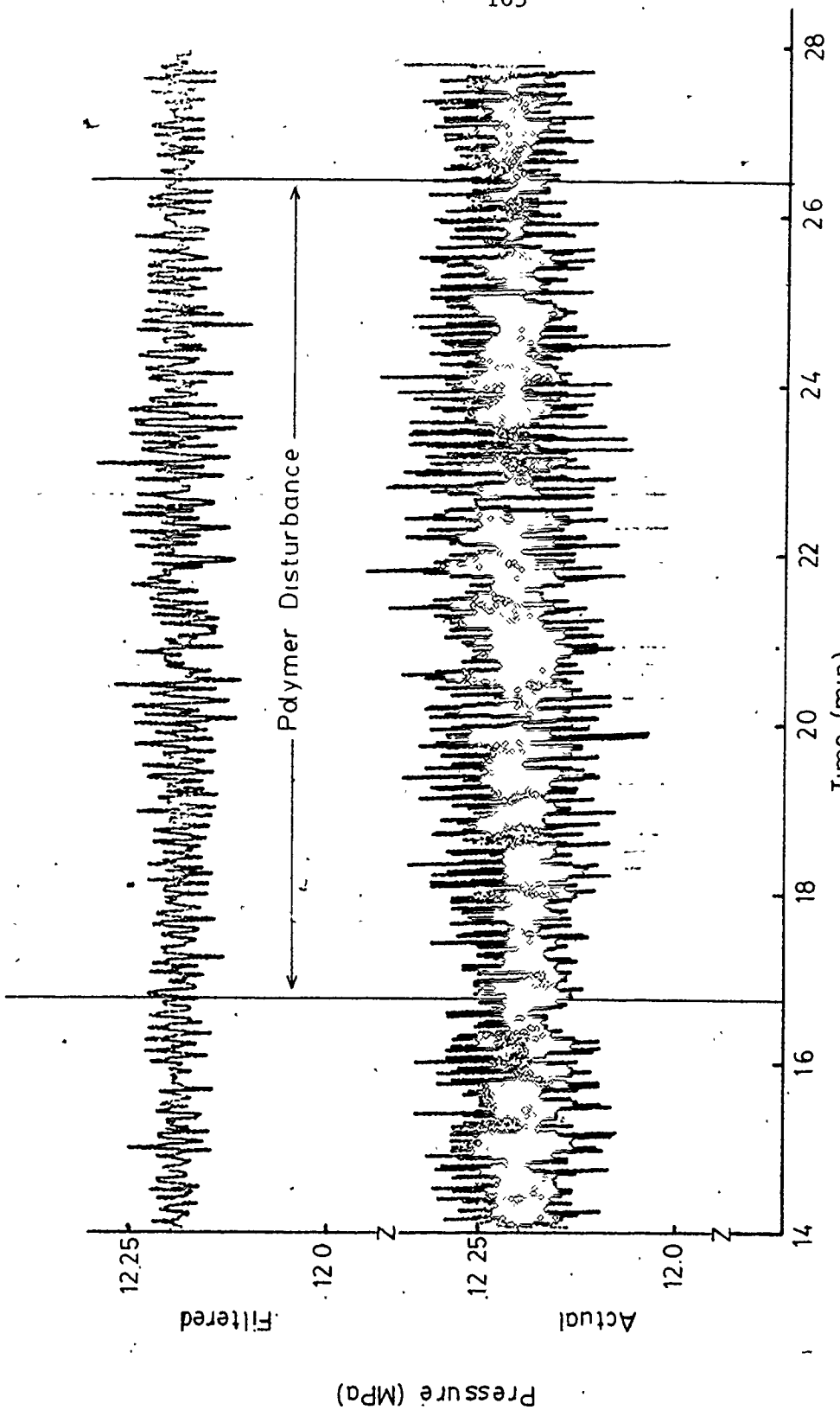

Figure 6.18 (b) Actual and Off-Line Filter Pressure of Figure 6.17

The unfiltered pressure shows considerable high frequency fluctuations that the 2 pole/2 zero filter and the off-line filter removed.

Comparing the off-line filtered pressure of Figure 6.18 to that of Figure 6.2, shows that the inclusion of the 2 pole/2 zero filter in the control loop, reduces the variance of this filtered pressure by between 33 and 50%. The control parameters selected for best tuning in the 2 pole/2 zero case are $K_c = 1.885 \times 10^{-2}$ M.P./kPa and $T_I = 0.7$ s. These are much higher values than those allowed in the unfiltered pressure experiment. For both cases, however, the control deteriorates during the polymer disturbances.

Because of the narrowness of the filter and the resulting 80% attenuation at high frequencies, another filter was constructed for $a = .3(2\pi)$ rad/s, $b = 3(2\pi)$ rad/s and $c = 1(2\pi)$ rad/s. This filter was implemented with a control frequency of 4 Hz; a frequency outside the bandwidth of the filter. The amplitude at 4 Hz is 0.86, 0.74 when the filter is cascaded with itself. The results for this filter cascaded with itself and PI control are shown in Figure 6.19 (a) and (b). The pressure data presented is the off-line filtered data. The variance of this case was further reduced by 20 to 40% over the previous 2 pole/2 zero filter. The final tuning parameters are 2.03×10^{-2} M.P./kPa and 0.8 s, very close to those used in the previous case. Again the control deteriorated during the polymer quality disturbance. The variances during this disturbance are about equal for both Figures 6.18 and 6.19.

Of all the filters used in combination with the PI algorithm, the data of Figure 6.19 shows the most success in the regulation of the

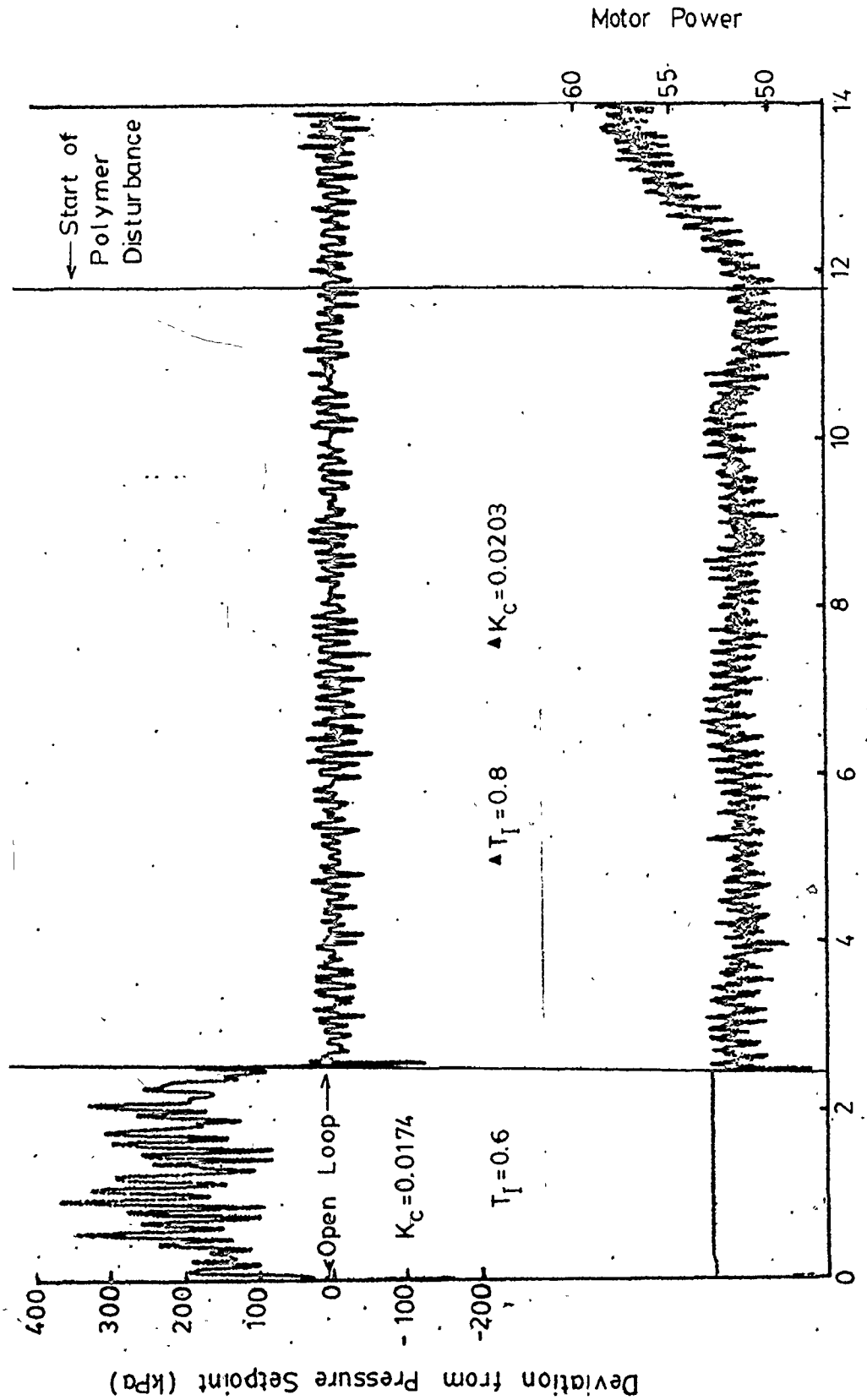

Figure 6.19 (a) Digital PI Control of Pressure, 2 Pole/2 Zero Filter, Control Frequency 4. Hz

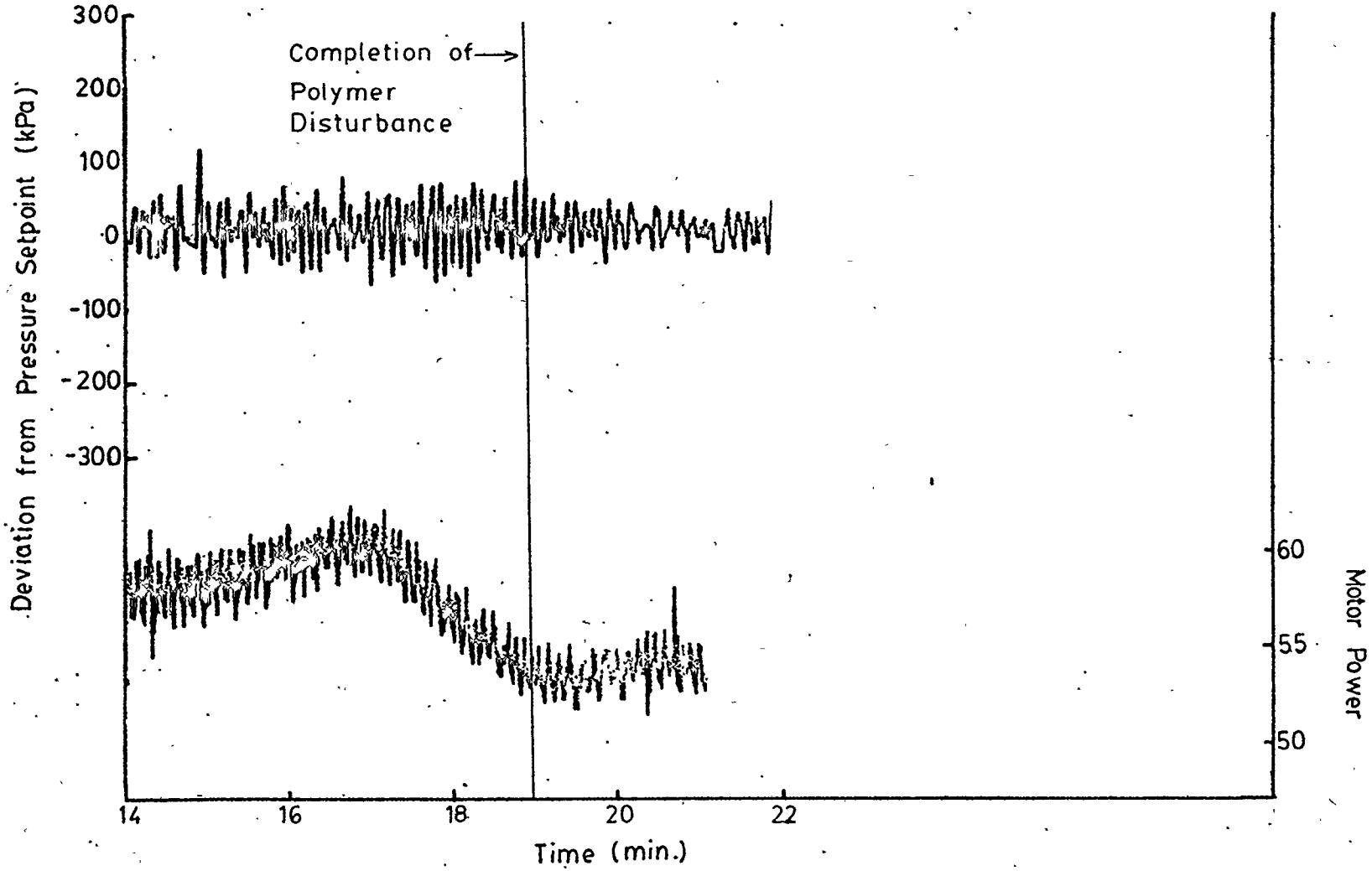

Figure 6.19 (b) Digital PI Control of Pressure, 2 Pole/2 Zero Filter, Control Frequency 4. Hz

8 s pressure surging. It is successful because the filter used attenuates the flight noise without an excessive amount of phase change introduced into the system. The controller can then concentrate more on controlling the 8 s surging and less on the flight noise, without too much danger of destabilizing the system.

However, the filter does considerably affect the process model. This was examined by developing a time series model for the 2 pole/2 zero filter used in Figure 6.17. This model is given in quation (6.20).

$$P_t = \frac{(\omega_0 + \omega_1 Z^{-1} + \omega_2 Z^{-2} + \omega_3 Z^{-3})\ U_{t-1}}{(1. - \delta_1 Z^{-1} - \delta_2 Z^{-2} - \delta_3 Z^{-3} - \delta_4 Z^{-4})} + \frac{(1 - \theta_1 Z^{-1} - \theta_2 Z^{-2} - \theta_3 Z^{-3})}{\nabla(1 - \phi_1 Z^{-1} - \phi_2 Z^{-2} - \phi_3 Z^{-3})} a_t \qquad (6.20)$$

ω_0	=	11.4	± 2.4	kPa/M.P.
ω_1	=	43.2	± 5.0	kPa/M.P.
ω_2	=	61.9	± 5.8	kPa/M.P.
ω_3	=	27.7	± 3.2	kPa/M.P.
δ_1	=	-0.818	± 0.072	
δ_2	=	0.279	± 0.095	
δ_3	=	0.314	± 0.082	
δ_4	=	-0.318	± 0.07	
θ_1	=	0.548	± 0.176	
θ_2	=	-0.397	± 0.129	
θ_3	=	0.569	± 0.067	
ϕ_1	=	0.679	± 0.159	
ϕ_2	=	-0.258	± 0.165	
ϕ_3	=	0.075	± 0.158	

This is quite a complex model in which the transfer function has a considerably increased number of parameters (8 versus 2 in the unfiltered

case, equation (5.11) or 4 in the low-pass filter case, equations (6.6) and (6.7). Even with the large number of parameters in equation (6.20) there are still a few significant lags in the auto and partial correlations of the residuals, indicating that even more parameters would be needed, in the noise model, to reduce the fitting residuals to pure white noise. However, (6.20) should represent the system fairly accurately (the transfer function portion is a very good fit) and is sufficient to study the effect of the filter on the system.

Table 6.2 shows the roots for all the terms of equation (6.20) and their corresponding natural frequencies. Unfortunately, because of the large number of parameters and the unexpected frequencies they identify, one cannot match up individual sections of the model to either the filter or the parameters identified in equation (5.1). The expected frequencies would be close to the values used in the filter, a = 0.3 Hz, b = 1.5 Hz, c = 1. Hz and the pressure surging at 0.125 Hz. Frequency 0.3 Hz appears in $\theta(Z^{-1})$ and 1.5 Hz appears in $\theta(Z^{-1})$, both part of the noise model. Part of the filter is affecting the noise model. Two of the roots of $\omega(Z^{-1})$ lie inside the unit circle in the Z^{-1} plane. This models a non-minimum phase system similar to the models for the low-pass filtered data. This is due to the filter attenuating high frequencies.

A comparison of equations (6.20) and (5.1) shows the vast difference between the process alone and the process including the filter. The first order system of equation (5.1) considered without the flight noise, would be much easier to control than the non-minimum phase system of model (6.20). This is why the PI controller cannot

TABLE 6.2

EVALUATION OF THE ROOTS OF EQUATION (6.20)

Term	Roots	Frequency
$\omega(Z^{-1})$	$-0.489 \pm 0.299i$	Non-minimum phase
	-1.255	-
$\delta(Z^{-1})$	$-0.893 \pm 0.485i$	0.16 Hz
	$1.387 \pm 1.059i$	1.30 Hz
$\theta(Z^{-1})$	$-0.234 \pm 1.206i$	0.36 Hz
	1.165	0.3 Hz
$\phi(Z^{-1})$	$0.655 \pm 2.415i$	0.39 Hz
	2.129	1.50 Hz

totally eliminate the 8 s surging even in the off-line filtered data of Figures 6.18 and 6.19

Figure 6.20 shows the melt temperature response for the data of Figure 6.17. The die wall temperature is always under regulation by the die analog PI temperature controller. However, as shown in Figure 4.4, this controller is poorly tuned and is not regulating the melt temperature properly, causing a cycling with a 1.5 min period. When the new polymer impulse enters the system, the melt temperature follows the control action to a new operating level. It returns to a point slightly above its former level with the return of the old polymer. The die temperature controller is completely unable to maintain the melt temperature at a constant operating level. Future research should look at regulating the melt temperature. The die heater power should be used to regulate the melt temperature instead of the die wall temperature currently regulated.

6.6 Summary

This chapter discusses the process control of the extruder using the combination of the digital PI algorithm and various filters. The filters studied are the low-pass filter, filters derived from Box and Jenkins time series models, bandstop filters and filters formed from a transfer function consisting of 2 poles and 2 zeroes.

The noise that is to be removed by the filter (approximately 1. Hz) lies in between the process disturbance frequency (0.125 Hz) and the control frequency (2. Hz or 4. Hz). The low-pass filter, filtered the control actions as well as the noise and introduced considerable phase lag in the loop, destabilizing the process at high-tuning parameters.

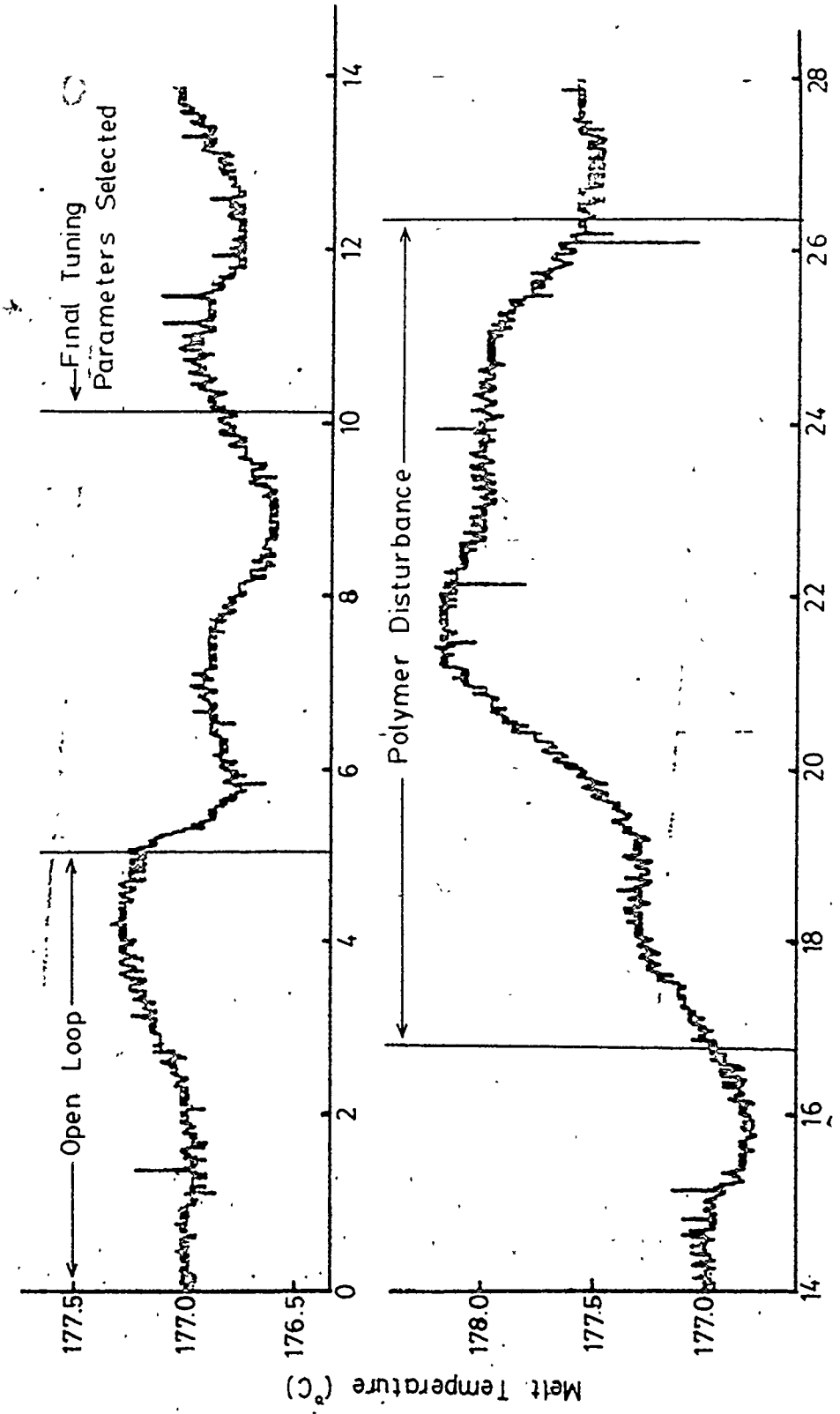

Figure 6.20 Temperature Response for Experiment of Figure 6.17

The inclusion of the low-pass filter in the open loop considerably changed the process transfer function as was demonstrated by two time series models.

The filters derived from Box and Jenkins seasonal models were found to be either inadequate for closed loop filtering or were a form of the bandstop filter. The bandstop filter also destabilized the loop at high tuning giving poor control.

The best control was achieved by using a 2 pole/2 zero filter which removed much of the system signal noise without destabilizing the system at higher control settings. However, this filter also affects the system transfer function and the control does not succeed in completely eliminating all the deviations due to the 0.125 Hz pressure surging.

CHAPTER SEVEN

SELF-TUNING AND MINIMUM VARIANCE CONTROL

7.1 Self-Tuning and Minimum Variance Control Theory

After using the PI algorithm (discussed in Chapter 6) to control the extruder pressure, the self-tuning regulator (STR) algorithm was implemented to control the same process. The PI algorithm was only able to partially compensate for the 8 s surging and the control deteriorated as a polymer disturbance entered the system. It was expected that the STR would give improved control due to its structure and its ability to compensate for changing process conditions. The STR structure, as shown below, is selected based on knowledge of the process and its disturbances. It is therefore better prepared to control both the process and its related disturbances. The STR tunes its parameters based on the discounted recursive least squares algorithm given below. The STR is also easy to implement, involving the addition of a 30 line FORTRAN computer subroutine to the control program (program listings are given in Appendix B).

The self-tuning algorithm has been presented by many authors (i.e. Borrison and Syding(1976) and Harris et al(1980)). The control is calculated by equation (7.1):

$$VU_t = \frac{-(\alpha_o + \alpha_1 Z^{-1} + \ldots + \alpha_m Z^{-m})\ Y_t}{(\beta_o + \beta_1 Z^{-1} + \ldots + \beta_\ell Z^{-\ell})} \qquad (7.1)$$

whose parameters ($\alpha_o \ldots \alpha_m$, $\beta_o \ldots \beta_\ell$) are determined by the discounted recursive least squares algorithm, equation (7.2).

$$\underline{\theta}_{t+1} = \underline{\theta}_t + \underline{K}_t \left[Y_t - \beta_o \nabla U_{t-f-1} + \xi \nabla U_{t-f-1} - \underline{\psi}^T_{t-f-1} \underline{\theta}_t\right]$$

$$\underline{K}_t = \underline{\underline{P}}_t \underline{\psi}^T_{t-f-1} \left[\lambda + \underline{\psi}_{t-f-1} \underline{\underline{P}}_t \underline{\psi}^T_{t-f-1}\right]^{-1} \tag{7.2}$$

$$\underline{\underline{P}}_{t+1} = \left[\underline{\underline{P}}_t - \underline{K}_t \left[\lambda + \underline{\psi}_{t-f-1} \underline{\underline{P}}_t \underline{\psi}^T_{t-f-1}\right] \underline{K}^T_t\right]/\lambda$$

where $\underline{\theta}_t = [\alpha_o \alpha_1 \ldots \alpha_m \ \beta_1 \beta_2 \ldots \beta_\ell]^T$

$\underline{\psi}_t = [Y_t \ Y_{t-1} \ldots Y_{t-m} \ \nabla U_{t-1} \ldots \nabla U_{t-\ell}]^T$

$\underline{\underline{P}}_t$ is the normalized covariance matrix of the parameter estimates

$\underline{K}_t$ is a vector weighing the error at time t

and $\underline{\theta}_t$ is the vector of calculated parameters.

The tuning parameter λ is a forgetting factor for past data. The asymptotic window length or the effective number of observations used in the estimation routine is $(1 - \lambda)^{-1}$. The range of $0.95 \leq \lambda \leq 1$ is usually chosen which gives effective window lengths of 20. to infinity (there is no discounting of past values for $\lambda = 1$).

The ξ in equation (7.2) is a constraining factor weighing the past control actions. A value of $\xi = 0$ will tune controller (7.1) to the minimum variance control equation, provided the structure (the values of m and ℓ) are correct. The constraining factor is generally very effective in reducing the variance of the manipulated variable without significantly increasing the variance of the controller variable. It is especially useful for non-minimum phase systems. These systems have unstable minimum variance controllers but can be

stabilized by constrained STR or M.V. controllers.

Generally, the values of m and ℓ are chosen from the minimum variance control structure. This can be most easily demonstrated through an example. Taking the time series model developed in Chapter 5, equation (5.1):

$$\nabla_s P_t = \frac{\omega_o(1 - \omega_s Z^{-s} - \omega_{s+1} Z^{-s-1})\, U_{t-1}}{(1 - \delta Z^{-1})} + \frac{(1 - \theta_1 Z^{-1} - \theta_2 Z^{-2})\, a_t}{(1 - \phi_1 Z^{-1} - \phi_2 Z^{-2})} \quad (5.1)$$

(5.1) can be rewritten to include the ∇_s term in the noise model (along with the $(1 - \omega_s Z^{-s} - \omega_{s+1} Z^{-s-1})$ term which cancels the ∇_s factor). (5.1) becomes (7.3):

$$P_t = \frac{\omega_o}{1 - \delta Z^{-1}} U_{t-1} + \frac{(1 - \theta_1 Z^{-1} - \theta_2 Z^{-2})}{(1 - \phi_1 Z^{-1} - \phi_2 Z^{-2})\, \nabla_s} a_t \quad (7.3)$$

The ∇_s term models the flight noise. Normally this non-stationary term would be compensated by a non-stationary control action. The controller would try to match the cycling due to the flight noise by a corresponding cycling in the control action. However, it is desired that the controller not take action based on the flight noise. Additionally, in most cases the flight noise will be removed by a filter eliminating the need for the ∇_s term in the model. Therefore the ∇_s term was replaced in the model by one of its roots, $(1 - Z^{-1})$, the difference operator. The ∇ term forces the minimum variance (M.V.) controller to include integral action, which eliminates any offsets or level changes in the process. Equation (7.3) becomes (7.4):

$$P_t = \frac{\omega_o}{1 - \delta Z^{-1}} U_{t-1} + \frac{(1 - \theta_1 Z^{-1} - \theta_2 Z^{-2})}{(1 - \phi_1 Z^{-1} - \phi_2 Z^{-2})\, \nabla} a_t \quad (7.4)$$

The general minimum variance controller has the following form:

$$\nabla^d U_t = \frac{\delta(Z^{-1})\ T(Z^{-1})\ P_t}{\omega(Z^{-1})\ \psi_1(Z^{-1})\ \phi(Z^{-1})} \tag{7.5}$$

All the factors of equation (7.5) are determined from the process transfer function plus noise time series model. $\psi_1(Z^{-1})$ is a polynomial in Z^{-1}, of order f (where f is the number of whole periods of delay in the transfer function part of the noise model), which predicts P_t in terms of past a_t's. For equation (7.4), f = 0, $\psi_1(Z^{-1}) = 1$. $T(Z^{-1})$ is determined from equation (7.6).

$$\theta(Z^{-1}) = \psi_1(Z^{-1})\ \phi(Z^{-1})\nabla^d + T(Z^{-1})\ Z^{-f-1} \tag{7.6}$$

For model (7.4), equation (7.6) becomes (7.7).

$$(1 - \theta_1 Z^{-1} - \theta_2 Z^{-2}) = (1 - Z^{-1})(1 - \phi_1 Z^{-1} - \phi_2 Z^{-2}) + T(Z^{-1})Z^{-1} \tag{7.7}$$

Using the values listed in Chapter 5 for equation (5.1) in equation (7.7) yields

$$T(Z^{-1}) = 1.588 - 2.296Z^{-1} + 0.869Z^{-2}$$

Finally the minimum variance controller calculated by (7.5) becomes:

$$\nabla U_t = \frac{-(1.588 - 2.742Z^{-1} + 1.514Z^{-2} - 0.244Z^{-3})\ P_t}{70.7\ (1 - 1.722Z^{-1} + 0.869Z^{-2})} \tag{7.8}$$

The ∇ term forces the controller to include integral action. The $(1 - 1.722Z^{-1} + 0.869Z^{-2})$ which models the 8 s surging in model (7.4), forces the controller to take control action matching this 8 s surging.

The denominator of equation (7.8) includes terms for the inverse of the plant dynamics and for the prediction for the noise model. This controller will compensate for any disturbances, to a system of model (7.4), in one sampling period.

Normally, the orders for m and ℓ would be selected from controller (7.8) as m = 3 and ℓ = 2. However, because of the relatively small value of the term $\alpha_3 = -0.244$, the order of m was selected as m = 2, to simplify the calculations. Initial guesses for the STR parameters can also be selected from (7.8).

In much of the literature on the STR algorithm, there is some controversy as to whether the β_0 parameter of equation (7.1) should be constant. Poor guesses of a fixed β_0 can cause problems of system stability and poor convergence. However, if β_0 is being estimated, poor behavior in the algorithm can occur when the parameters converge (such as momentary "bursts" in the parameter values). Usual practice is to estimate β_0 until the parameters converge and then to set it to this constant value. For the STR used in this thesis, β_0 was fixed, mainly to simplify the calculations by reducing the matrix sizes and the computation time. The value of β_0 was taken as ω_0. This is a good estimate that would avoid any problems of stability or convergence.

7.2 Self-Tuning Regulator Experiments

The self-tuner theory presented in the previous section was implemented on the extruder to compare it to the digital PI algorithm. It was hoped that the larger structure and the parameter following characteristics of the STR would yield improved control over the PI cases.

Figure 7.1 shows the results for the STR with a 0.5 s control interval, acting on the unfiltered pressure data. A short period of tuning the STR constraining factor follows 5 min of open loop data. Note the small amount of offset from the setpoint during the open loop period and its immediate correction when the loop is closed. ξ = 6.9 kPa/M.P. is chosen as the "best" tuning for the STR constraining factor. As in the PI control experiments, the STR was tested for its ability to regulate a disturbance in polymer quality. The STR was very successful in eliminating any long term drifts or offsets caused by the polymer disturbance. This ability was due to the inclusion of integral action in the controller. The pressure data looks very similar to the unfiltered PI control presented in Figure 6.1. However, by comparing the graphs of the control actions taken, presented in Figures 6.1 and 7.1, one can see that the STR takes considerably more control action than the PI algorithm, especially during the polymer disturbance.

Figure 7.2 shows the pressure data of Figure 7.1 filtered off-line by a low-pass filter. This removed the high frequency pressure components that would not be affecting the product, leaving the 8 s pressure surging. The 8 s surging is quite noticeable with a variance comparable to that of Figure 6.2 but considerably higher than the PI algorithm in combination with the 2 pole/ 2 zero filters. The unfiltered STR achieved comparable results to the unfiltered PI but takes considerably larger control actions. This means that the extruder motor is doing more work, with greater electrical usage and more wear on the moving parts, for the same level of control.

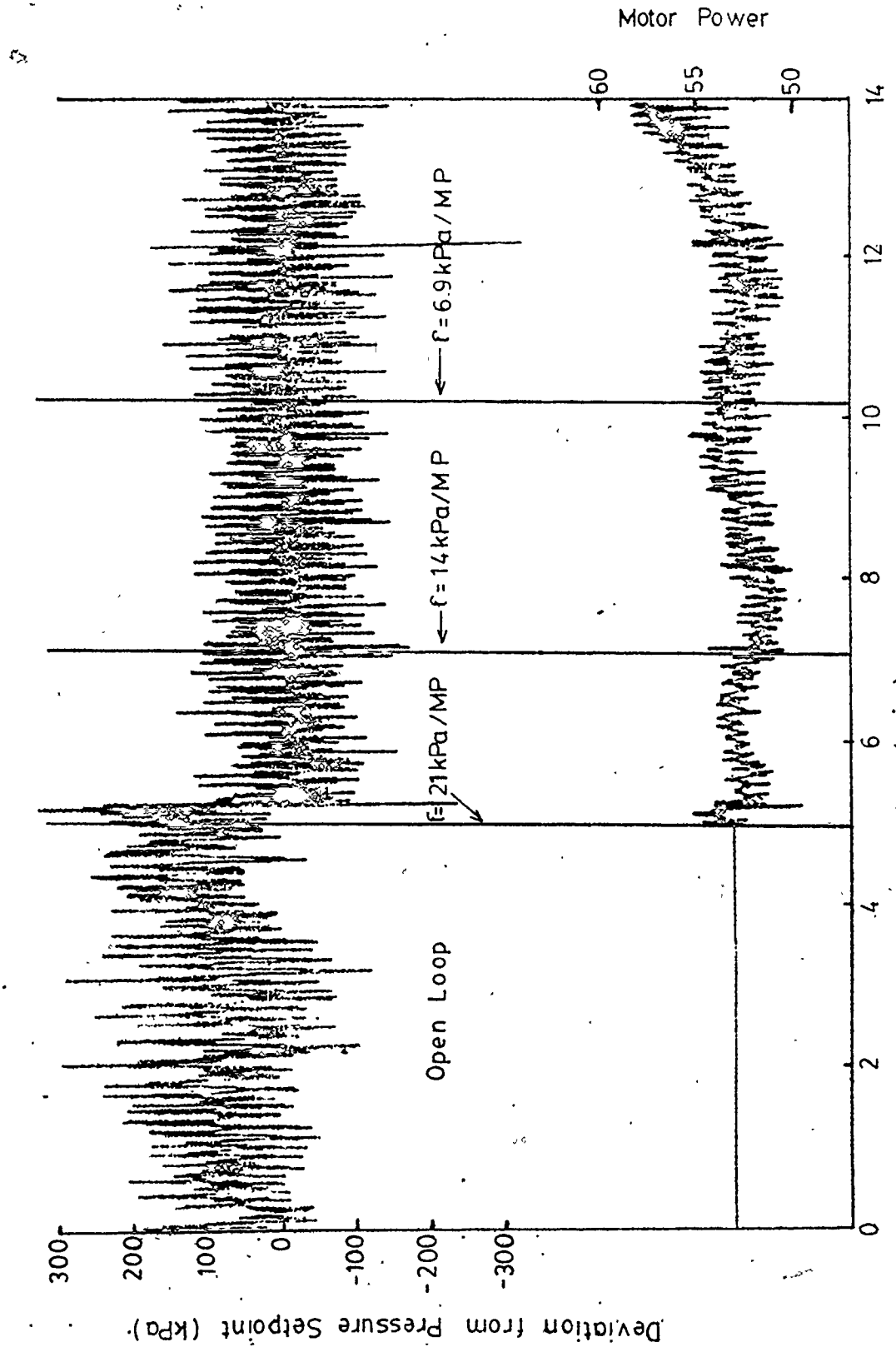

Figure 7.1 (a) Self-Tuning Regulation of Pressure

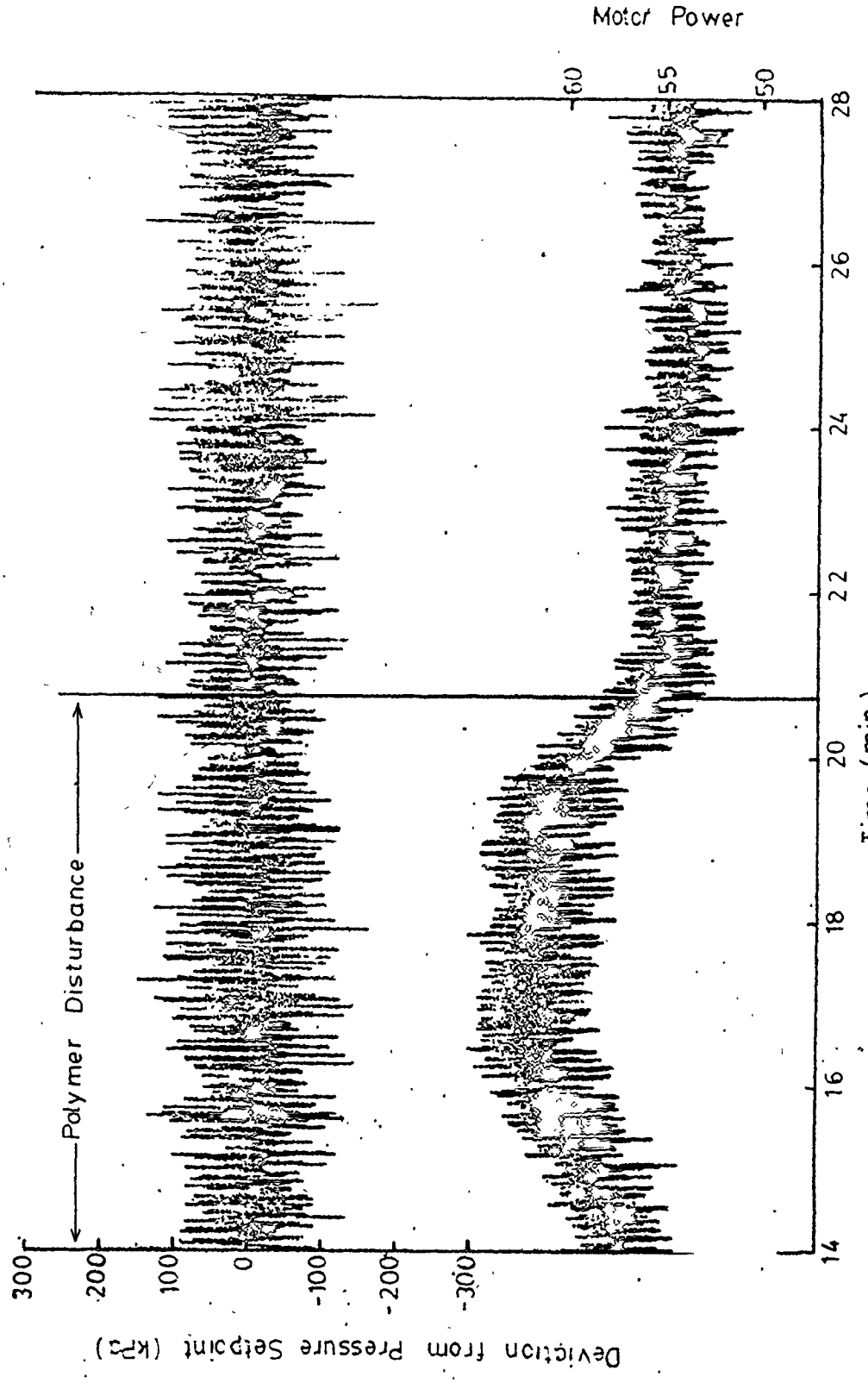

Figure 7.1 (b) Self-Tuning Regulation of Pressure

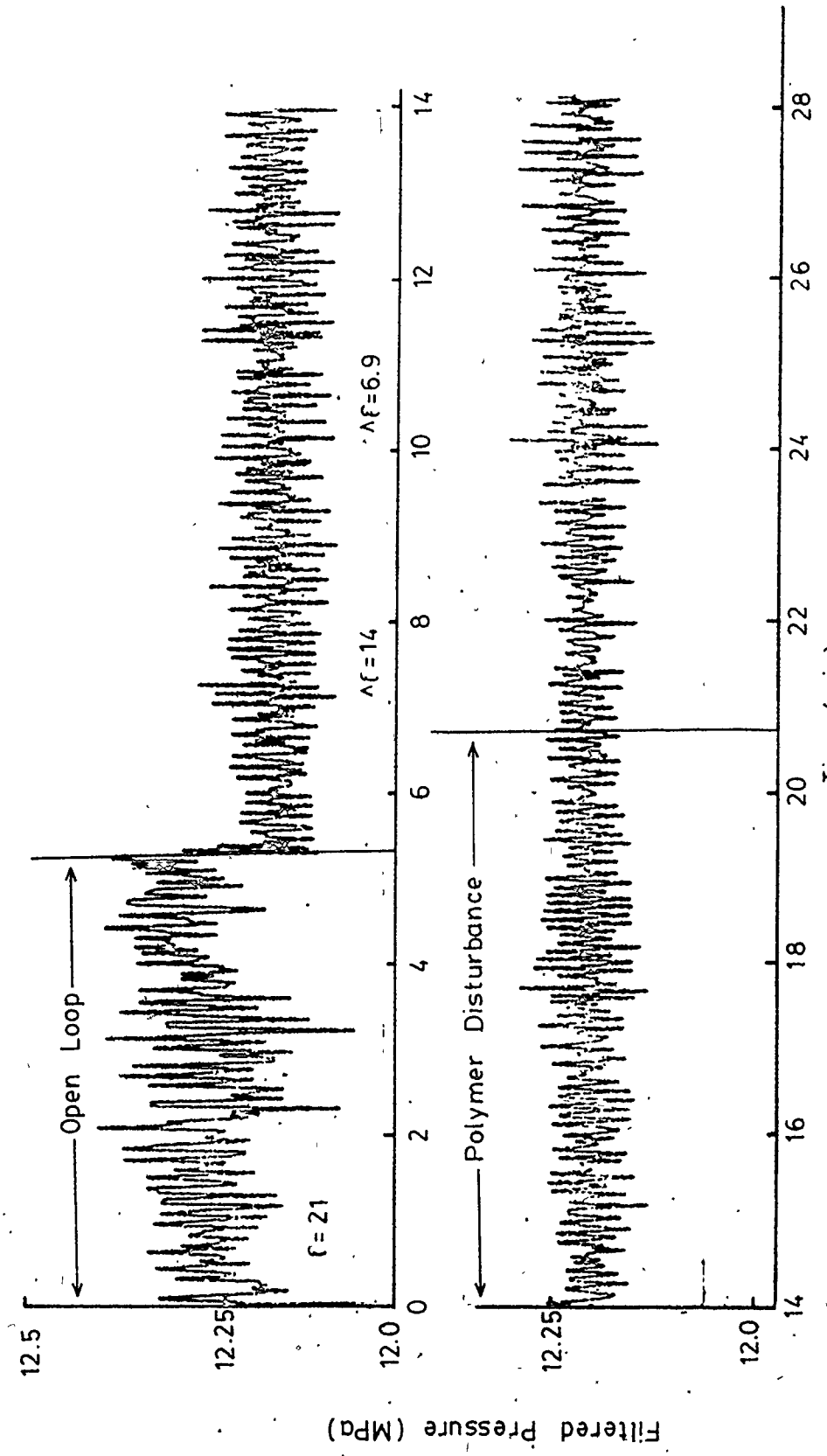

Figure 7.2 Pressure Data of Figure 7.1 Filtered Off-Line

As in the case for the unfiltered PI controller, the STR is taking control action on the flight noise, thereby not effectively regulating the 8 s surging. In the STR case, it can tune itself to try and more optimally (for its present structure) eliminate the signal noise, which is seen as the most significant disturbance. Therefore, it will take larger high frequency control actions than the PI algorithm.

A typical STR controller equation, found by taking representative tuning parameters, is presented in the first row of Table 7.1. The STR has tuned its poles into a controller that will regulate a sinusoidal disturbance of 0.186 Hz, that is alternating in sign at every sample. In other words, it is modelling a sine wave of frequency 0.186 Hz overlayed with another disturbance of 1. Hz. This is the STR tuning for a compromise between the 8 s surging, the flight noise and the level of constraining of the controller. This compromise is ineffective in regulating either the flight noise or the surging. This tuning is what one would expect the STR would do for the case where the flight noise is an actual process disturbance which the STR would be desired to regulate. However, it is actually desired that the STR ignore the flight noise for both control and estimation.

At a sampling frequency of 2 Hz, the flight noise, which lies between 0.8 Hz and 1. Hz (for 50 to 60 r/min), is close to the Nyquist frequency of 1. Hz. The STR would have difficulty identifying the flight noise at these frequencies and therefore, the constraining factor can be relatively low. In order to study this effect on STR with control

TABLE 7.1

CONTROLLERS DETERMINED BY STR TUNING

Experiment	Controller (P_t in units kPa)	Comments
Unfiltered	$VU_t = \frac{-(0.625 + Z^{-1})\ P_t}{76.(1.+1.59Z^{-1}+0.9Z^{-2})}$	frequency = 0.186 Hz identify a sinusoid of 0.186 Hz frequency alternating in sign at each sample
Unfiltered 0.25 s control interval	$VU_t = \frac{-(0.75-0.56Z^{-1}+0.625Z^{-2})P_t}{145.(1-0.48Z^{-1}+0.90Z^{-2})}$	numerator d = 0.95 f = 0.33 Hz denominator d = 0.91 f = 0.37 Hz
	$VU_t = \frac{-.75(1-0.75Z^{-1}+0.83Z^{-2})P_t}{145.(1-0.48Z^{-1}+0.90Z^{-2})}$	
	$\approx -0.75/45.$	gain
Cascaded first 2 pole/2 zero filter	$VU_t = \frac{-2.9\ P_t}{91.(1+0.8Z^{-1}+0.8Z^{-2})}$	d = 0.89 f = 0.35 Hz identifying filter
Cascaded first 2 pole/2 zero filter disturbance	$VU_t = \frac{-(3.75+3.75Z^{-1}-1.875Z^{-2})P_t}{91.(1+1.44Z^{-1}+0.96Z^{-2})}$	numerator roots Z^{-1} = 2.73 (2.Hz) =-0.73 denominator d = 0.98 f = 0.20 Hz
Minimum variance controller equation (7.8)	$VU_t = \frac{-(1.588-2.742Z^{-1}+1.514Z^{-2}-0.244Z^{-3})P_t}{70.7(1-1.722Z^{-1}+0.869Z^{-2})}$	numerator f = 2.56 Hz d = 0.74 f = 0.0676 Hz denominator d = 0.93 f = 0.125 Hz

frequency of 4 Hz was implemented. This case needed a very high constraining factor (75.8 kPa/M.P. as opposed to 6.9 kPa/M.P. for the previous case, 2 Hz control frequency). Table 7.1 shows the controller parameters. These parameters have been tuned by the STR to become equivalent to one gain term. This reduces the controller to an integral controller. The STR determines that almost all the disturbance corresponds to the high frequency signal noise that it tries to track with equally quick control actions. The high constraining prevents the controller from tuning to a sinusoidal response to compensate even more effectively for the flight noise.

In an attempt to remove the flight noise and achieve improved control, the fourth order Butterworth bandstop filter of section 6.4 was implemented in combination with the STR algorithm. The STR was allowed to run for the first 400 control intervals on the unfiltered pressure data. After the 400 intervals, the filter was included in the closed loop. Immediately, the system became unstable. The addition of the filter destabilized the system. A very large value of 275 kPa/M.P. was needed for the constraining factor, to stabilize the system. At this level of constraint, the STR was taking almost no control action and was unable to regulate the system. The STR poles remained outside the unit circle (in the Z^{-1} plane) when the filter was added to the system, indicating that the controller itself was stable, while the system was not. These results were very similar to those achieved using the PI algorithm and the same bandstop filter. Further attempts to use this filter were abandoned.

Figure 7.3 (a) and (b) shows the results for the twin cascaded 2 pole/2 zero filter previously used for the data of Figure 6.17. Figure 7.4 (a) and (b)gives the pressure results that have been filtered off-line to remove the high frequencies. The variances were equivalent to the same experiment using the PI algorithm. During the new polymer impulse, the algorithm had a small amount of offset from the setpoint pressure. The control action taken during the polymer disturbance was bigger under STR control than under PI control. Again for this case, the performance of the STR was inferior to the comparable digital PI experiment. In addition when first initiated, the STR became unstable. It was quickly stabilized by increasing the constraining factor. When the constraining factor was subsequently lower, the STR remained stable. The problem was due to the STR initially tuning the algorithm into a controller that cycled between software limits in the control action. This system non-linearity did not allow the STR to retune to a stable system. This problem can occur during the initial period of self tuning control when the algorithm only has a limited amount of information. The STR may then find poor, unstable estimates for the control parameters.

The plot of the parameters determined by the STR are presented in Figure 7.5 (a) and (b). After the initial tuning period, the parameter values converge to a controller approximated by $VU_t = -(2.9 + 0(Z^{-1}) + 0(Z^{-2}))P_t / (91.(1. + 0.8Z^{-1} + 0.8Z^{-2}))$. The zeroes are reduced to a gain term and the poles model a damped sinusoid with a frequency of 0.35 Hz. This is very close to the frequencies that appear in the noise portion of the time series model (6.20), and

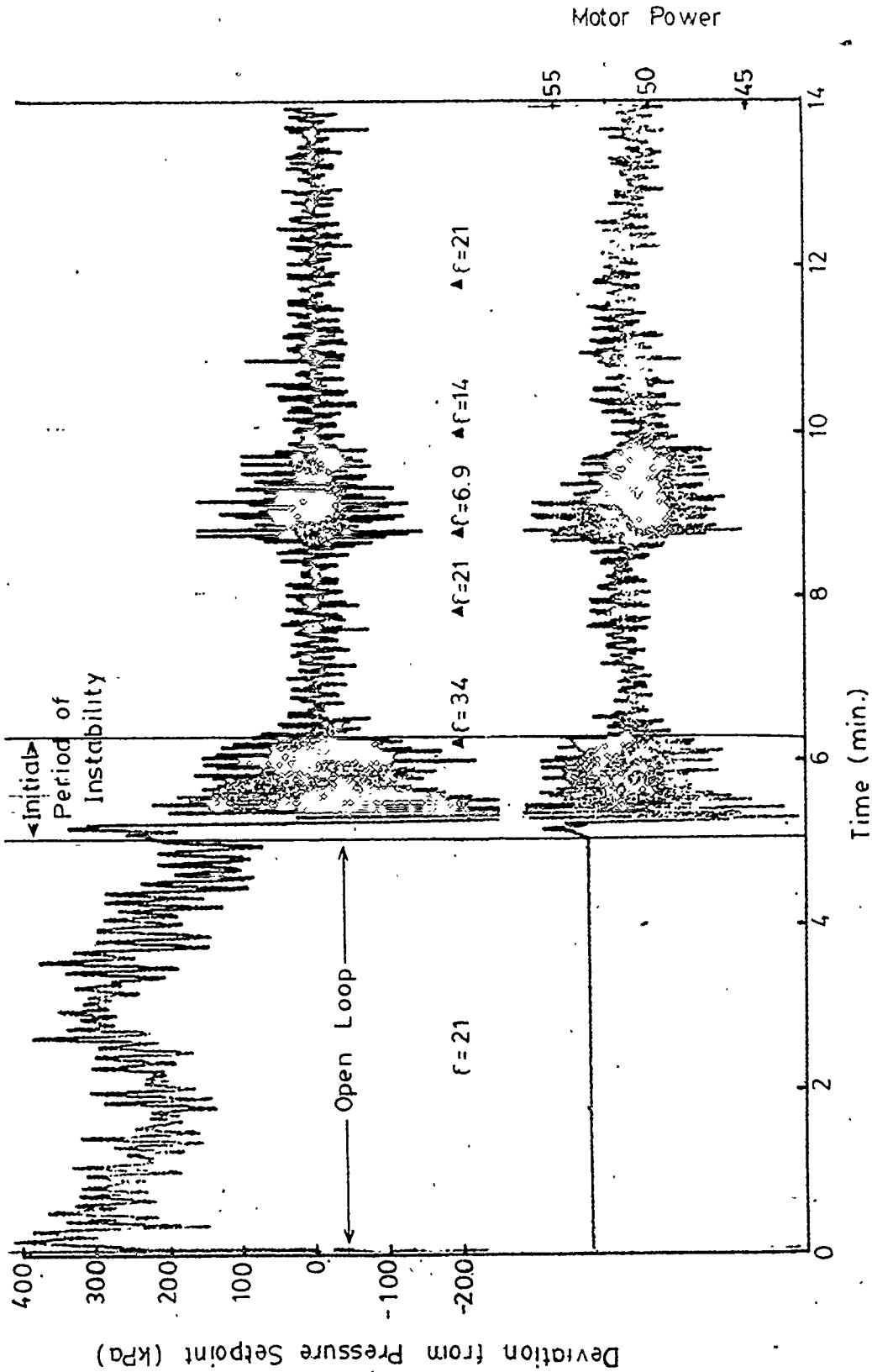

Figure 7.3 (a) Self-Tuning Regulation of Pressure, 2 Pole/2 Zero Filter

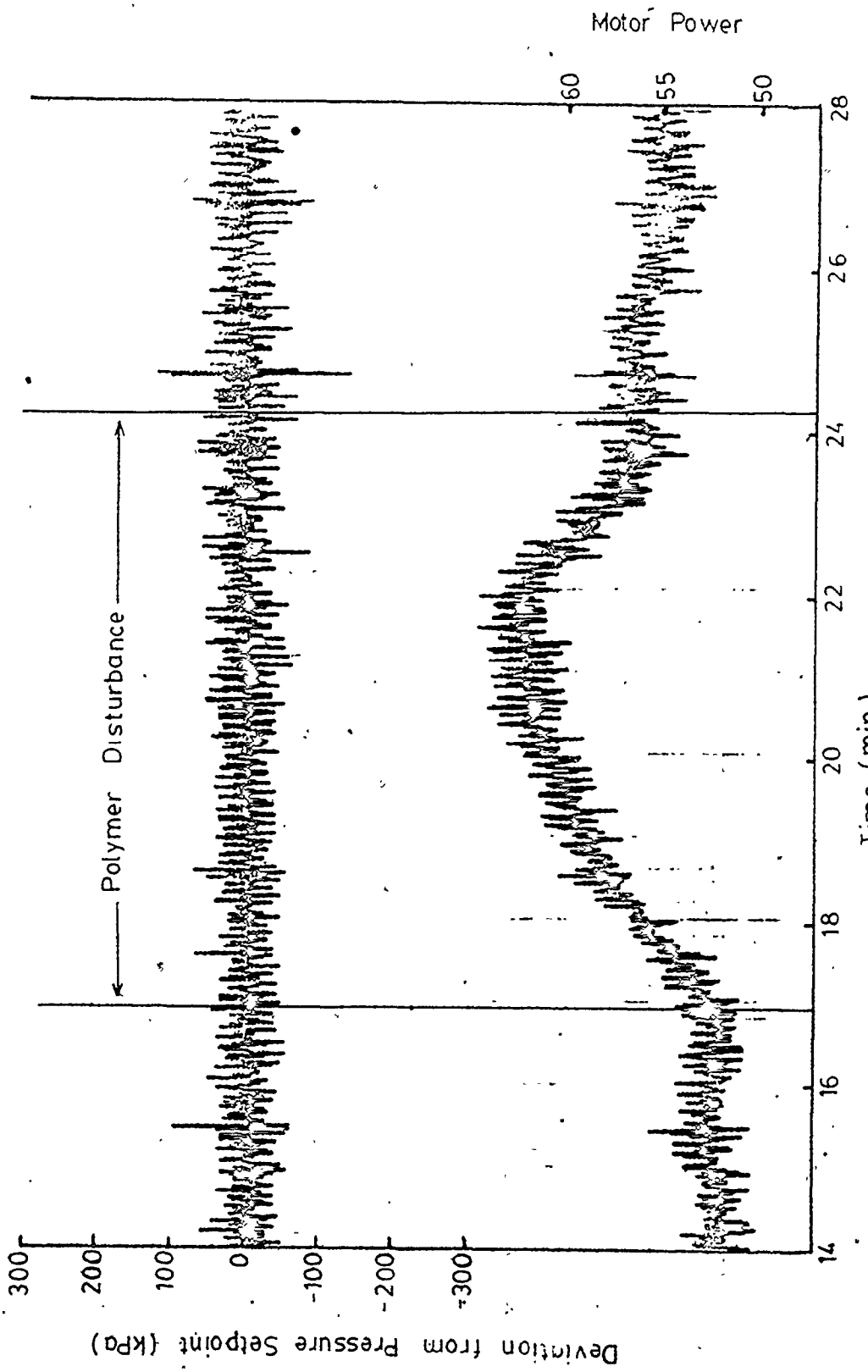

Figure 7.3 (b) Self-Tuning Regulation of Pressure, 2 Pole/2 Zero Filter

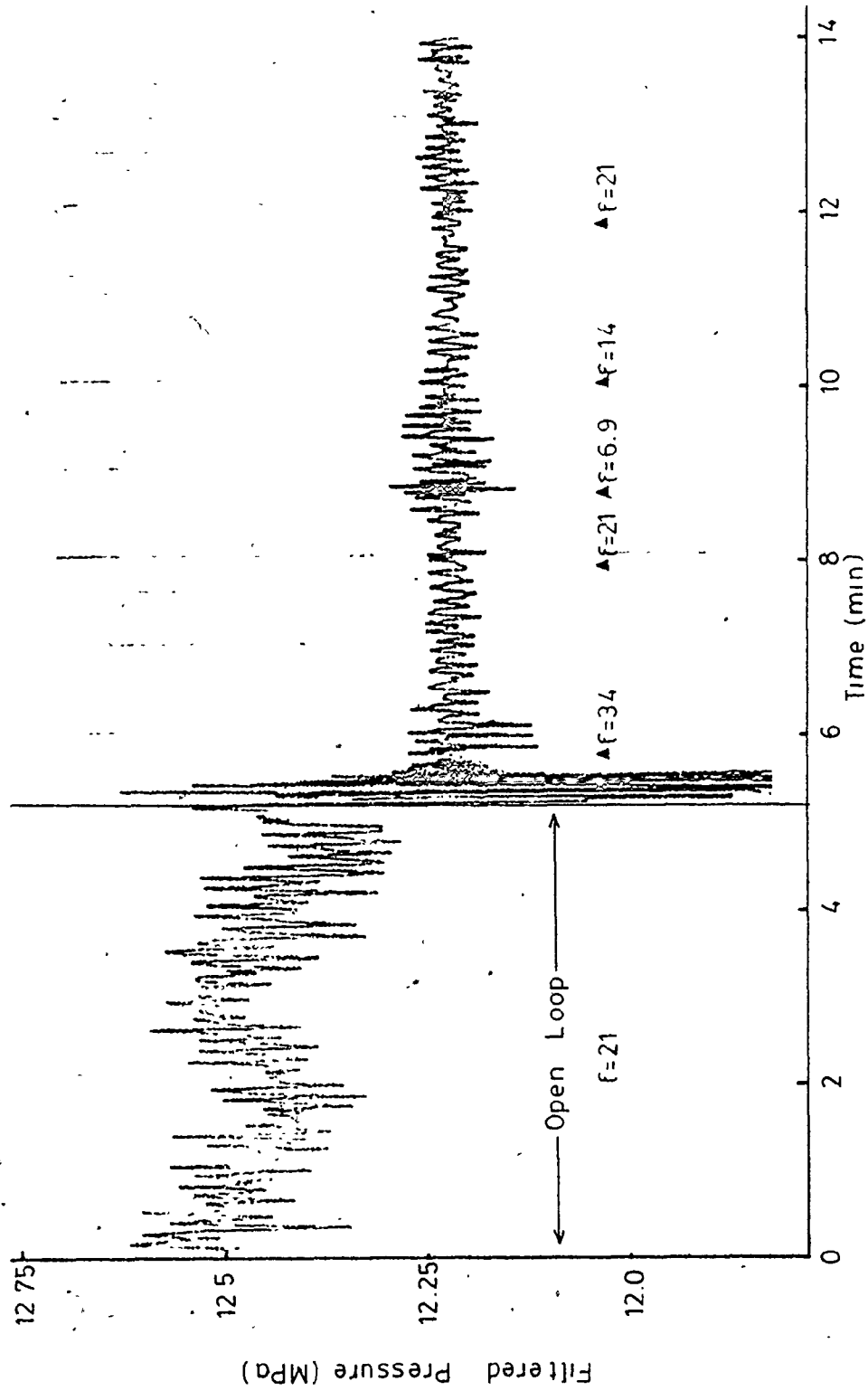

Figure 7.4 (a) Pressure Data of Figure 7.3 (a), Filtered Off-Line

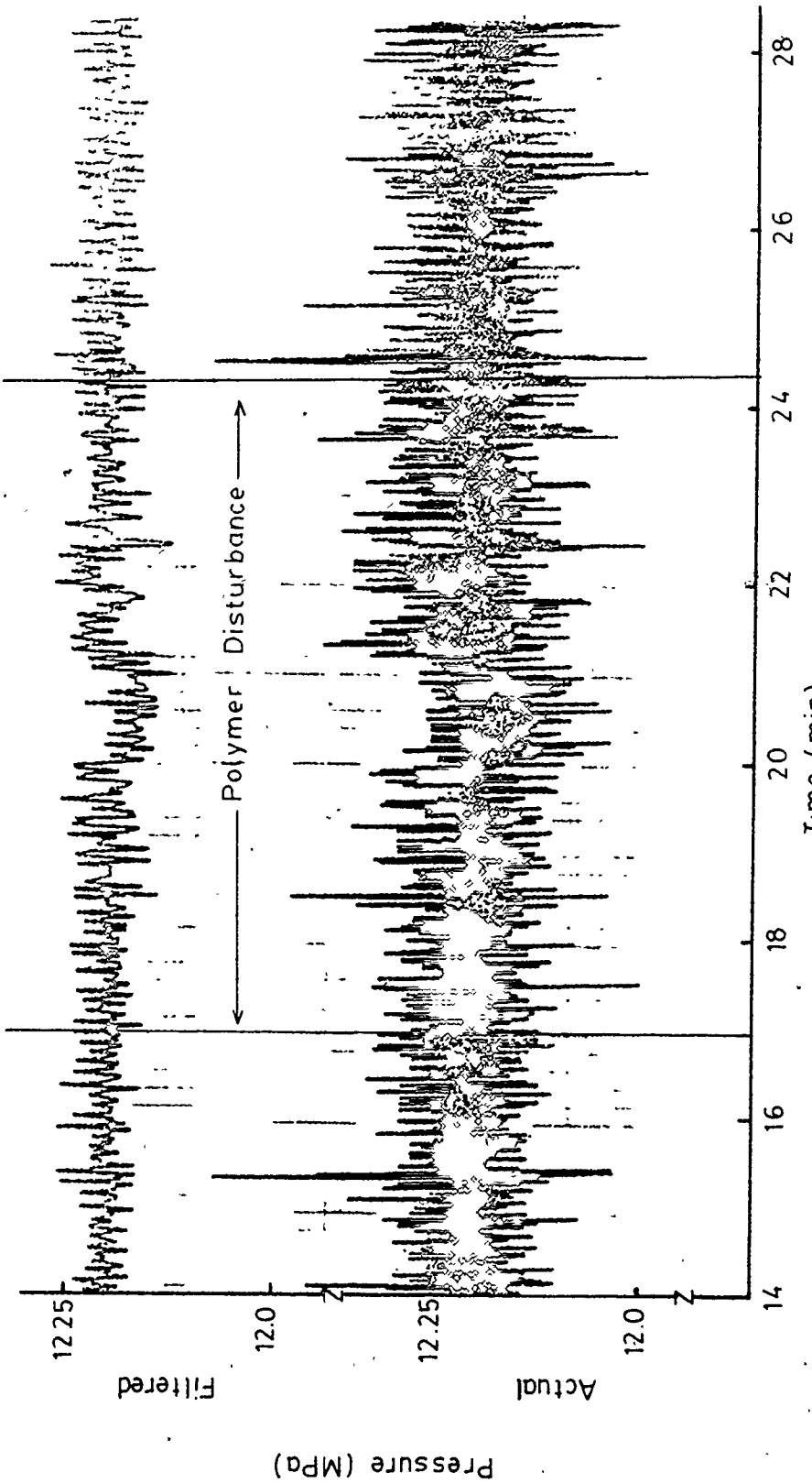

Figure 7.4 (b) Pressure Data of Figure 7.3 (b), Filtered Off-Line

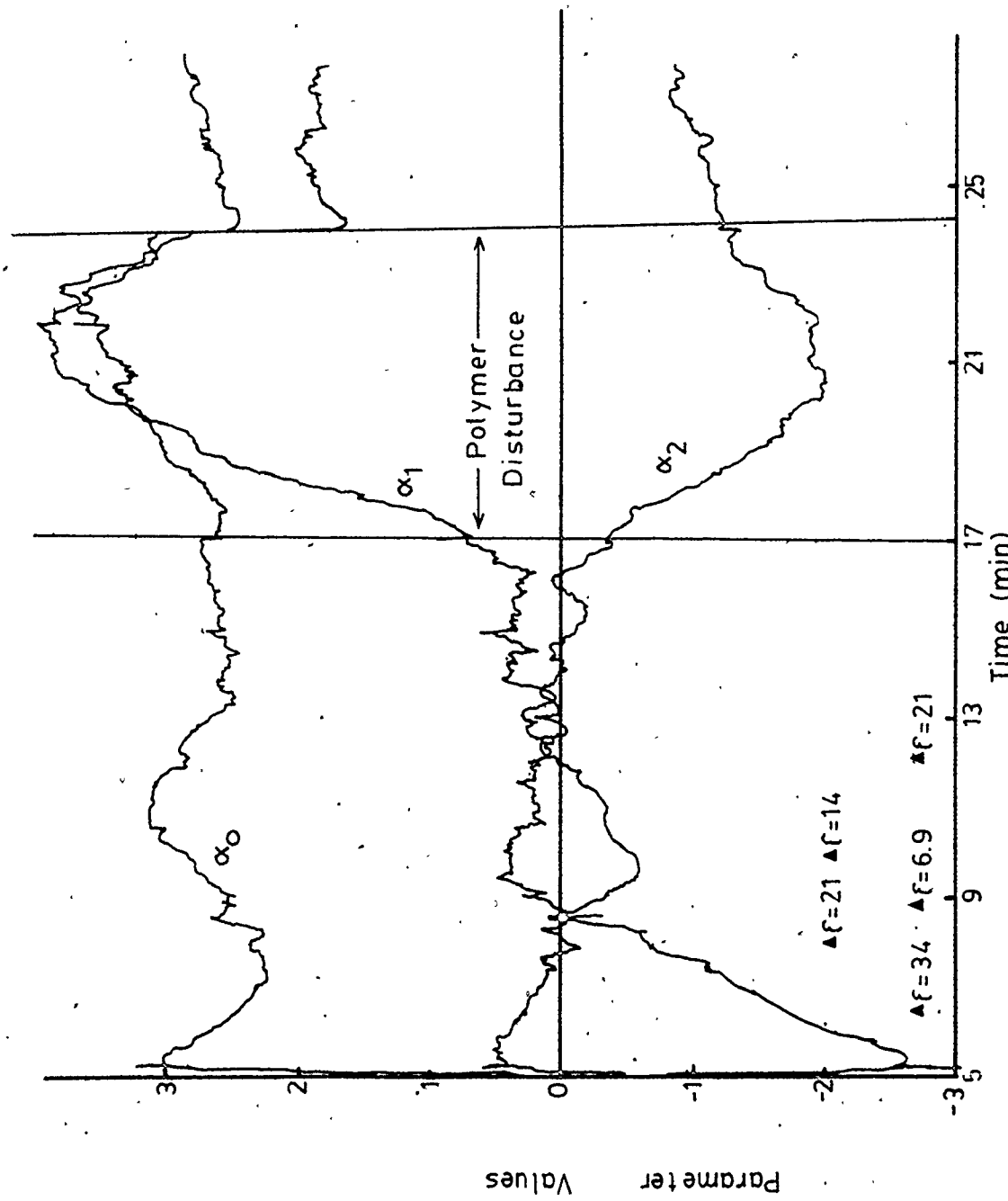

Figure 7.5 (a) Controller Parameters for Data of Figure 7.3

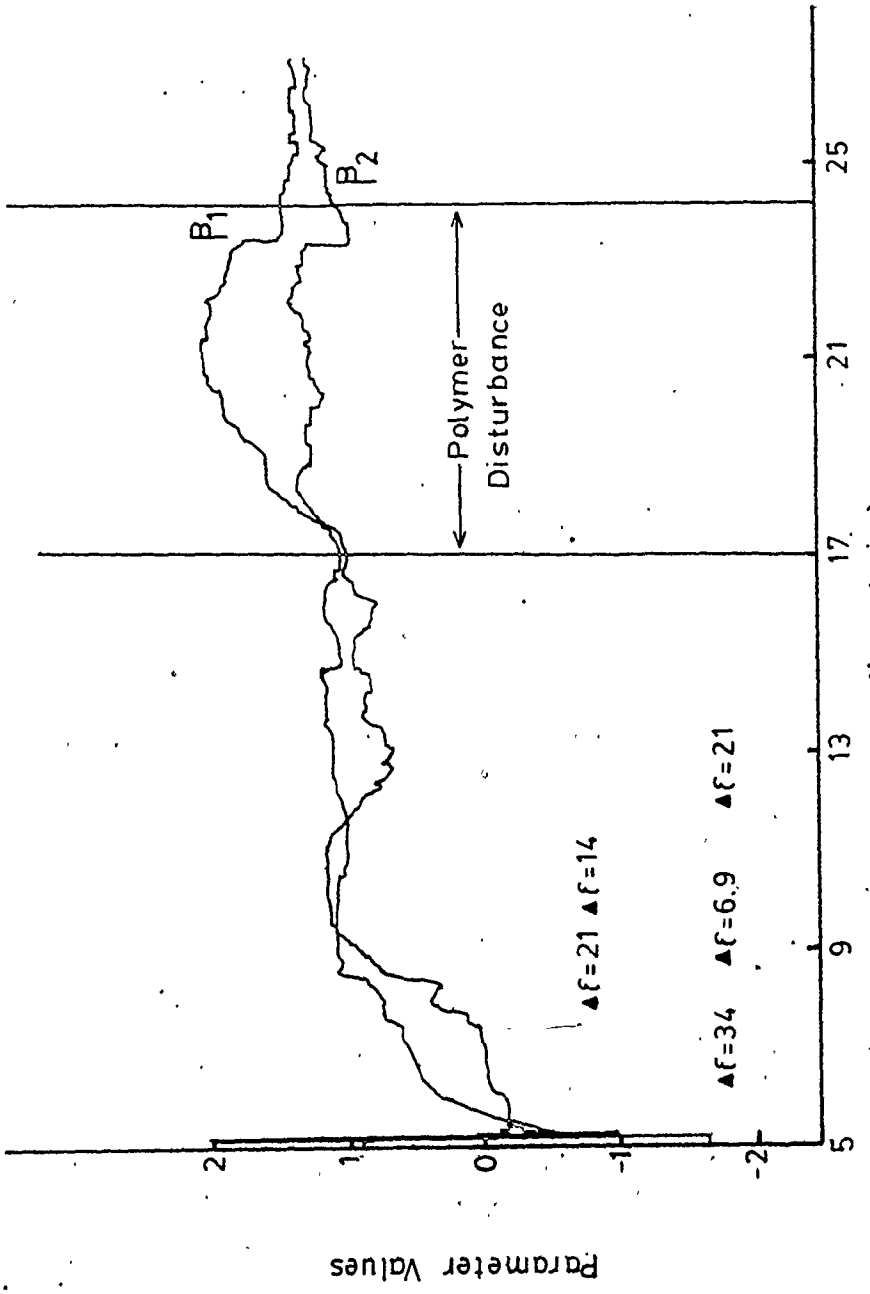

Figure 7.5 (b) Controller Parameters for Data of Figure 7.3

the lower corner frequency (.3 Hz) of the filter. The poor response of this controller, filter combination is due to the STR trying to compensate for the filter. Note that the β values for $\zeta = 6.9$ yield an unstable controller.

During the polymer disturbance, the STR parameters changed considerably, yielding the controller given in Table 7.1. The new polymer has moved the extruder to a new operating level. In combination with the filter, this new operating level may have a considerably different time series model, meaning that the STR would tune to a very different controller.

The other 2 pole/2 zero filter, discussed in section 6.4, using a 4. Hz control interval was also implemented on the extruder. However, it proved difficult to stabilize, requiring a large constraining factor of 138. kPa/M.P. At this large constraining factor, the control was poorer than the PI controller using this same filter. A plot of the parameters showed that they fluctuated and did not appear to be converging to steady state values.

The performance of the STR, as compared to the digital PI algorithm was disappointing. There was no noticeable improvement in pressure control by the STR over the digital PI controller. At first glance, this is a surprising result. The larger structure and parameter updating characteristics of the STR should provide superior control. However, one must remember that the STR will tune itself depending on the disturbances and noise present in accordance with the type of controller structure used.

Table 7.1 summarizes the approximate controllers to which the STR converges. The M.V. controller, equation (7.8) is included for

comparison. The table also summarized what part or frequency of the noise structure each STR is compensating. In each case the STR is doing a good job controlling the parts of the process that it identifies as the most important. However, actually, it is not desired that the STR regulates the flight noise, or compensate for a filter. The STR defeats the use of bandstop filters by identifying the dynamics of the filter and trying to invert these dynamics in the controller, eliminating most of the advantage originally gained by filtering. The controller is not allowed to tune to the desired control equation that would control the real 8 s disturbance.

This can be elucidated by studying the block diagrams of various controller/filter configurations. The minimum variance controller presented in section 7.1, equation (7.5), is derived for a general block diagram, without measurement dynamics, such as presented by Figure 7.6 (a). G_c is the controller transfer function, G_p is the process transfer function and G_N is the noise model. For the case of Figure 7.6 (a), the minimum variance (M.V.) controller would be determined by equation (7.9)

$$U_t = \frac{-\hat{N}_t\ (f+1)}{G_p}$$

$$= \frac{-\hat{G}_N}{G_p} P_t = G_C P_t \qquad (7.9)$$

where $\hat{G}_N$ represents a model optimally predicting the noise $\hat{N}_t$. The rest of the controller, $1/G_p$, is an inversion of the process. This

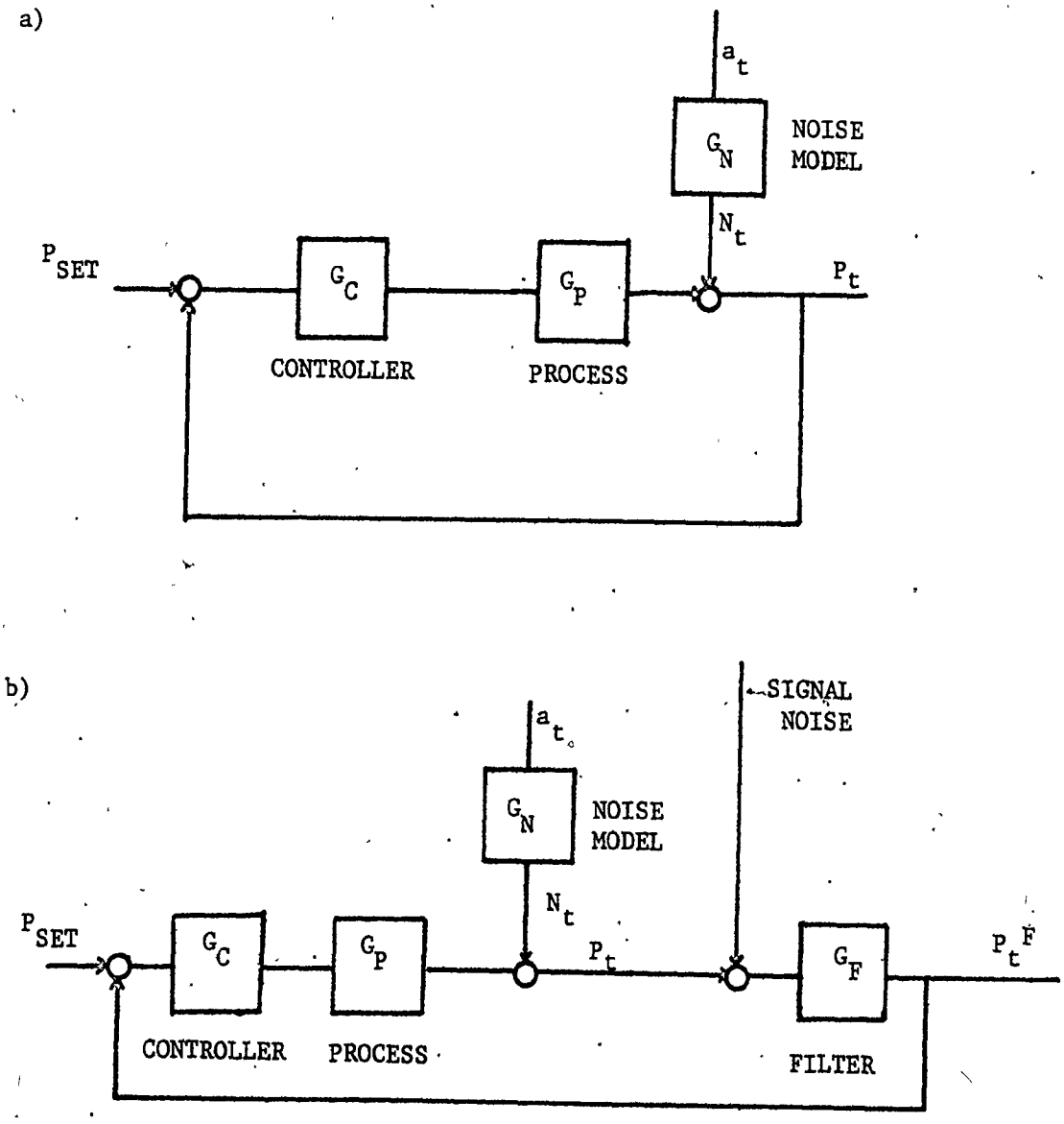

Figure 7.6 Block Diagrams: Various Controller/Filter Configurations

c)

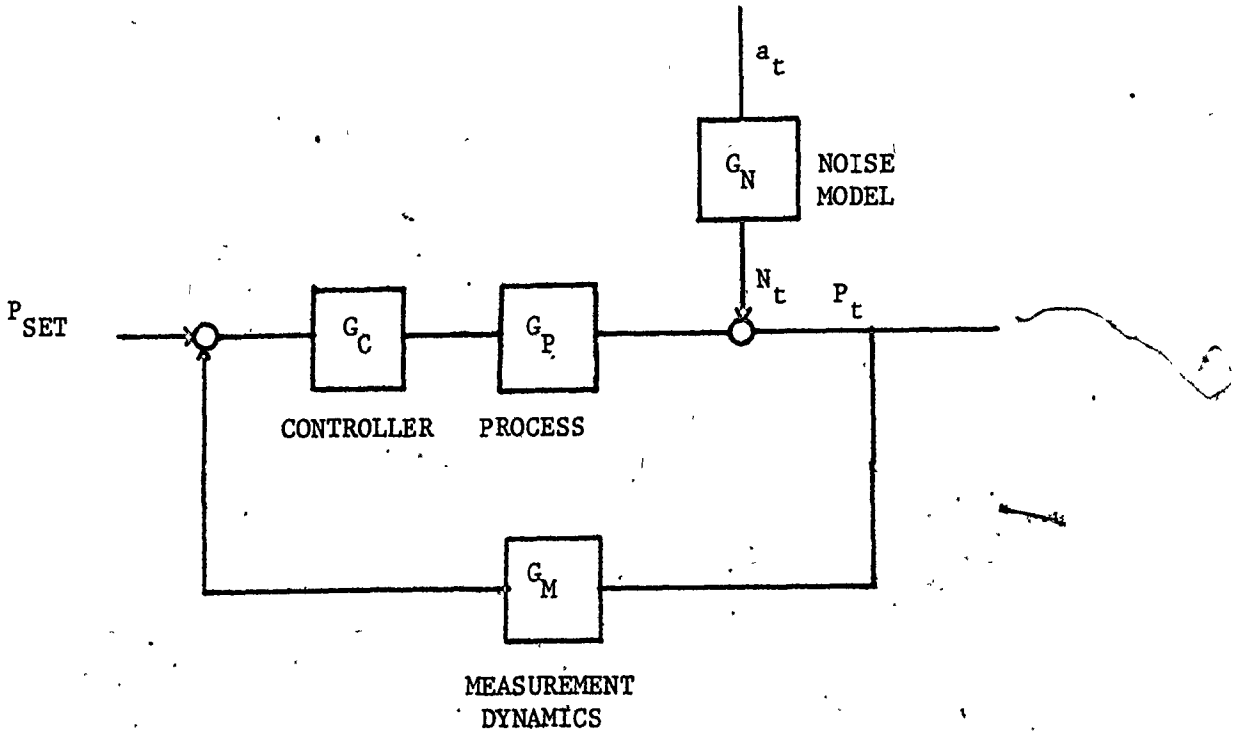

Figure 7.6 Block Diagrams: Various Controller/Filter Configurations

procedure is briefly discussed in section 7.1. For more detail refer to Box and Jenkins(1976).

The block diagram presented in Figure 7.6 (b) includes a filter model (G_F) in the loop forward transfer function. Note that the filter is in the forward transfer function part of the diagram and not the measurement loop. This is because, in this case, one is interested in regulating the filtered pressure data and not the raw signal. The open loop time series models presented in the previous chapter, equations (6.6), (6.7) and (6.20), include the filter in the process transfer function, in the forward transfer function part of the loop.

For the case of Figure 7.6 (b), the M.V. controller would be determined by equation (7.10)

$$G_C = \frac{-\hat{G}_N}{G_P G_F} \qquad (7.10)$$

As shown by the time series models using filtered data, equations (6.6), (6.7) and (6.20), the filter is identified as part of the process model, mostly affecting the transfer function part of the model. Since the STR algorithm tries to find an estimate for the control as close as possible to the M.V. controller, it would be affected by the filter in the same way.

This can also be discussed from a spectral analysis viewpoint. The spectrum of a time series is a plot of its variance verse frequency. A property of white noise is that its spectrum is constant over all frequencies. This means that the variance of a white noise series is equal at all frequencies.

The STR tries to find a controller that will regulate the controlled variable to approximate as close as possible a white noise series. Filters are included in control loops to remove undesired frequencies from the noise model. Unfortunately, the filter is not perfect and will affect the process Bode plot by attenuating other desired frequencies. The spectrum of the noise would therefore not be flat. The STR will try to flatten the spectrum by in effect inverting the filter.

If the noise is high frequency and is being removed by a low-pass filter with a cutoff frequency much higher than the control frequency, the M.V. controller would not be affected. The dynamics of the filter will be so fast in relation to the sampling frequency of the controller that G_F would be reduced to a unity gain in the time series model. This filter would then not affect the dynamics of the loop as seen by the self tuner and would not affect the controller found by the recursive least squares algorithm.

Figure 7.6 (c) shows a similar block diagram for a system with measurement dynamics G_M. In this case, one wants the STR to identify the measurement dynamics but control should be based only on the process and noise. In this case the measurement dynamics can be included in the recursive least squares algorithm. The RLS algorithm will then be able to separately identify the controller.

A similar identification of the filter in the RLS for the case of Figure 7.6 (b) would mean that the filter would be eliminated from the identification routine and the noise would not be removed.

It is recommended that future work be carried out in this area. Simulations could be used to study the effects of filters on the STR control algorithm. One could also continue to look at using a deterministic model for the flight noise. Other approaches could possibly identify the flight noise explicitly under closed loop conditions by using the flight noise as a dither signal.

7.3 Summary of Extruder Pressure Control

Chapter 6 and the previous sections of this chapter describe various attempts to regulate the extruder pressure using different control algorithms and filters. From the experimental results, various recommendations can be made for the regulation of pressure in most extruders. These recommendations can be broken into three cases.

The first case is when one is only interested in maintaining the extruder at some mean operating level, in the face of long term drifts or disturbances. This would be the case where the pressure surging is absent or does not have a major effect on the product. In general, all the stable controllers were very successful in regulating the long term drifts and the disturbance caused by an impulse change in polymer, because they include integral action.

Since, in this case, it is not desired to regulate short term disturbances, it is recommended that the pressure data be filtered by a low-pass filter to remove all the noise and any surging information. The filtered pressure can then be sampled at a low frequency, (a few times every minute) much smaller than the filter cutoff frequency. Because of the vary fast first order dynamics of the extruder pressure,

the transfer function of the extruder model would be reduced to a gain term (the effect of any step in extruder screw speed would be completed by the next sampling period). The noise model would consist only of the non-stationarities (the drifts) because the other disturbances would be removed by the filter. This noise model can be represented by a random walk model ($N_t = a_t/(1 - Z^{-1})$). PI or integral controllers are both very effective for these types of disturbances.

The next case is when one wishes to regulate the extruder for pressure surging when a high frequency signal noise due to the screw rotation is not a significant part of the system. This would occur when the pressure transducer is located in the adapter or the die or some other place where it would not pick up a signal noise. Other possibilities are that the signal noise may be too small to be significant, or the frequency of the surging may be low enough to make low-pass filtering practical (the low-pass cutoff frequency must be higher than half the control frequency). The pressure for this case could then be easily controlled by either the PI or the STR algorithms.

An STR of order $m = 3$ and $\ell = 2$, as used in Chapter 7, is recommended for this case because its optional structure and parameter updating would allow the STR to better control the process and to compensate for any changes in the process conditions. The experiments in this thesis do not show the STR giving superior control over the digital PI controller. However, in all cases, the process model that was used to identify the STR structure was later modified by the addition of a filter or flight noise to the system. This degrades the performance of the STR because it tunes itself to compensate for the

filter or the flight noise. Without the flight noise, the STR would function without these modifications and therefore should give excellent control.

The final case is the one looked at in most detail in this thesis. In this case, the pressure signal contains both pressure surging and a flight noise too close to the surging frequency to be removed by low-pass filtering. In most extruders, the die or adapter can be redesigned to include the pressure transducer and eliminate the problem. If this is not possible, it is recommended to use the digital PI algorithm in combination with the 2 pole/2 zero filter. The STR is not recommended for this case.

CHAPTER 8

SUMMARY, CONCLUSIONS AND RECOMMENDATIONS

8.1 Summary and Conclusions

This thesis presents the interfacing, modelling and control of a plasticating extruder using a minicomputer control system. The regulation of extruder pressure is studied by using the screw speed as manipulated variable. Steady state information, step tests and time series analysis are used to develop dynamic models for the transfer function between screw speed and pressure and to model the disturbances associated with the extruder pressure.

The system time constant is found to be very rapid, approximately 0.4 s. The most important disturbance associated with the extruder pressure consists of a non-stationary pressure surging with a period of 8 s due to the periodic breaking up of the tip of the solid region. There is also signal noise at the same frequency as the screw rotation. This is due to the screw flight passing the tip of the pressure transducer.

A time series model for the process is presented in equation (5.1). This model is an improvement over previous models presented in the literature. The transfer function relating pressure to screw speed is a first order model. The noise model has terms modelling both the extruder pressure surging and the flight noise.

In order to approximate smaller disturbances in polymer quality, the extruder was switched from one type of polymer to another by

introducing the new polymer into the extruder hopper. This change caused a second order response in pressure and temperature.

Digital PI and self-tuning regulator algorithms were implemented on the extruder to regulate the pressure. As expected, both controllers were able to successfully control for long term drifts in the pressure level and a disturbance caused by a change in polymer quality. If one is interested in the long term regulation of the extruder pressure, it is recommended that any surging or flight noise information be removed by low-pass filtering. An integral controller can then be used to regulate the process.

For the case where signal noise is not present in the extruder, it is recommended that a self-tuning regulator using the structure of equation (7.8), be used to regulate the pressure. No signal noise would be present if the pressure transducer is situated in the die or the adapter region of the screw.

Various filters were used to eliminate the signal noise. However, all the filters substantially changed the process transfer function. This affected the ability of the controllers to regulate the process. The combination of controller and filter that was found to be best able to control the process was the digital PI algorithm with a twin cascaded 2 pole/2 zero filter, presented in section 6.5.

The STR was found to be inferior to the PI controller. This unexpected result is due to the self-tuning regulator tuning itself to compensate for a filter in the loop or the flight noise, and not for the elimination of the process disturbances. Experiments showed the poor control results achieved by the STR algorithm when it is used with

filters that have dynamics that are comparable to the sampling frequency.

Filters implemented include the standard signal processing methods of Butterworth low-pass and bandstop filters. These filters were found to add too much system phase lead or lag. Other means of eliminating the flight noise were studied. The most important of these methods was the seasonal Box and Jenkins time series models presented in section 6.3. A seasonal difference term was used to model the flight noise but was found to be unsuitable for loop control. Another Box and Jenkins seasonal filter which removes sinusoids of one frequency was found to be similar to a bandstop filter. However, the sinusoidal filter amplified the high frequencies.

In summary, the contributions of this thesis are:

1.) a much improved dynamic model for both the transfer function and the disturbances associated with plasticating extruders.

2.) applying stochastic control theory in the form of time series analysis and self-tuning regulators to extruders.

3.) the first attempt to control pressure surging in an extruder.

4.) presenting problems associated with using digital bandstop filters in closed loop control.

5.) presenting the frequency response of seasonal Box and Jenkins time series models applied as filters.

8.2 Recommendations for Future Research

Much of the work in this thesis concentrates on the construction and implementation of bandstop filters in control loops. It is shown that these filters have a detrimental effect on the open loop transfer

function and the closed loop control. This is especially true for the cases where a self-tuning regulator is used for the control algorithm. Research on the application of the bandstop filters with the STR control algorithm should continue. Simulations could be used to study the effects of filters on the transfer functions and the STR algorithm. A method of modifying the STR algorithm to take account of filters in the closed loop should be developed.

The possibility of redesigning the extruder adapter, so that the pressure transducer can be placed in this area, should be explored. Placing the transducer in this region would eliminate the signal noise presently experienced which is caused by the screw flight passing the tip of the transducer. This would enable one to control the extruder pressure without the control algorithm being corrupted by the flight noise or filters designed to remove this noise. This would also verify that high frequency pressure disturbances are not present in the die. The effect of high frequency screw speed actions on the die pressure can also be observed.

The long term objective of the research on the extruder system is to regulate the entire extruder system. The die heater power is presently interfaced to the computer. As is discussed in section 6.4, it is recommended that this heater power be used to regulate the melt temperature and not the die wall temperature. It is the melt temperature that needs to be regulated to maintain product quality.

The extrudate thickness measurement device and the take-up mechanism speed control should be completed and interfaced to the computer. This would allow one to develop a dynamic model relating

the thickness to step changes in both screw speed and take up mechanism speed. One can also analyze the disturbances associated with the extrudate thickness. It would be especially interesting to determine the relation between the pressure surges in the extruder and thickness. The thickness measure should also be modified to study the dynamic behaviour of die swell. This can be achieved by recording the thickness of the extrudate for steps in screw speed while the extrudate is allowed to fall freely without being pulled by the take up mechanism.

REFERENCES

Antoniou, A., Digital Filters: Analysis and Design, McGraw-Hill Book Co., New York, N.Y. (1979).

Borison, A. and R. Syding "Self-Tuning Control of an Ore Crusher", Automatica, 12, 1-7. (1976).

Box, G.E.P. and G.M. Jenkins, Times Series Analysis, Forecasting and Control, Revised Edition, Holden-Day, San Francisco, California (1976).

Brauner, N., R. Lavie and Z. Tadmor, "Control of a Plasticating Extruder", Int. IFAC Conf. on Instrum. and Autom. in the Pap., Rubber and Plastics Ind., 3rd Proc., Brussels, Belg., 6, 353-360 (1978).

Chin, P.A., Plasticating Extrusion Interfacing and Control, M. Eng. Thesis, McMaster University (1979).

DiStefano, J.J., A.R. Stubberud and I.J. Williams, Theory and Problems of Feedback and Control Systems, Schaum's Outline Series, McGraw-Hill Book Co., New York, N.Y. (1967).

Dormeier, S., "Digital Temperature Control - A Way to Improve the Extrusion Process", Antec Preprints, 25, 216-219 (1979).

Dormeier, S., "Extruder Control", 4th IFAC Conference in the Paper, Rubber, Plastics and Polymerization Industries, Ghent, Belgium, June 1980.

Fenner, R.T., A. P.D. Cox and D.P. Isherwood, "Surging in Screw Extruders", Antec Preprints, 24, 494-497, (1978).

Fingerle, D., "Autogenic Melt Temperature Control System for Plastic Extrusion", J. of Elastomers and Plastics, 10, 293-312. (1978).

Fontaine, W., Analysis and Modelling of the Dynamic Behavior of a Plasticating Extruder, Ph.D. Dissertation, Ohio State University (1975).

Franklin, G.F. and J.D. Powell, Digital Control of Dynamic Systems, Addison-Wesley Publ. Co., Reading, Massachusetts, (1980).

Frederickson, A.A., Jr., "A Flat Die Extruder Control System Using Distributed Digital Processors", Antec Preprints, 24, 561-564 (1978).

Griffith, R.M. and J.T. Tsai, "Shape Changes During Drawing of Non-Circular Extruded Profiles", Polymer Engng. Sci., 20 (18), 1181-1187 (1980).

Harris, T., "DGDAC Manual", Internal Report, Dept. of Chemical Engineering, McMaster University (1979).

Harris, T., Topics in Stochastic Control with Applications to a Tubular Reactor, Ph.D. Thesis, McMaster University (1980).

Harris, T., J.F. MacGregor and J.D. Wright, "Self-Tuning and Adaptive Controllers: An Application to Catalytic Reactor Control", Technometrics, 22 (2), 153-164 (1980).

Jury, E.I., Sampled-Data Control Systems, John Wiley & Sons Inc., New York, N.Y.,(1965).

Kaiser, J.F., "Design Methods for Sampled Data Systems", in Digital Signal Processing, Ed. Rabiner, L.R. and C.M. Rader, IEEE Press, New York, N.Y. (1972).

Kochhar, A.K. and J. Parnaby, "Dynamic Modelling and Control of Plastics Extrustion Processes", Automatica, 13, 177-183 (1977).

Kochhar, A.K. and J. Parnaby, "Comparison of Stochastic Identification Techniques for Dynamic Modelling of Plastic Extrustion Processes", Int. Mech. Eng. (Lond.) Proc., 192, 299-309 (1978).

Kuo, B.C., Digital Control Systems, SRL Publ. Co., Champaign, Illinois, (1977).

Lindorff, D.P., Theory of Sampled-Data Control Systems, John Wiley & Sons Inc., New York, N.Y., (1965).

MacGregor, J.F., "Optimal Choice of the Sampling Interval for Discrete Process Control", Technometrics, 18 (2), 151-160, (1976) and Technometrics, 19 (2), 224 (1977).

Maddock, B.H., "Measurement and Analysis of Extruder Stability", Soc. Plastics Engrs., J., 20, 1277-1283, (1964).

Oppenheim, A.V. and R.W. Schafer, Digital Signal Processing, Prentice-Hall, Englewood Cliffs, N.J. (1975).

Parnaby, J., A.K. Kochhar and B. Woods, "Development of Computer Control Strategies for Plastics Extruders", Polymer Engng. Sci., 15 (8), 594-605 (1975).

Patterson, I., P. Branchi and J. Paris, "Valve Control of Extruder Output", Antec Preprints, 25, 166-169 (1979).

Patterson, I. and T. de Kerf, "The Dynamic Behavior of Extruders", Antec Preprints, 24, 483-487 (1978).

Rabiner, L.R. and B. Gold, Theory and Application of Digital Signal Processing, Prentice-Hall Inc., Englewood Cliffs, New Jersey (1975).

Rader, C.M. and B. Gold, "Digital Filter Design Techniques in the Frequency Domain", in Digital Signal Processing, Eds. Rabiner, L.R. and C.M. Rader, IEEE Press, New York, N.Y. (1972).

Rastogi, L.K., "A Flat Die Extruder Control System Using Distributed Microcomputers", Proceedings Joint Aut. Control Conference, 375-388, (1978).

Saucedo, R. and E.E. Schiring, Introduction to Continuous and Digital Control Systems, MacMillan Co., New York, N.Y., (1968).

Schott, N.R., Analysis of Plastics Extruder Dynamics, Ph.D. Dissertation, University of Arizona (1971).

Smith, C.L., Digital Computer Process Control, International Textbook Co., (1972).

Tadmor, Z. and I. Klein, Engineering Principles of Plasticating Extrusion, Robert E. Krieger Publ. Co., Huntingdon, New York (1978).

Tadmor, Z., S.D. Lipshitz and R. Lavie, "Dynamic Model of a Plasticating Extruder", Polymer Eng. Sci., 14 (2), 112-119 (1974).

Tou, J.T., Digital and Sampled-Data Control Systems, McGraw-Hill Book Co., New York, N.Y., (1959).

Vlachopoulos, J., Private Communication (1981).

Wright, J.O., An Implementation of Digital Extrustion Control with an Embedded Microprocessor, Ph.D. Dissertation, Ohio State University (1975).

Zverev, A.I., Handbook of Filter Synthesis, John Wiley and Sons, Inc., New York, N.Y. (1967).

NOTATION

a - constant in equation (2.1)
lower cutoff frequency equation (6.19)

a_t - white noise sequence

AR - amplitude ratio

B - constant depending on die resistance and polymer viscosity

b - upper cutoff frequency equation (6.19)

c - $\Omega_u - \Omega_e$ equation (6.16)
- midpoint frequency of 2 pole/2 zero filter

d - order of non-stationary disturbances
- damping factor of AR(2) model
- $\Omega_u - \Omega_e$ equation (6.16)

e_n - error signal

f_o - frequency of AR(2) model

G_C - controller equation

G_F - filter model

G_M - measurement dynamic model

G_N - noise model

G_P - process model

H - filter transfer function

$\underline{K}$ - vector weighing past parameters and present errors in controlled variable

K_c - controller gain

K_p - number of periods of dead time equation (2.5)

N_t - noise component of model

P - melt pressure

$\underline{\underline{P}}$ - normalized covariance matrix of parameter estimates

P_{SET} - melt pressure setpoint

Q - volumetric flowrate

s - laplace transform variable
- integer number of sampling periods representing period of signal noise

T - melt temperature

T_I - controller integral action

T_s - sampling period

$T(Z^{-1})$ - feedforward portion of equation (7.5)

$TACH_t$ - tachometer reading at time t

U - screw speed manipulated variable

X_t - manipulated variable

Y_t - measured variable

Z - Z-transform variable

α - parameter in STR algorithm

β - parameter in STR algorithm

∇ - difference operator $(1 - Z^{-1})$

∇_s - seasonal difference operator $(1 - Z^{-S})$

$\delta(Z^{-1})$ - polynomial in time series transfer function representing the system dynamic terms

θ - frequency of noise to be removed equation (6.13)

$\underline{\theta}$ - vector of parameters

$\theta(Z^{-1})$ - moving average terms of noise model

$\theta_f(Z^{-1})$ - moving average term of stochastic filter

λ - forgetting factor

ξ - damping factor
- constraining factor, STR algorithm

ζ - time constant

$\phi(Z^{-1})$ - autoregressive terms of noise model

$\phi_f(Z^{-1})$ - autoregressive terms of stochastic filter

Ψ - vector of past control actions and controlled variables

ω - frequency

ω_o - cutoff frequency

Ω_e - lower cutoff frequency

Ω_u - upper cutoff frequency

ω_W - frequency in W-domain

$\omega(Z^{-1})$ - polynomial in time series transfer function compensating for past inputs

APPENDIX A

CALIBRATION PROCEDURES

A.1 Introduction

All the extruder process signals interfaced to the minicomputers communicate through the Data Aquisition and Control system (DGDAC) described in section 3.1. The DGDAC can transmit or receive a 0 to 10 V signal that is stored in the computer as a 12 bit number. This means that the 0 to 10 V reading is converted into an integer value scaled to lie between 0 and 4095. Calibrations must be performed to convert the computer values into engineering units.

When performing calibrations, it is usually best to calibrate the entire loop at once. This is done by comparing the computer measurement directly with the process measurement, without calibrating the intervening circuitry. This avoids the need to do many calibrations for each measurement. This method is used for all the calibration procedures reported in this thesis.

All the calibrations require a computer program that accesses the DGDAC and records the values of the process variables in computer units. These values should be recorded at small time intervals, by the teletype situated close to the extruder. These values can also be recorded in a disk file, at a faster rate, so that they can be accessed at a later time.

A schematic of the extruder instrumentation panel is given in Figure A. 1 for later reference.

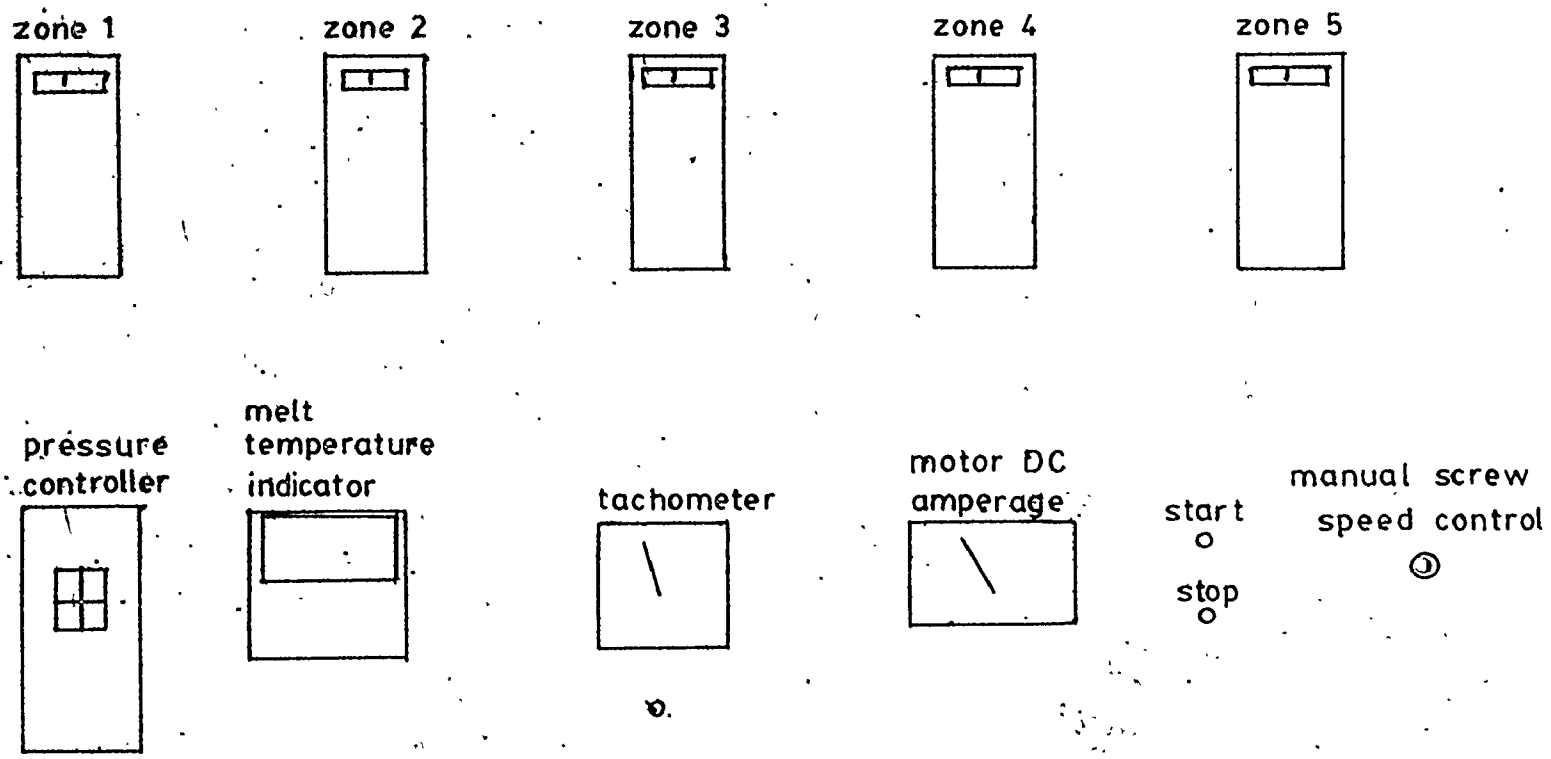

Figure A.1 Schematic of Extruder Instrumentation Panel

Before calibrating always allow the electronics at least half an hour to warm up.

A.2 Tachometer Calibration

1) Place a mark on the torque-arm speed reducer. This is the part of the extruder which rotates at the same rate as the screw and can be seen through the gap left by the engine guard. The mark should be in a bright colour so that it can be easily noticed while the screw is rotating.

2) Select a screw speed. While the computer records the tachometer readings in computer units, record the time needed for a set number of screw rotations (i.e. 10). Repeat this step at least twice for each screw speed setting.

3) The values can now be used to fit a calibration curve. Note that this procedure can only be used for speeds below 60. r/min. At faster speeds the line passes too quickly to be timed accurately. The calibration curve should be extrapolated from low settings to find values at high speeds.

The calibration curve for screw speed is given in Figure A.2.

A.3 Melt Temperature Calibration

1) Disconnect the melt thermocouple from the digital temperature indicator (pins 2 and 3).

2) Short out pins 2 and 3, the thermocouple connections. The temperature reading should approximate the room temperature.

3) Use a milli-volt source to simulate the thermocouple input. This should match with J thermocouple tables after the voltage is compensated

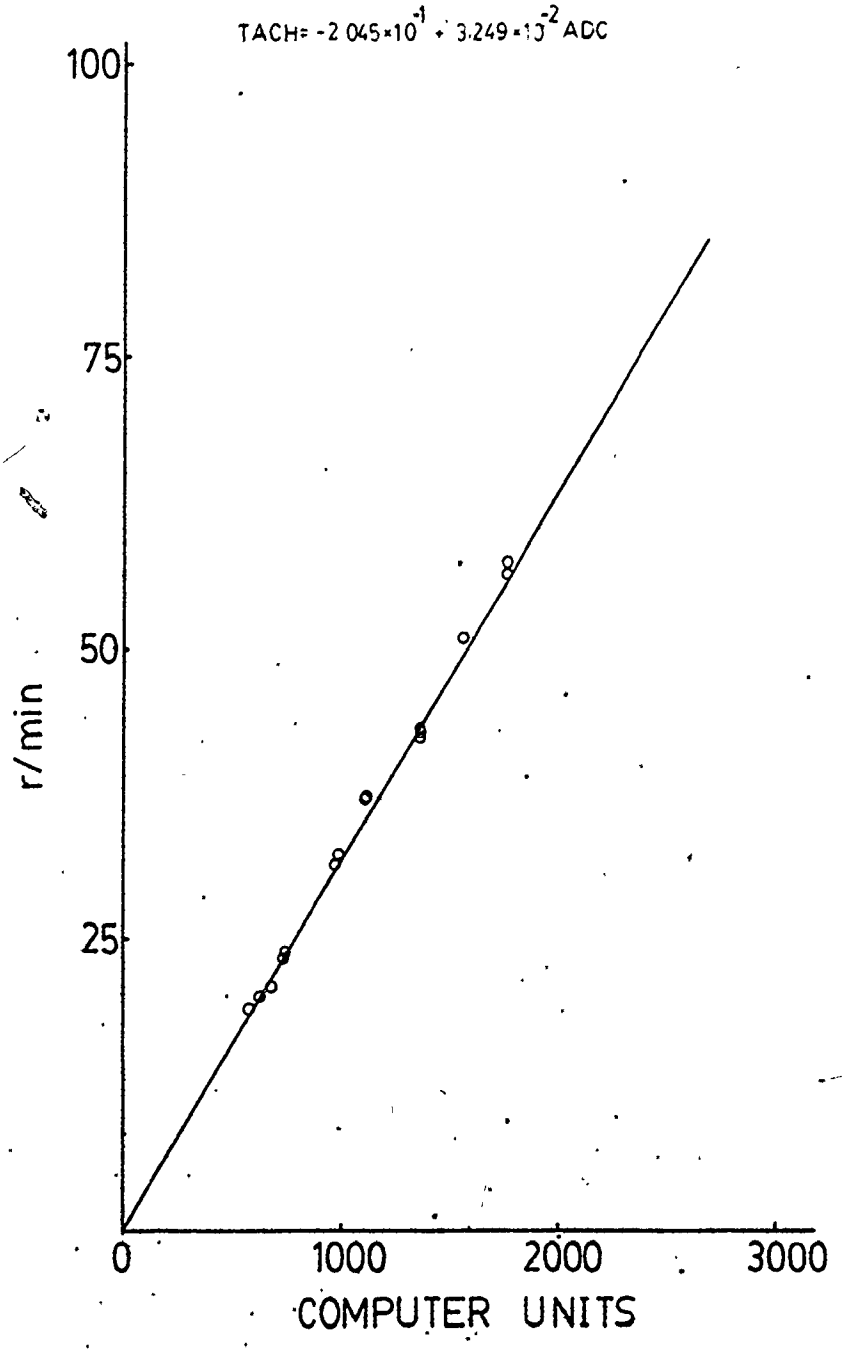

Figure A.2 Calibration Curve for Screw Speed

for the room temperature. Record these readings on the computer.

The calibration curve for the melt temperature is given in Figure A.3.

A.4 Die and Zone Temperature Calibrations

1) Disconnect all the thermocouples leading to the die and zone temperature controllers.

2) Using the melt temperature indicator, as in the calibration procedure for melt temperature, determine the millivolt setting for a selected temperature reading by the digital indicator.

3) The same millivolt signal is applied to each temperature controller in turn while the computer records the readings. Note that the controllers have different loads than the melt temperature indicator and the millivolt source will need some adjustment to have the same millivolt value.

4) The temperature determined from the melt indicator is used in the calibration versus the computer units recorded by the teletype. Note that the temperature readings on the front dial of the temperature controllers are generally off by a few degrees. This is a small offset that should be constant through the entire range of the calibration.

The calibration curves for the die and zone temperatures are given in Figures A.4 through A.8.

A.5 Pressure Calibration

Note that the pressure amplifier has been modified to a times 5.74 amplification. This allows a smaller range of pressures to be more accurately represented.

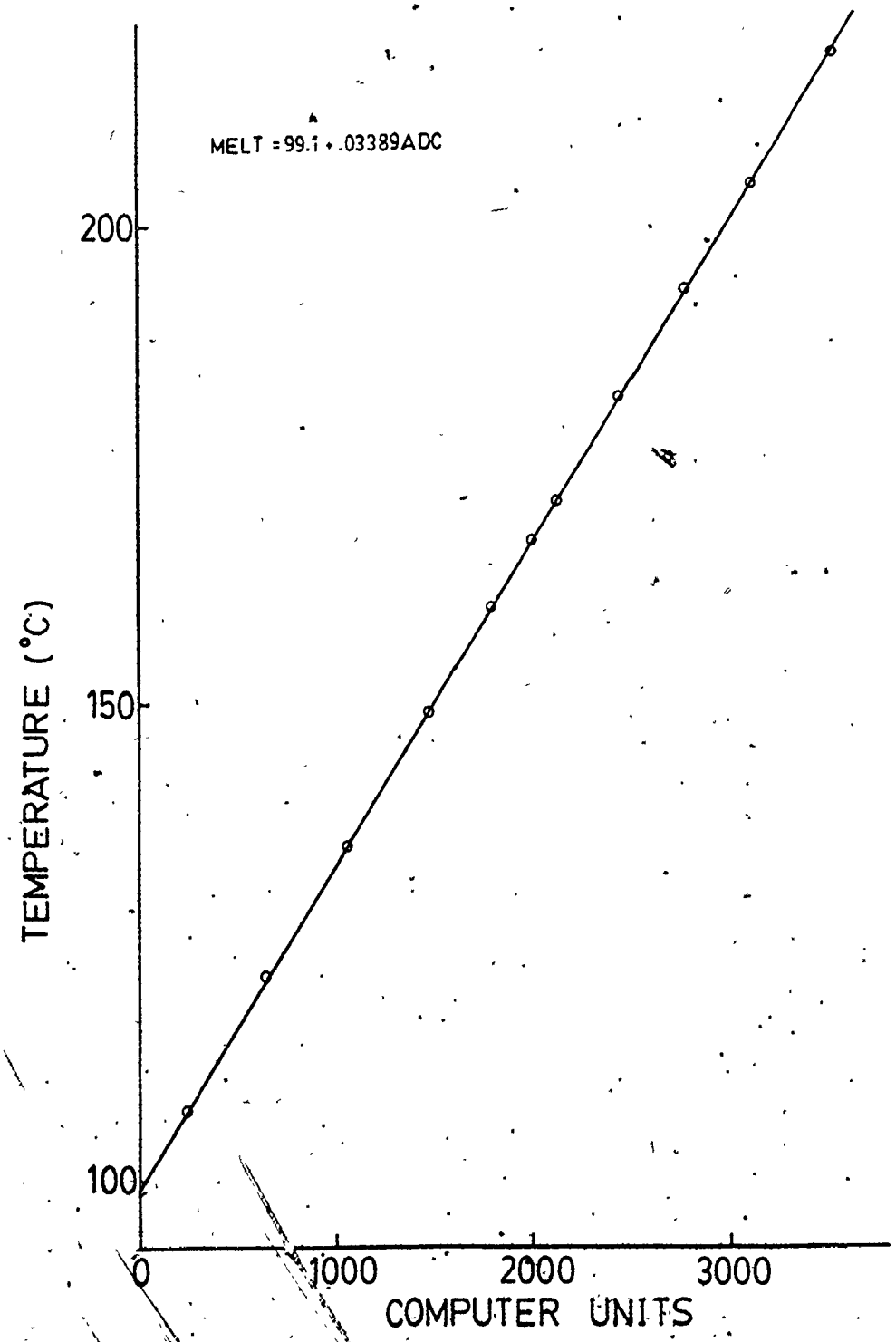

Figure A.3 Calibration Curve for Melt Temperature

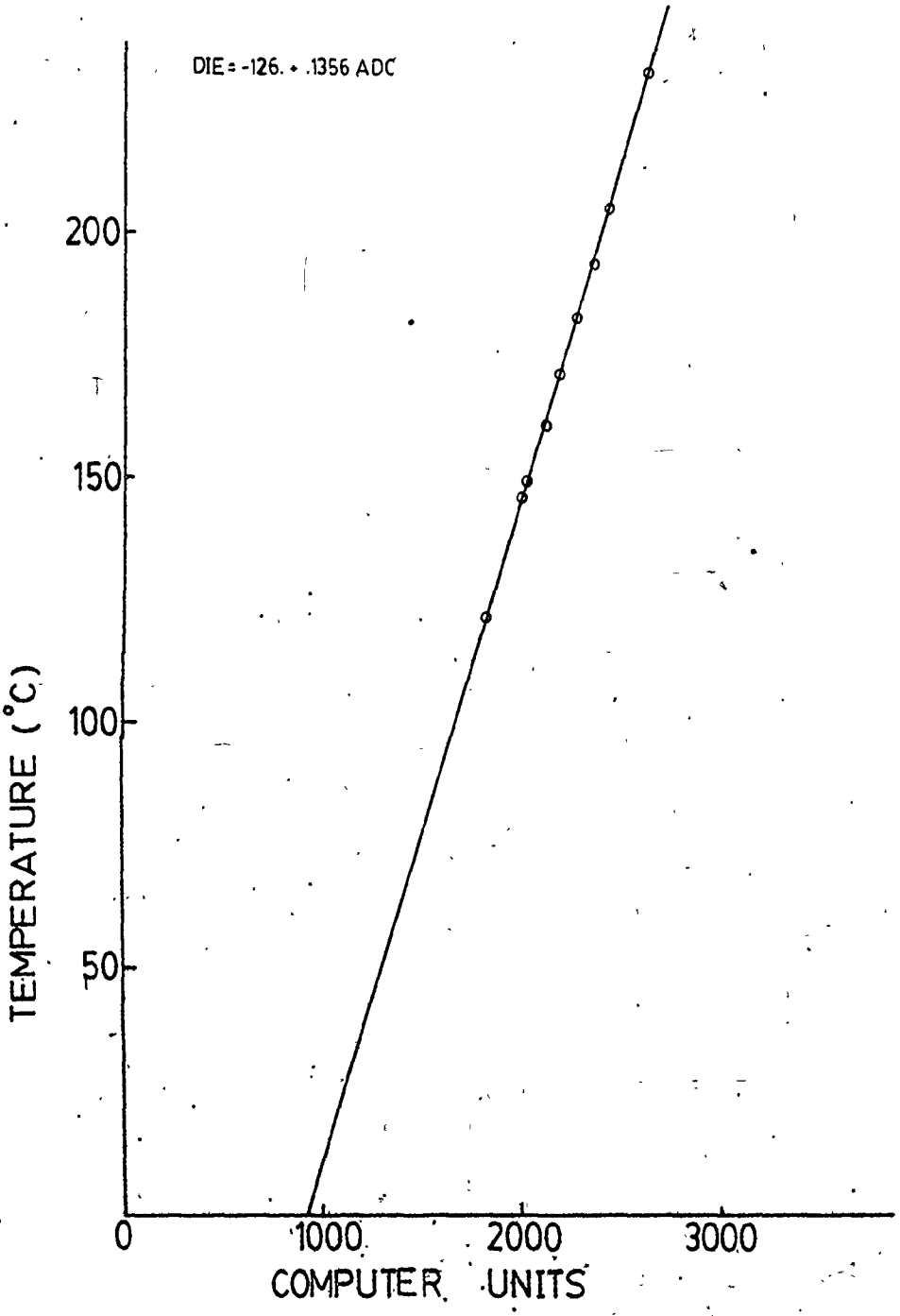

Figure A.4 Calibration Curve for Die Temperature

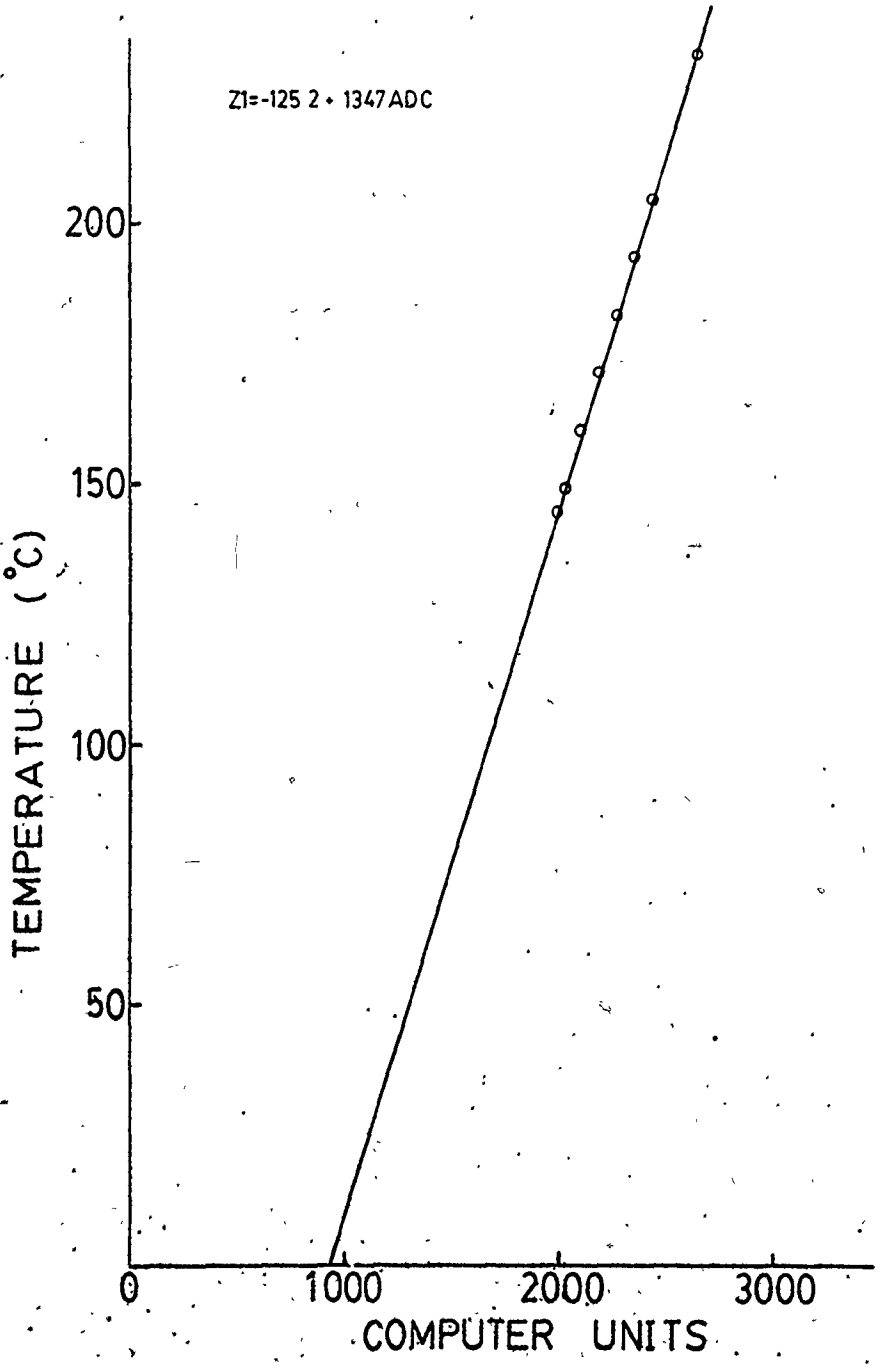

Figure A.5 Calibration Curve for Zone 1 Temperature

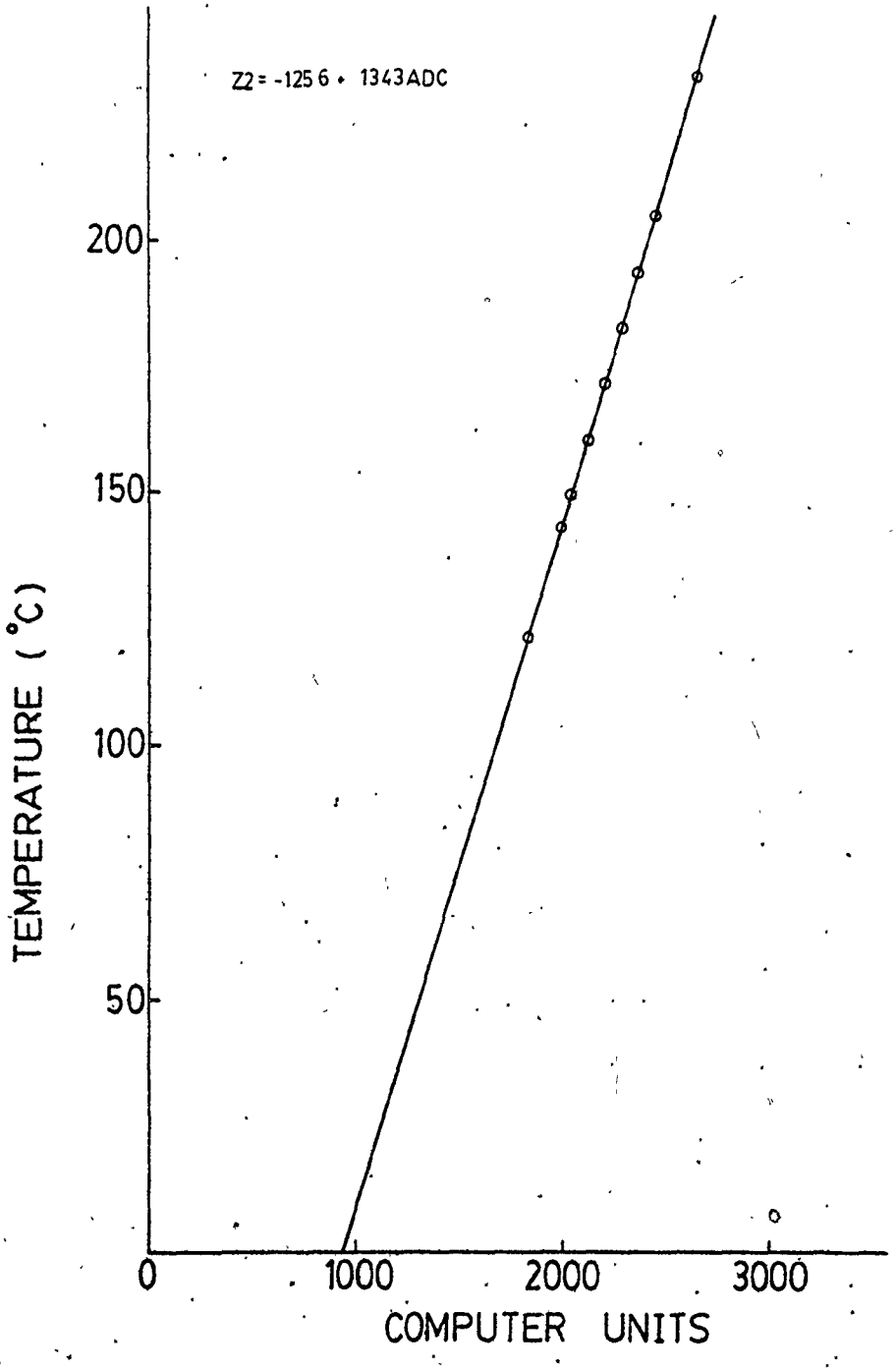

Figure A.6 Calibration Curve for Zone 2 Temperature

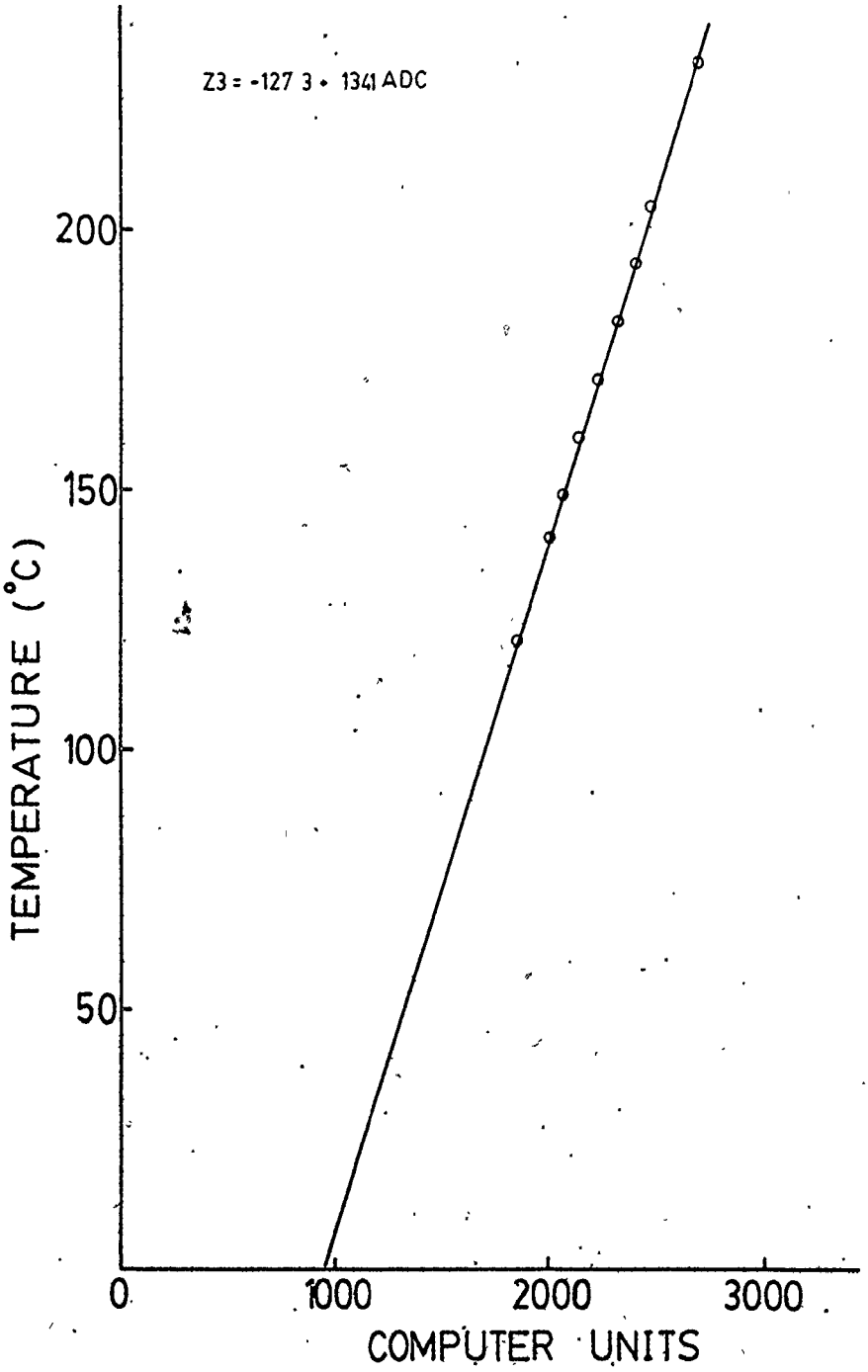

Figure A.7 Calibration Curve for Zone 3 Temperature

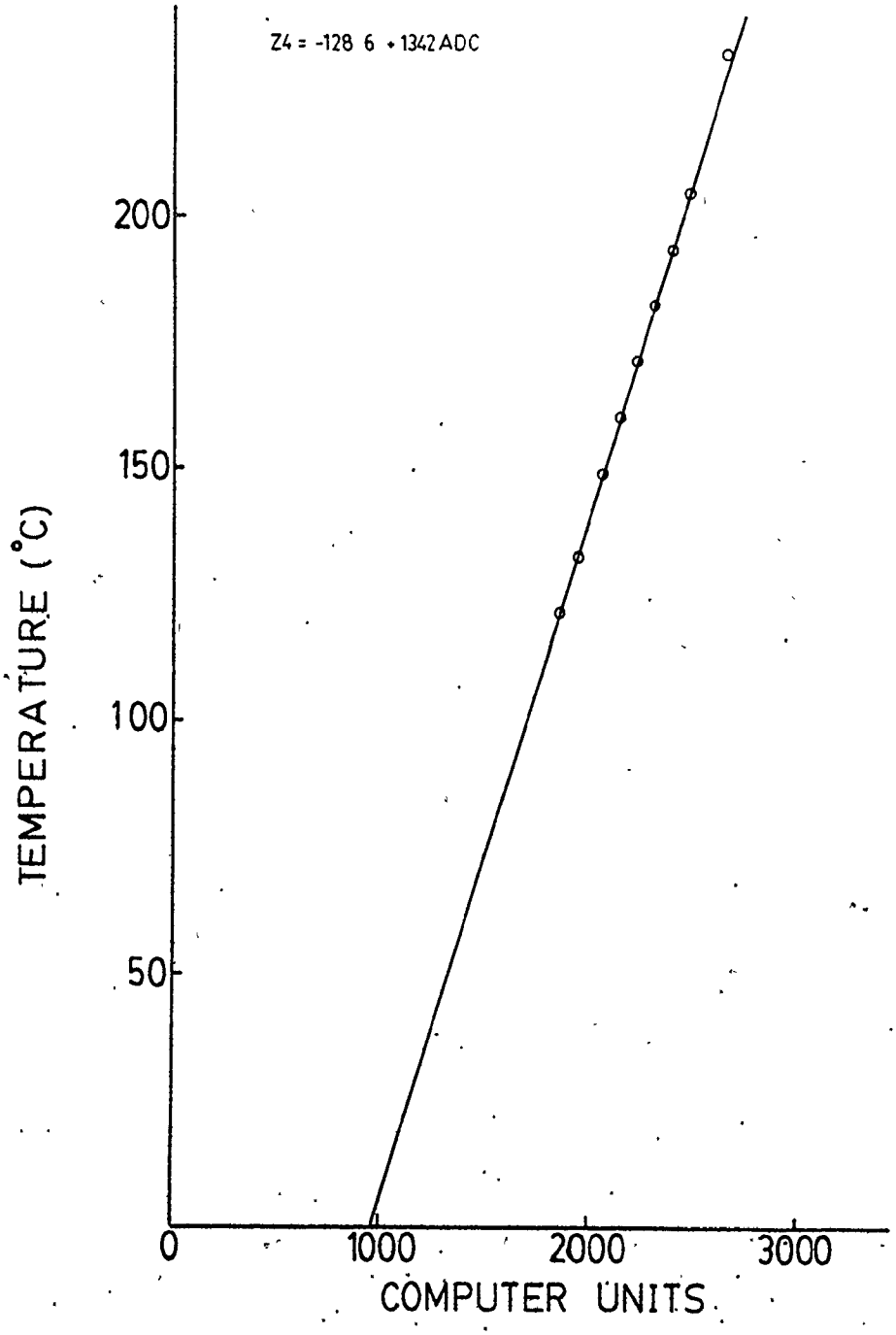

Figure A.8 Calibration Curve for Zone 4 Temperature

1) Select a screw speed.

2) Determine the pressure by recording the value off the dial on the analog pressure controller. Record the computer values.

The calibration curve for the pressure is given in Figure A.9.

A.6 Verifying the Calibrations

If the calibrations are performed in the same units as those used by the indicators on the control panel, these dials can be easily and quickly used to roughly verify the computer readings. It was found that all five of the temperature controllers and the tachometer showed a small offset from the calibrated values. The temperature can be checked by placing the thermocouples at a known temperature. The calibrations for the die and zone temperatures were verified by placing the thermocouples in a boiling water bath and comparing the computer readings with a thermometer. In this manner, it was determined that the offset was due to inaccuracies in the temperature controllers and not in the calibrations.

The calibrations should be redone periodically to maintain their accuracy.

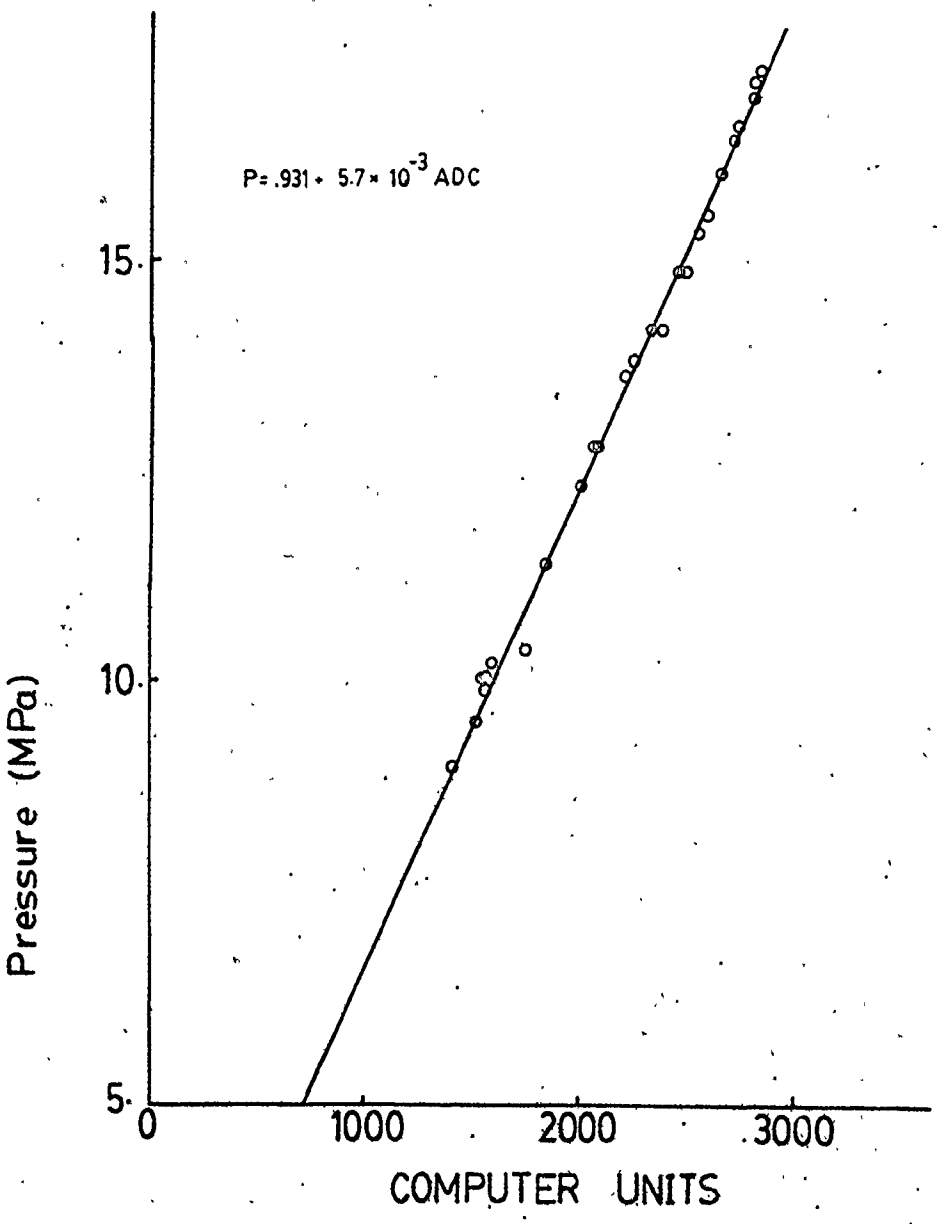

Figure A.9 Calibration Curve for Pressure

APPENDIX B

COMPUTER PROGRAM LISTING

File Name : STP 1. MC

```
C
C     COMPUTER PROGRAM TO RUN THE EXTRUDER
C     MAIN PROGRAM GIVEN HIGHEST PRIORITY
C     ACCEPTS INPUT FROM TTO1 FOR D2A
C         AND SELECTS OVERLAY OPTION
C
      PARAMETER ITTO1=50, ITTI1=51, IFLCH=20, ID=5
      PARAMETER IOLCH=22, IDTOAS=3, IATODS=4
      EXTERNAL DAAD, DAAD2, DAAD3, STEP1, STEP2, STP3
      COMMON// TSI, G, G1
C
      COMMON/DGDC2/ DATUM(IDTOAS), ANALG(IATODS)
      COMMON/BLCK1/ DISK, RPM
      INTEGER DATUM, ANALG
      EQUIVALENCE (PSET, RPM)
      LOGICAL START, DISK
      TYPE 'EXECUTING ON TTO1'
C
C     OPENNING CHANNELS TO $TTO1
C
      STEP=18.5
      CALL OPEN(ITTO1, '$TTO1' 2, IER)
      CALL OPEN(ITTI1, '$TTI1', 2, IER)
      CALL DCLR(IER)
      DISK=.FALSE.
      CALL OVOPN(IOLCH, 'STP1.OL', IER)
      GOTO 1012
 15   WRITE(ITTO1, 155)
 155  FORMAT(/, ' RPM?', 2X, Z)
      START=.FALSE.
C
C     DATA LOGGING LOOP
C
 1    READ(ITTI1) RPM
      IF(.NOT.START) GOTO 156
      CALL DESTROY(6, IER)
      CALL DESTROY(ID, IER)
      IF(DISK) CALL CLOSE(IFLCH, IER)
 156  IF(RPM.EQ.0.) GOTO 1002
      DELT=RPM-STEP
      IF((RPM.LT.18.5).OR.(RPM.GT.90.)
     1          .OR.(ABS(DELT).GT.10.)) GOTO 200
      DATUM(1)=STEP*40.95+.5
      STEP=RPM
      START=.TRUE.
      CALL INITT(1)
      CALL ITASK(DAAD, ID, 10, IER)
      GOTO 1
```


cont'd...

```
C
 200  WRITE(ITTO1,157) RPM
 157  FORMAT(' OUTSIDE LIMITS ',F7.2)
      GOTO 15
C
C     ERROR CONDITION
C
 1000 WRITE(ITTO1) 'STOP'
      CALL RESET
      STOP
C
C     LOAD OVERLAY CORRESPONDING TO OPTION
C          1 - STOP
C          2 - PRBS TEST
C          3 - CONTROL ALGORITHM
C          4 - DATA LOGGING
C
 1012 CALL FOVLD(IOLCH,STP3,0,IER)
 1002 WRITE(ITTO1,102)
 102  FORMAT(' OPTION?',1X,Z)
      RPM=STEP
      READ(ITTI1) LETTER
      IF((LETTER.LT.1).OR.(LETTER.GT.4)) GOTO 1002
      IF((LETTER.NE.2).AND.(LETTER.NE.3)) GOTO 16
      I=LETTER-1
      CALL INITT(I)
      CALL FOVRL(STP3,IER)
 16   GOTO (1000,1005,1003,15),LETTER
C
C     LOAD PRBS TEST OVERLAY
C
 1005 CALL FOVLD(IOLCH,STEP1,0,IER)
      CALL ITASK(DAAD2,ID,10,IER)
      GOTO 1012
C
C     LOAD SELF-TUNER OVERLAY
C
 1003 CALL FOVLD(IOLCH,STEP2,0,IER)
      CALL ITASK(DAAD3,ID,10,IER)
```

cont'd....

```
 1006 READ(ITTI1) LETTER
      IF((LETTER.LT.1).OR.(LETTER.GT.5)) GOTO 1006
C
C     OPTIONS STR INPUT
C          1 - STOP STR EXPERIMENT
C          2 - CHANGE TSI
C          3 - CHANGE PSET
C          4 - CHANGE G
C          5 - CHANGE G1
C
      GOTO(1007,1020,1021,1022,1023),LETTER
 1020 WRITE(ITTO1)' TSI'
      READ(ITTI1) TSI
      IF(TSI.LT.0.) GOTO 1020
      GOTO 1006
 1021 WRITE(ITTO1) ' PSET'
      READ(ITTI1) PSET
      IF(PSET.LT.0.) GOTO 1021
      GOTO 1006
 1022 WRITE(ITTO1) ' G'
      READ(ITTI1) G
      IF(G.LT.0.) GOTO 1022
      GOTO 1006
 1023 WRITE(ITTO1)' G1'
      READ(ITTI1) G1
      IF(G1.LT.0.) GOTO 1023
      GOTO 1006
C
C     CONTROL COMPLETED
C
 1007 WRITE(ITTO1) ' END OF CONTROL RUN'
      CALL DESTROY(ID,IER)
      CALL DESTROY(6,IER)
      CALL DESTROY(12,IER)
      CALL DESTROY(14,IER)
      IF(DISK) CALL CLOSE(IFLCH,IER)
      IF(DISK) CALL CLOSE(21,IER)
      CALL FOVRL(STEP2,IER)
      GOTO 1012
      END
```

File Name : RLS. MC

```
      PARAMETER NP=5, NL=5, ISK=600, IFL2=21
      TASK RLS
C
C     TASK TO PREFORM RECURSIVE LEAST SQUARES
C     ASSUMES P MARIX INITIALIZED SYMETRIC
C
      COMMON// TSI, G, G1, II, U, X, TH(NP), PH(NP), YM, FL
      COMMON/BLCK1/ DISK
      LOGICAL DISK
      REAL K(NL), THETA(NL), PHI(NL), P(NL, NL)
      N=NL-1
C
C     INITIALIZE P MATRIX AND PHI VECTOR
C
      DO 10 I=1, NL
        PH(I)=0.
        DO 10 J=1, NL
          P(I, J)=0.
          IF(I. NE. J) GOTO 10
          P(I, J)=10.
 10   CONTINUE
 1    CALL SUSP
C
C     STORE COMMON VARIABLES
C
      Y=YM
      DO 2 I=1, NL
        PHI(I)=PH(I)
 2      THETA(I)=TH(I)
C
      SUM=PHI(NL)*PHI(NL)*P(NL, NL)
C
C     LAMDA + PHI * P * PHI
C
      DO 9 I=1, N
        SUM=SUM+PHI(I)*PHI(I)*P(I, I)
        IJ=I+1
        DO 9 J=IJ, NL
 9        SUM=SUM+2.*PHI(I)*PHI(J)*P(I, J)
      DEN=SUM+FL
      ERRS=0.
C
C     CALCULATE K VECTOR
C
      DO 19 I=1, NL
        SUM=0.
        DO 29 J=1, NL
          PP=P(I, J)
          IF(I. GT. J) PP=P(J, I)
 29       SUM=SUM+PP*PHI(J)
        K(I)=SUM/DEN
```

cont'd...

```
 19      ERRS=ERRS+PHI(I)*THETA(I)
       ERRS=Y-ERRS
C
C      CALCULATE PARAMETER VECTOR
C
       DO 5 I=1,NL
         DO 4 J=I,NL
 4         P(I,J)=(P(I,J)-K(I)*K(J)*DEN)/FL
 5       THETA(I)=THETA(I)+K(I)*ERRS
       IF(II.LE.(ISK+20)) GOTO 51
C
C      RECORD PARAMETER VALUES
C
       DO 40 I=1,NL
 40      TH(I)=THETA(I)
 51    IF(DISK) WRITE(IFL2,102) II,(TH(I),I=1,NL)
 102   FORMAT(I6,9F5.2)
       GOTO 1
       END
```

File Name : STEP 1. MC

```
      OVERLAY STEP1
C
C     THIS FILE OVERLAYS STP3. MC
C
      PARAMETER IDTOAS=3, IATODS=4, ITTO1=50, IFLCH=20, ID=6
      PARAMETER ICHPR=25
      TASK DAAD2
C
C     TASK TO RUN PRBS TEST
C
      EXTERNAL WAITT, WRTE
      COMMON/DGDC0/NMBR(2)
      COMMON/DGDC1/SCD2A(IDTOAS), SCA2D(IATODS)
      COMMON/DGDC2/DATUM(IDTOAS), ANALG(IATODS)
      COMMON/DGDC3/IWRD, ISTL
C
      COMMON/BLCK1/DISK, RPM
      COMMON/BLCK2/ MESK, TENTH, ITIME
      COMMON/BLCK4/ FIRST, P1(8), PAV(8)
      COMMON/BLCK3/DIE, P, TACH, MELT
      COMMON/BLCK6/ PP
      COMMON// TSI, G, G1, I, RPMN, Y
      LOGICAL DISK, TENTH, FIRST
      REAL MELT
      INTEGER SCA2D, ANALG, DATUM, SCD1A
C
C     OPENING PRBS DATA FILE
C
      Y=0.
      TSI=0.
      CALL OPEN(ICHPR, 'PRBS', 1, IER)
      ILINE=1
      IF(IER.NE.1) GOTO 99
C
      CALL DATAI(IER)
      FIRST=.TRUE.
      ITIME=50
      DLRPM=1.
      RPMN=RPM
      ILINE=8
      CALL ITASK(WRTE, 12, 12, IER)
      CALL ITASK(WAITT, ID, 7, IER)
      IF(IER.NE.1) GOTO 99
C
C     PRBS DATA ACQUISITION
C
      DO 150 I=1, 10000
        READ(ICHPR, END=151) SGN
        RPMN=RPM+SGN*DLRPM
        DATUM(1)=RPMN*40.95+.5
          CALL FILTER
```

cont'd...

```
          CALL CAL
          DATUM(2)=(P-1.5)*3000.+.5
          CALL DATAO(IER)
C
C     RECORDING EXPERIMENTAL DATA
C
        CALL RELSE(12,IER)
 150  CONTINUE
C
C     END OF PRBS TEST
C
 151  WRITE(ITTO1),' END OF PRBS TEST RETURNING TO MAIN'
      CALL CLOSE(ICHPR,IER)
      ILINE=4
      IF(IER.NE.1) GOTO 99
      CALL DESTROY(ID,IER)
      ILINE=2
      IF(IER.NE.1) GOTO 99
      IF(DISK) CALL CLOSE(IFLCH,IER)
      ILINE=3
      IF(IER.NE.1) GOTO 99
      CALL OVKIL(STEP1)
 99   WRITE(ITTO1) ' ERROR IN DARD',ILINE,IER
      CALL RESET
      STOP
      END
```

File Name : STEP 2. MC

```
      OVERLAY STEP2
C
C     THIS FILE OVERLAYS STP3.MC
C     SELF-TUNING CONTROLLER
C
      PARAMETER IDTOAS=3, IATODS=4, ITTO1=50, ID=6, ID2=12, ISK=600
      PARAMETER NP=5, NA=3, NB=2, ID3=14
      TASK DAAD3
      EXTERNAL WAITT, RLS, WRTE
      COMMON/DGDC0/NMBR(2)
      COMMON/DGDC1/SCD2A(IDTOAS), SCA2D(IATODS)
      COMMON/DGDC2/DATUM(IDTOAS), ANALG(IA
      COMMON/DGDC3/IWRD, ISTL
C
      COMMON/BLCK1/ DISK, RPM
      COMMON/BLCK2/MESK, TENTH, ITIME
      COMMON/BLCK3/DIE, P, TACH, MELT
      COMMON/BLCK4/ FIRST, P1(8), PAV(8)
      COMMON/BLCK5/ TM, UTT
      LOGICAL DISK, TENTH, FIRST
      REAL MELT
      INTEGER SCA2D, ANALG, DATUM, SCD2A
      COMMON//TSI, G, G1, II, UT, Y, CONT(NP), PHI(NP), YM, FL
      EQUIVALENCE (PSET, RPM)
C
C     INITIALIZING CONTROL PARAMETERS
C
      FIRST=.TRUE.
      ITIME=250
      BOP=1.026
      CONT(1)=.586
      CONT(2)=-.703
      CONT(3)=.1
      CONT(4)=-1.722
      CONT(5)=.869
      FL=.98
      TSI=.3
C
      CALL DATAI(IER)
      CALL CAL
      UT=RPM
      CALL ITASK(WRTE, ID2, 12, IER)
      CALL ITASK(RLS, ID3, 14, IER)
      PSET=1.77
      WRITE(ITTO1, 101) PSET
 101  FORMAT(' PSET = ', F6.3, /3X, 'II', 4X, 'U', 5X, 'Y', 7X,
     1          'P', 2X, 'PSET', 3X, 'TACH', 1X, 'MELT', 1X, 'TSI', /)
      CALL WAIT(1, 2, IER)
      Y=0.
      U3=0.
      U2=0.
      U1=0.
      U=0.
      UP=0.
```


cont'd...

```
      NC=NA+NB
      CALL ITASK(WAITT,ID,7,IER)
C
      DO 150 II=1,10000
        CALL FILTER
        CALL CAL
        DATUM(2)=(P-1.5)*3000.+.5
        IF(DATUM(2).LT.0) DATUM(2)=0
          CALL DATAO(IER)
        ILINE=1
        IF(IER.NE.0) GOTO 999
C
C     MINIMUM VARIANCE AND SELF-TUNING CONTROL CALCULATIONS
C
        PSI=(P-PSET)*100.
        BO=BOP+TSI
        IF(II.LT.ISK) GOTO 146
        U=-(PSI*CONT(1)+Y*CONT(2)+Y1*CONT(3))
        U=(U-CONT(4)*U1-CONT(5)*U2)/80
        IF(ABS(U).GE.5) U=ABS(U)/U*5
        IF((UT+U).GT.90.) U=90.-UT
        IF((UT+U).LT.18.5) U=18.5-UT
        CALL RELSE(ID3,IER)
        ILINE=2
        IF(IER.NE.1) GOTO 999
  146   UT=UT+U
        DATUM(1)=UT*40.95+.5
        CALL DATAO(IER)
C
C     RESET PHI VECTOR
C
        DO 1 I=2,NA
          K=NA-I+2
    1     PHI(K)=PHI(K-1)
        PHI(1)=Y
        Y1=Y
        Y=PSI
        DO 2 I=2,NB
          K=NC-I+2
    2     PHI(K)=PHI(K-1)
        PHI(NA+1)=U2
        U3=U2
        U2=U1
        U1=U
        YM=Y-BOP*U2
C
C     RECORDING EXPERIMENTAL DATA
C
        CALL RELSE(ID2,IER)
  150 CONTINUE
C
C     ERROR DETECTED
C
  999 WRITE(ITTO1) 'ERROR IN DAAD'
      CALL RESET
      STOP
      END
```

File Name : STP 2. MC

```
      PARAMETER ITTO1=50, ITTI1=51, IFLCH=20
      SUBROUTINE INITT(IFLNUM)
C
C     SUBROUTINE TO NAME AND INITIALIZE DATA FILES
C
      COMMON/BLCK1/ DISK, RPM
      INTEGER FLNM(4), DTAR(3), TMAR(3)
      LOGICAL DISK
      DISK=.FALSE.
C
C     DETERMINE IF FILE IS NEEDED
C
 5    WRITE(ITTO1,102)
 102  FORMAT(' DISK FILE? ',Z)
      READ(ITTI1,101) LETTER
 101  FORMAT(A1)
      IF((LETTER.NE.'Y ').AND.(LETTER.NE.'N ')) GOTO 5
      IF(LETTER.NE.'Y ') RETURN
C
C     WRITE DISK HEADER; FILE NAME, DATE, TIME
C
      DISK=.TRUE.
      IFL=IFLCH
      DO 200 I=1,IFLNUM
      WRITE(ITTO1,104) I
 104  FORMAT(' NAME: FILE #',I1,2X,Z)
      READ(ITTI1,100) FLNM
 100  FORMAT(4A2)
      CALL CFILW(FLNM,1,IER)
      IF(IER.NE.1) GOTO 99
      CALL OPEN(IFL,FLNM,2,IER)
      CALL DATE(DTAR,IER)
      CALL TIME(TMAR,IER)
      WRITE(IFL,130) FLNM,DTAR,TMAR
 130  FORMAT(' FILE NAME  ',4A2,' DATE ',I3,2('/',I2),
     1          '  TIME',I3,2(':',I2))
        IFL=IFL+1
 200  CONTINUE
      RETURN
C
C     HERE ON ERROR
C
 99   WRITE(ITTO1) ' INITT',IER
      CALL RESET
      STOP
      END
```

File Name : STEP 3. MC

```
C
C       THIS FILE OVERLAYS STP3.MC
C       PI CONTROLLER; DIGITAL VELOCITY EQUATION
C
        PARAMETER IDTOAS=3, IATODS=4, ITTO1=50, IFLCH=20, ID=6
        PARAMETER ID2=12, ISK=600
        OVERLAY STEP2
        TASK DAAD3
        EXTERNAL WAITT, WRTE
        COMMON/DGDCO/NMBR(2)
        COMMON/DGDC1/SCD2A(IDTOAS), SCA2D(IATODS)
        COMMON/DGDC2/DATUM(IDTOAS), ANALG(IATODS)
        COMMON/DGDC3/IWRD, ISTL
C
        COMMON/BLCK1/ DISK, RPM
        COMMON/BLCK2/MESK, TENTH, ITIME
        COMMON/BLCK3/DIE, P, TACH, MELT
        COMMON/BLCK4/ FIRST, P1(8), PAV(8)
        LOGICAL TENTH, DISK, FIRST
        REAL MELT, KC
        INTEGER SCA2D, ANALG, DATUM, SCD2A
        COMMON// TSI, KC, TI, II, UT, PSI
C
C       INITIALIZING TASKS AND PARAMETERS
C
        CALL DATAI(IER)
        ILINE=1
        IF(IER.NE.0) GOTO 99
        CALL CAL
        UT=RPM
        PSET=1.77
        WRITE(ITTO1,101) PSET
 101    FORMAT(' PSET = ',F6.3,/,3X,'II',2X,'U',5X
     1          ,'Y',3X,'PSET',3X,'TACH',1X,'MELT',1X,'TSI',/)
        KC=.4
        TI=1.
        CALL ITASK(WRTE, ID2, 12, IER)
        ILINE=2
        IF(IER.NE.1) GOTO 99
        ITIME=250
        CALL WAIT(ITIME, 1, IER)
        ILINE=4
        IF(IER.NE.1) GOTO 99
        Y=0.
        FIRST=.TRUE.
        SAMP=ITIME/1000.
        ILINE=8
        CALL ITASK(WAITT, ID, 7, IER)
```

cont'd...

```
      IF(IER.NE.1) GOTO 99
C
      DO 150 II=1,10000
        CALL FILTER
        CALL CAL
C
C     DIGITAL PI CONTROL CALCULATIONS
C
        U=0.
        PSI=(PSET-P)*100.
        IF(II.LT.ISK) GOTO 146
        U=KC*((PSI-Y)+PSI/TI*SAMP)
        IF(ABS(U).GE.5) U=ABS(U)/U*5.
        IF((UT+U).GT.90.) U=90.-UT
        IF((UT+U).LT.18.5) U=18.5-UT
 146    UT=UT+U
        DATUM(1)=UT*40.95+.5
        DATUM(2)=(P-1.5)*3000.+.5
        IF(DATUM(2).LT.0) DATUM(2)=0
        CALL DATAO(IER)
        Y=PSI
        CALL RELSE(ID2,IER)
 150  CONTINUE
C
C     ERROR DETECTED
C
 99   WRITE(ITTO1) ' ERROR IN DAAD',ILINE,IER
      CALL RESET
      STOP
      END
```

```
      OVERLAY STP3
      PARAMETER IDTOAS=3, IATODS=4, ITTO1=50, IFLCH=20, ID=6
      PARAMETER ILAG=1
      TASK DAAD
C
C     TASK OF LOW PRIORITY TO SCAN DGDAC
C        AND TO WRITE TO DISK AND TTO1
C
      EXTERNAL WAITT
      COMMON/DGDC0/NMBR(2)
      COMMON/DGDC1/SCD2A(IDTOAS), SCA2D(IATODS)
      COMMON/DGDC2/DATUM(IDTOAS), ANALG(IATODS)
      COMMON/DGDC3/IWRD, ISTL
C
      COMMON/BLCK1/ DISK, RPM
      COMMON/BLCK2/ MESK, TENTH, ITIME
      COMMON/BLCK3/DIE, P, TACH, MELT
X     COMMON/BLCK4/ FIRST, P1(8), PAV(8)
      LOGICAL DISK, FIRST, TENTH
      REAL MELT
      INTEGER SCA2D, ANALG, DATUM, SCD2A
      WRITE(ITTO1, 120) RPM
 120  FORMAT(' RPM   = ', F5.1, //, '    TIME'
     1              , 4X, 'DIE', 3X, 'P', 3X, 'TACH'
     2              , 2X, 'MELT', /)
      SEC=-8.
      ITIME=250
      LOOP=32
      SECIN=.25
      CALL DATAI(IER)
C
C     OUTPUT STEP AND RECORD INITIAL CONDITIONS
C
      IF(DISK) WRITE(IFLCH, 110) RPM
 110  FORMAT(' RPM = ', F5.1)
      ILINE=8
      CALL ITASK(WAITT, ID, 7, IER)
      IF(IER.NE.1) GOTO 99
C
C     PRINTOUT INITIAL CONDITIONS + INITIAL STEP RESPONSE
C
      FIRST=.TRUE.
      DO 145 J=1, ILAG
        DO 140 I=1, LOOP
          TENTH=.TRUE.
          CALL REC(MESK, MESS)
          TENTH=.FALSE.
          CALL DATAI(IER)
```

cont'd...

```
          SEC=SEC+SECIN
          CALL CAL
          IF(DISK) WRITE(IFLCH,100) SEC,DIE,P,TACH,MELT
          DATUM(2)=(P-1.5)*3000.+.5
          IF(DATUM(2).LT.0) DATUM(2)=0
          CALL DATAO(IER)
 140      CONTINUE
          WRITE(ITTO1,100) SEC,DIE,P,TACH,MELT
 145   CONTINUE
       DATUM(1)=RPM*40.95+.5
       CALL DATAO(IER)
C
C      LOOP TO RECORD STEP TEST DATA
C
 147   DO 149 I=1,LOOP
         TENTH=.TRUE.
         CALL REC(MESK,MESS)
         TENTH=.FALSE.
         CALL DATAI(IER)
         CALL CAL
         DATUM(2)=(P-1.5)*3000.+5
         IF(DATUM(2).LT.0) DATUM(2)=0
         CALL DATAO(IER)
       SEC=SEC+SECIN
C
C      RECORDING EXPERIMENTAL DATA
C
       IF(DISK) WRITE(IFLCH,100) SEC,DIE,P,TACH
      1                ,MELT
 149     CONTINUE
C
C      WRITE TO $TTO1 EVERY 8 SEC
C
         WRITE(ITTO1,100) SEC,DIE,P,TACH,MELT
 100   FORMAT(F8.2,F6.1,F6.3,F5.1,F7.1)
       GOTO 147
 99    WRITE(ITTO1) ' ERROR IN DAAD',ILINE,IER
       CALL RESET
       STOP
       END
```

```
      PARAMETER IDTOAS=3, IATODS=4
      BLOCK DATA
C
C     BLOCK DATA SUBROUTINE TO DETERMINE DGDAC
C         I/O PORT NUMBERS
C
      COMMON/DGDC0/NMBR(2)
      COMMON/DGDC1/SCD2A(IDTOAS), SCA2D(IATODS)
      COMMON/DGDC2/DATUM(IDTOAS), ANALG(IATODS)
      COMMON/DGDC3/IWRD, ISTL
      INTEGER SCA2D, ANALG, DATUM, SCD2A
      DATA NMBR/IDTOAS, IATODS/
C
C     2000K - ZONE FOUR TEMPERATURE
C     2001K - PRESSURE
C     2002K - ZONE TWO TEMPERATURE
C     2003K - TACHOMETER
C     2013K - MELT TEMPERATURE
C     3000K - DIE TEMPERATURE
C     3001K - ZONE THREE TEMPERATURE
C     3002K - ZONE ONE TEMPERATURE
C
      DATA SCA2D/3000K, 2001K, 2003K, 2013K/
C
C     4001K - CHART RECORDER
C     4002K - EXTRUDER MOTOR POWER
C     4003K - DIE HEATER POWER
C
      DATA SCD2A/4002K, 4001K, 4003K/
      END
```

```
      PARAMETER IDTOAS=3, IATODS=4
      SUBROUTINE CAL
C
C     SUBROUTINE TO PERFORM CALIBRATIONS
C
      COMMON/DGDC2/DATUM(IDTOAS), ANALG(IATODS)
      COMMON/BLCK3/DIE, P, TACH, MELT
      COMMON/BLCK6/ PP
      INTEGER ANALG, DATUM
      REAL MELT
C
C     Z1 - ZONE 1 TEMPERATURE
C     Z2 - ZONE 2 TEMPERATURE
C     Z3 - ZONE 3 TEMPERATURE
C     Z4 - ZONE 4 TEMPERATURE
C     DIE - DIE TEMPERATURE
C     MELT - MELT TEMPERATURE
C     TACH - TACHOMETER
C     P - FILTERED PRESSURE
C     PP - UNFILTERED PRESSURE
C
X     Z1=-193.4+.2425*ANALG(5)
X     Z2=-194.1+.2418*ANALG(4)
X     Z3=-197.2+.2413*ANALG(3)
X     Z4=-199.5+.2415*ANALG(2)
      DIE=-194.8+.2440*ANALG(1)
      MELT=205.5+.05995*ANALG(4)
      P=.135+ANALG(2)*8.2E-4
      PP=.135+PP*8.2E-4
      TACH=-2.045E-1+ANALG(3)*3.249E-2
      RETURN
      END
```

File Name : STP 6. MC

```
      PARAMETER ITTO1=50, IUNITS=1
      TASK WAITT
C
C     TASK TO WAIT FOR SPECIFIED PERIOD
C
      LOGICAL TENTH
      COMMON/BLCK2/MESK, TENTH, ITIME
      MESK=0
      MESS=1
 1    CALL WAIT(ITIME, IUNITS, IER)
      IF(IER. NE. 1) GOTO 999
      IF(. NOT. TENTH) GOTO 999
      IER=-1
 2    CALL XMT(MESK, MESS, $999)
      GOTO 1
C
C     ERROR MESSAGE
C     NEGETIVE NUMBER FOR IER MEANS
C         ERROR IN XMT STATEMENT
C

 999  WRITE(ITTO1, 1000) IER
 1000 FORMAT(' ERR WAITT', I4)
      IF(IER. EQ. 1) GOTO 2
      CALL RESET
      STOP
      END
```

File Name : STP 7. MC

```
      PARAMETER IDTOAS=3, IATODS=4, LOOP=10
X     PARAMETER ISKIP=1000
C
C     SUBROUTINE TO FILTER PRESSURE DATA
C         LOWPASS FILTER - FOURTH ORDER BUTTERWORTH
C
      SUBROUTINE FILTER
      COMMON/DGDC0/NMBR(2)
      COMMON/DGDC1/SCD2A(IDTOAS), SCA2D(IATODS)
      COMMON/DGDC2/DATUM(IDTOAS), ANALG(IATODS)
      COMMON/DGDC3/IWRD, ISTL
C
      COMMON/BLCK2/ MESK, TENTH, ITIME
      COMMON/BLCK4/ FIRST, P1(8), PAV(8)
      COMMON/BLCK6/ PP
      COMMON/BLCK7/ PF, PF1
      LOGICAL TENTH, FIRST
      INTEGER SCA2D, ANALG, DATUM, SCD2A
C
      IF(.NOT.FIRST) GOTO 2
X     II=1
      ITIME=50
      DO 10 I=1,8
        P1(I)=ANALG(2)
        PAV(I)=ANALG(2)
 10   CONTINUE
      PF1=ANALG(2)/18.002
      FIRST=.FALSE.
 2    CONTINUE
      DO 1 I=1, LOOP
```

cont'd...

```
      TENTH=.TRUE.
      CALL REC(MESK,MESS)
      TENTH=.FALSE.
      CALL DATAI(IER)
X     PA1=ANALG(2)
X     IF(II.LT.ISKIP) GOTO 1
      PA=(ANALG(2)+2.*P1(1)+P1(2)+1016.6*PAV(1)-486.8*PAV(2))/533.8
      PA1=(PA+2.*PAV(1)+PAV(2)+1016.6*PAV(3)-500.6*PAV(4))/520.
      DO 11 J=1,7
        K=8-J
        P1(K+1)=P1(K)
        PAV(K+1)=PAV(K)
11    CONTINUE
      P1(1)=ANALG(2)
      PAV(3)=PA1
      PAV(1)=PA
X     DATUM(2)=PA1+.5
X     CALL DATAO(IER)
1     CONTINUE
      PP=ANALG(2)
      ANALG(2)=PA1+.5
X     II=II+1
      RETURN
      END
```

```
      PARAMETER ITTO1=50, IFLCH=20, IWR=30
      TASK WRTE
C
C     TASK TO WRITE DATA
C
      REAL MELT
      LOGICAL DISK
      COMMON/BLCK1/ DISK, PSET
      COMMON/BLCK3/ DIE, P, TACH, MELT
      COMMON/BLCK5/ TM, UTT
      COMMON/BLCK6/ PP
      COMMON// TSI, G, G1, II, UT, Y
C
 1    CALL SUSP
      IF(DISK)WRITE(IFLCH, 100) II, UT, Y, P, TACH, MELT, TSI, PP
      IF(MOD(II, IWR). EQ. 0) WRITE(ITTO1, 100)
     1                  II, UT, Y, P, TACH, MELT, TSI, PP
100   FORMAT(I6, F6. 2, F7. 2, F6. 3, F5. 1, F6. 1, F5. 2, F6. 3)
      GOTO 1
      END
```

```
      PARAMETER ITTO1=50, IFLCH=20, IWR=30
      TASK WRTE
C
C     TASK TO WRITE DATA
C
      REAL MELT
      LOGICAL DISK
      COMMON/BLCK1/ DISK, PSET
      COMMON/BLCK3/ DIE, P, TACH, MELT
      COMMON/BLCK5/ TM, UTT
      COMMON/BLCK6/ PP
      COMMON// TSI, G, G1, II, UT, Y
C
 1    CALL SUSP
      IF(DISK)WRITE(IFLCH, 100) II, UT, Y, P, TACH, MELT, G, G1, PP
      IF(MOD(II, IWR). EQ. 0) WRITE(ITTO1, 100)
     1                  II, UT, Y, P, TACH, MELT, G, G1, PP
100   FORMAT(I6, F6. 2, F7. 2, F6. 3, F5. 1, F6. 1, 2F5. 2, F6. 3)
      GOTO 1
      END
```

APPENDIX C

START UP AND SHUTDOWN PROCEDURES

C.1 Start Up Procedure

All the instrumentation discussed in this section is shown in the schematic of the extruder instrumentation panel, Figure A.1.

1) For safety reasons, make sure that the main 220 volt power supply switch located on the wall above the instrument box is switched off. Then switch on all the amplifiers and the voltage to current converter that are located inside the instrument panel.

2) Close and lock the door of the instrument panel and then turn on the main 220 volt power switch.

3) Turn the power switch, on the front of the instrumentation panel, to the ON position. This will start the heating elements controlled by the analog temperature controllers but not the extruder motor.

4) Do not start the extruder motor until the melt temperature indicator has reached the desired temperature and remained there for at least 20 minutes. This ensures that all the polymer present in the extruder barrel has completely melted. If the extruder motor is started when the extruder is cold, the screw will break (although a shear pin should break first). For all the experiments in this thesis, the desired temperature was taken as above 165°C. After the extruder motor is started, there is an initial period before the extrudate temperature reaches steady state. This initial period can be considerably shortened by heating the extruder for a longer period of time. Leaving the extruder heating for over 3 h generally reduces the start up time to less than 15 min.

5) After the extruder has warmed, flip the power switch on the side of the take up mechanism to the ON position and then press the start button on the front of the take up mechanism control panel. Turn on the air supply to the drying nozzle and the water supply to the cooling trough and plug in the pump motor. Regulate the water supply and recycle valve until the water level remains unchanged. For most experiments, the pump and the water supply do not need to be used because the water in the bath remains cold enough to freeze the extrudate for a long period. This eliminates the chance of the water overflowing the trough. Alternatively, the pump and the water can be used for short periods to replace heated water with fresh cold water.

6) Start the computer program and then using option 4, the step test overlay, step up to approximately 30, in motor power. With the extruder in manual mode and the manual screw speed control dial set at 25. r/min, open the feed shute and then start the extruder motor .

7) When the extrudate starts to be produced from the die, draw it through the bath, under the bars at the bottom of the tank, and through the dryer nozzle and take up mechanism wheels.

8) Switch the extruder from manual to automatic. The extruder is now under computer control.

C.2 Shutdown Procedures

1) Using option 4 in the computer program, step down to approximately 28. r/min on the tachometer dial. Remember that as the extruder slows, the extrudate thins and therefore the take up wheels may need tightening.

2) With the manual screw speed control dial set at 25. r/min, switch to normal control.

3) Close the feed shute and let the extruder empty of polymer.

4) Once the extruder has emptied, stop the extruder motor and the take up mechanism, pull out the pump motor plug and shut off the water flow and the air supply.

APPENDIX D

STEP TEST DATA

The data of Figures 4.6 and 4.7 on a reduced time scale.

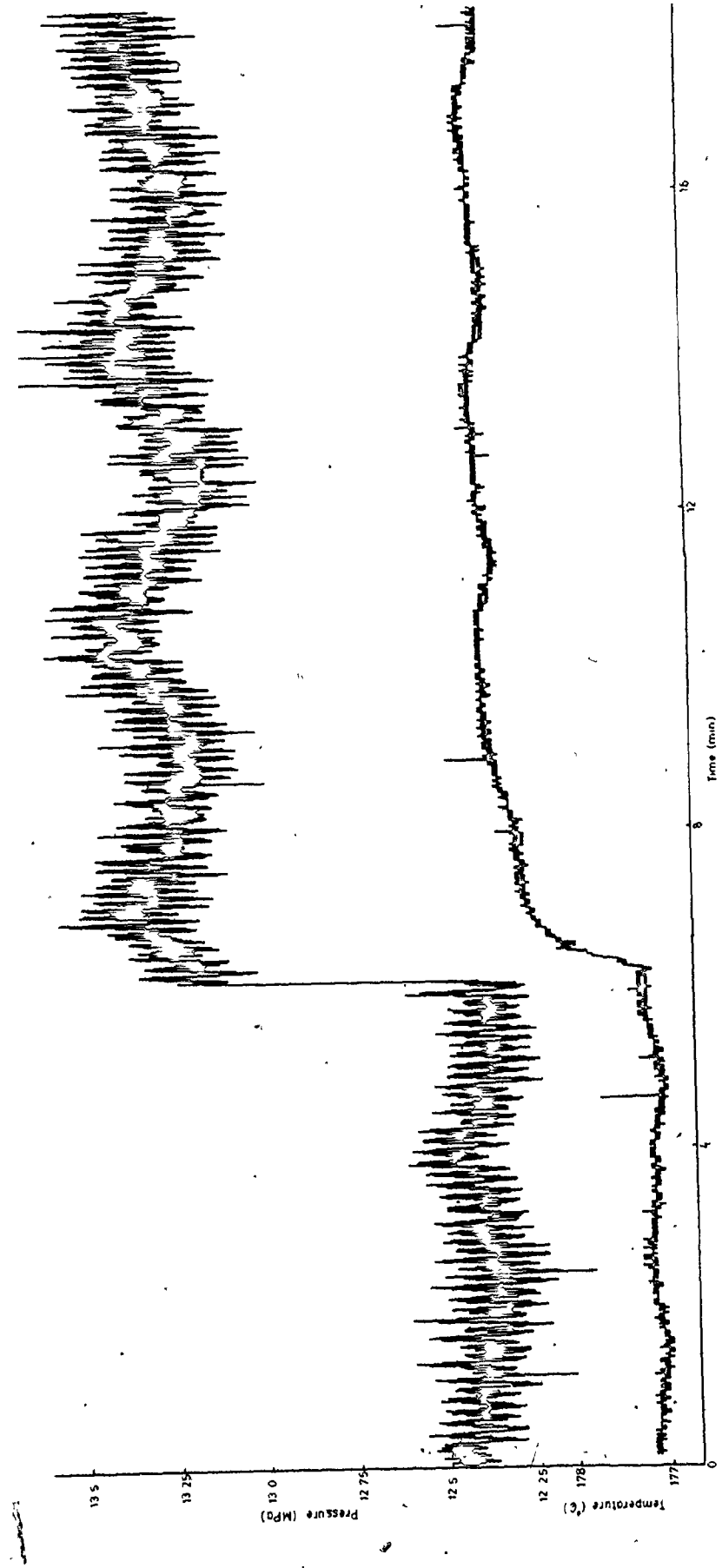
Pressure (MPa)
13 5
13 25
13 0
12 75
12 5
12 25
Temperature (°C)
178
177
0
4
8
12
16
Time (min)